Geologica Acta, Vol.9, Nos 3-4, September-December 2011, 329-350
DOI: 10.1344/105.000001695
Available online at www.geologica-acta.com

geologica acta

The Chuacús Metamorphic Complex, central Guatemala: geochronological and geochemical constraints on its Paleozoic - Mesozoic evolution

L.A. SOLARI [1] [*] **A GÓMEZ-TUENA** [1] **F. ORTEGA-GUTIÉRREZ** [2] **C. ORTEGA-OBREGÓN** [2]

[1] **Centro de Geociencias, Universidad Nacional Autónoma de México**
Campus Juriquilla, 76230 Querétaro, México. E-mail: solari@servidor.unam.mx

[2] **Instituto de Geología, Universidad Nacional Autónoma de México**
Ciudad Universitaria, 04510, México D.F., México

* Corresponding author

ABSTRACT

The Chuacús Metamorphic Complex is located in Central Guatemala, between the Polochic and Motagua fault zones. It is made up of complexly intercalated, mafic and felsic high-grade gneisses, amphibolites, pelitic and quartzofeldsphatic metasediments and subordinate marbles. Mafic dikes and lenses metamorphosed to amphibolite and eclogite facies are tholeiitic and similar to mid-ocean ridge basalts. In contrast, metamorphosed intrusives (gabbro, diorite and granite) are calc-alkaline and have the geochemical signature of arc magmas. Laser Ablation Inductively Coupled Plasma Mass Spectrometry U-Pb zircon geochronology allows the recognition of three episodes of metamorphism. The first eclogite facies metamorphism (M1) is bracketed between Ordovician magmatism in the northern Chuacús Metamorphic Complex and the neighboring Rabinal granitic suite; the second corresponds to an Upper Triassic period of arc magmatism and migmatization (M2); the third high-grade metamorphic event (M3) occurred during the Late Cretaceous.

The tectonic evolution of the Chuacús Metamorphic Complex began during the Early Paleozoic as a basin in the Rheic Ocean that received detrital material from the Maya Block, Acatlán and southeastern México. The Chuacús Metamorphic Complex evolved to an active margin that subducted to HP conditions during the Mid-Late Paleozoic, and then was exhumed and involved in two tectonothermal events during the Upper Triassic and Late Cretaceous. The Chuacús Metamorphic Complex was accreted to the southern Maya Block during the Late Cretaceous, as a result of the convergent tectonics between the latter and either the Greater Antillean arc or the Chortís Block.

KEYWORDS | **Chuacús Complex. Guatemala. U-Pb geochronology. Maya Block. Caribbean. Basement Tectonics.**

INTRODUCTION

The tectonic limit between the North America and Caribbean plates is composed of a complex mosaic of crustal blocks, which are juxtaposed and limited by faults (e.g., Ortega-Gutiérrez et al., 2007; Rogers et al., 2007; Brueckner et al., 2009; Ratschbacher et al., 2009) (Fig. 1). Those crustal blocks range in age from the Proterozoic (e.g. Yoro area, central Honduras, Manton, 1996) to Early-Late Paleozoic and Mesozoic (Altos Cuchumatanes, Guatemala, Solari et al., 2009, 2010a; Maya Mountains, Belize, Martens et al., 2010; Rabinal suite, Guatemala, Ortega-Obregón et al., 2008; Chuacús Complex, Ortega-Gutiérrez et al., 2004; Ratschbacher et al., 2009; Las Ovejas Complex, Ratschbacher et al., 2009), and were finally amalgamated during the Late Mesozoic-Cenozoic (Harlow et al., 2004; Ortega-Gutiérrez et al., 2004; Martens et al., 2007; Brueckner et al., 2009; Ratschbacher et al., 2009). Recent works shed light on the tectonic evolution of the Motagua fault zone as the complex tectonic limit between the North America and Caribbean plates (Harlow et al., 2004; Brueckner et al., 2009; Pindell et al., 2006; Pindell and Kennan, 2009). The tectonic significance of the continental blocks involved in the suturing, however, is still a matter of debate, especially on the southernmost edge of the North America plate (i.e., the Maya Block). The classical view on the tectonic limit is represented by a suture along the Motagua fault, involving the Maya Block (North America plate) to the north, and the Chortís Block (Caribbean plate) to the south (e.g., Dengo, 1969). More recently, several works have added complexity to such a simple model, involving the collision of the Greater Antilles to the south of the Maya Block during the Late Cretaceous, prior to docking of the Chortís Block (e.g., Pindell and Barret, 1990; Harlow et al., 2004; Giunta et al., 2006; Brueckner et al., 2009; Pindell and Kennan, 2009; Ratschbacher et al., 2009). Further complications have arisen from the works of Ortega-Gutiérrez et al. (2007) and Ortega-Obregón et al. (2008), who suggested and argued for the existence of discrete crustal blocks or suspect terranes in the southern Maya Block, extending from central Guatemala across the Motagua suture zone to well inside the Chortís Block of southern Guatemala and Honduras (e.g. Rogers et al., 2007). One of the key localities to test the possible existence of those crustal entities, and one of the least studied, is the Sierra de Chuacús in central Guatemala. This paper presents new geochronological and geochemical data of crustal rocks in the Sierra de Chuacús in order to provide further constraints to its tectonic evolution and the ongoing discussions on its allochthonous vs. autochthonous nature and tectonic evolution.

PREVIOUS WORKS

The Sierra de Chuacús is located in central Guatemala, between the Polochic and Motagua faults (Fig.1 and 2). The Chuacús Metamorphic Complex is made up of an intricate sequence of polydeformed, locally retrograded high-grade metamorphic rocks, both igneous and sedimentary in origin. Previous works report Silurian ages with Grenvillian protoliths in the northern sector of the Sierra de Chuacús (Gomberg et al., 1968). The presence of a Carboniferous high-grade metamorphic event affecting a Grenvillian protolith was identified by Ortega-Gutiérrez et al. (2004) in El Chol, in the middle of the Sierra de Chuacús. Martens et al. (2005, 2007) questioned the precision of that age and reported a Triassic age for similar rocks. A recent work by Ratschbacher et al. (2009) reported Proterozoic ages in the northern Sierra de Chuacús, with some discordant analyses yielding imprecise lower intercepts in the 638-477Ma range. Another sample they dated in the southern Sierra de Chuacús yielded Proterozoic and Devonian inheritance, as well as Triassic magmatic ages that postdate eclogite metamorphism and were later affected by high-temperature (HT) metamorphism during the Late Cretaceous. Petrological data suggest the existence of a HT eclogite facies event (~680-750°C, ~22-24kbar, Ortega-Gutiérrez et al., 2004; Martens et al., 2007; Ratschbacher et al., 2009), which cooled to about 580-600°C and 10-14kbar during decompression (Ortega-Gutiérrez et al., 2004; Ratschbacher et al., 2009). While there is still debate about the existence of one or two eclogite facies from metamorphic pulses affecting the Chuacús Metamorphic Complex; pre-Carboniferous according to Ortega-Gutiérrez et al. (2004), pre-Triassic according to Ratschbacher et al. (2009), or after the Triassic but before the Late Cretaceous according to Martens et al. (2007); these authors agree on Late Cretaceous cooling and exhumation (broad K-Ar, Ar and Rb-Sr age range of ~75 to ~66Ma, see also Ortega-Obregón et al., 2008).

Metamorphic and igneous rocks of comparable age and metamorphic grade are present elsewhere in southern México and central-north Guatemala. In the Acatlán Complex of southern México, basement of the Mixteco terrane, megacrystic granites have yielded ~480-440Ma magmatic ages, similar to the ages calculated for rift-related tholeiites in the same unit (Miller et al. 2007; Keppie et al. 2008a, b). They are intimately associated with high pressure metamorphism that occurred either during the Cambro-Ordovician (Vega-Granillo et al., 2007) or the Devonian-Mississippian and was associated with the closure of the Rheic Ocean (e.g. Nance et al., 2006, and references therein). In southeastern México, the Guichicovi complex is characterized by Grenvillian granulites (Weber and Köhler, 1999) intruded by Permian granites (La Mixtequita Massif, Torres et al., 1999). The Chiapas Massif crops out farther to the southeast, toward the Guatemala border. The massif is characterized by Ordovician S-type granites and amphibolites (Pompa-Mera et al., 2008), as well as widespread Late Permian granites that intrude medium to high-grade metasediments and orthogneisses, with Nd model

ages between 1.0 and 1.4Ga (Schaaf et al., 2002; Weber et al., 2006a, 2007, 2008). The metasediments of the Lower Santa Rosa Formation, which crop out in the Chiapas Massif, were recently dated by Weber et al. (2009), establishing the maximum depositional ages as defined by youngest zircons clustering around 315-325 and 331-341Ma. In Central Guatemala, just north of the Baja Verapaz Fault Zone, Ortega-Obregón et al. (2008) dated several peraluminous granites between 453 and 462Ma (lower intercepts of discordant data, U-Pb by Isotope-Dilution Thermal Ionization Mass Spectrometry (ID-TIMS)) and placed them at the very edge of what they considered to be the tectonic southern limit of the Maya Block. In the Maya Mountains of Belize, Martens et al. (2010) reported an Early Devonian Laser Ablation Inductively Coupled Plasma Mass Spectrometry (LA-ICPMS) age of 406Ma for rhyolites interbedded with conglomerates, which confirms the ~405-420Ma ages previously published by Steiner and Walker (1996).

GEOLOGY OF THE CHUACÚS METAMORPHIC COMPLEX

The Chuacús Metamorphic Complex is a polymetamorphic, originally high-grade and essentially metasedimentary formation, which bears textural and mineralogical evidence of at least one eclogite-facies event following a P-T decompressional path that could have departed near the field of ultrahigh pressure metamorphism (UHPM) and, in any case, representing continental subduction (e.g. Ortega-Gutiérrez et al., 2004; Martens, 2009). The Chuacús Metamorphic Complex is mainly composed of quartzofeldspathic, garnet and mica bearing gneisses; two micas, garnet, kyanite, rutile schists; minor marbles and calcsilicates and abundant orthogneisses, which range from mafic (garnet, hornblende, rutile and plagioclase) to granitic in composition. A large, Late Cretaceous shear zone, named Baja Verapaz Shear Zone by Ortega-Obregón et al. (2008) limits the Chuacús Metamorphic Complex in the north. The kinematics of the

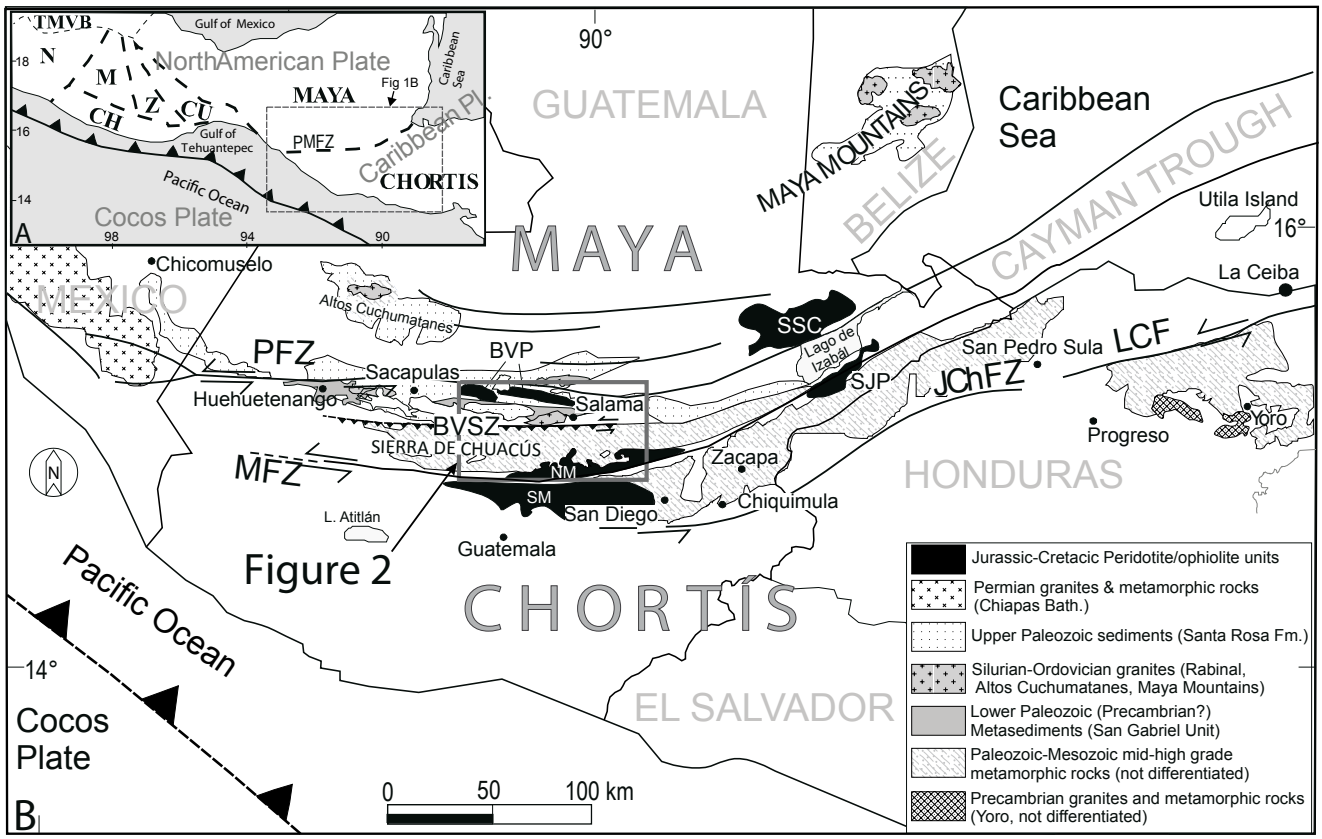

FIGURE 1 | **A) Main tectonic subdivision of crustal blocks in southern Mexico and Central America. N: Náhuatl-Guerrero terrane; TMVB: Trans-Mexican Volcanic Belt; M: Mixteco terrane; CH: Chatino terrane; Z: Zapoteco terrane; CU: Cuicateco terrane; MAYA: Maya Block; CHORTIS: Chortís block. Nomenclature after Sedlock et al. (1993). PMFZ: main (simplified) trace of the Polochic-Motagua fault zone. B) Schematic geological map showing basement rocks of central Guatemala, southeasternmost Mexico, and northwestern Honduras. Geology is recompiled from Kesler et al. (1970); Anderson et al. (1973); Steiner and Walker (1996); Weber et al. (2005, 2006); and unpublished data by the authors. PFZ: Polochic Fault Zone; MFZ: Motagua Fault Zone; BVFZ: Baja Verapaz Fault Zone; JChFZ: Jocotán-Chamelecón Fault Zone; LCF: La Ceiba Fault. Main ophiolitic bodies are shown in black: SSC: Sierra de Santa Cruz; BVP: Baja Verapaz; SJP: S. Juán de Paz; NM: north Motagua unit, ophiolite and mélange; SM: south Motagua unit, ophiolite and mélange. Modified from Ortega-Obregón et al. (2008).**

Baja Verapaz Shear Zone indicates thrusting to the NNE with a minor left-lateral component. It mainly affected a sequence of low-grade pre-Ordovician slates and phyllites, informally named the San Gabriel sequence, as well as some igneous units belonging to the Ordovician Rabinal Granite Suite (Ortega-Obregón et al., 2008). At the southern edge of the Baja Verapaz Shear Zone the low metamorphic grade increases to amphibolite facies, where the Chuacús Metamorphic Complex actually begins. Chuacús Metamorphic Complex orthogneisses present a large age range and variable degrees of deformation. However, intrusive contacts are often visible in fresh outcrops. One of the Chuacús Metamorphic Complex exposures which deserves a more detailed description is the El Chol. At this location, banded mafic gneisses are intimately associated with metamorphosed granitic-trondhjemitic dikes. Local pods of granitic melt, slightly discordant to concordant with the main foliation, strongly suggest that the mafic bands are migmatitic restites, whereas the granitic veins are neosomatic leucosomes. It is important to underline that El Chol is the only locality in the Chuacús Metamorphic Complex where at least three deformation events are superposed and clearly distinguishable. Pegmatites are also widespread throughout the entire Chuacús Metamorphic Complex, ranging from decimetric bands to more than several hundreds of meters wide. Eclogite is the most important lithology recognized in several outcrops. These high-pressure rocks are mainly present as deformed lenses in leucocratic and deformed gneisses, indicating a remnant of an important metamorphic event (cf. Ortega-Gutiérrez et al., 2004, for representative microprobe analyses).

The high-pressure metamorphism is widespread in the southern Sierra de Chuacús between El Chol and the northern Motagua allochthonous units, which constitute the tectonic southernmost limit of the Chuacús Metamorphic Complex. Eclogite-facies metamorphism is not recognized, however, in the western Chuacús (e.g. Kesler et al., 1970; Ratschbacher et al., 2009) or in the easternmost known outcrops, which are located in the southern Sierra de Las Minas (easternmost outcrops of Fig. 2).

MAIN PETROGRAPHIC FEATURES

The following petrological data summarize and complement previous work (Ortega-Gutiérrez et al., 2004) on some fundamental petrographic and textural

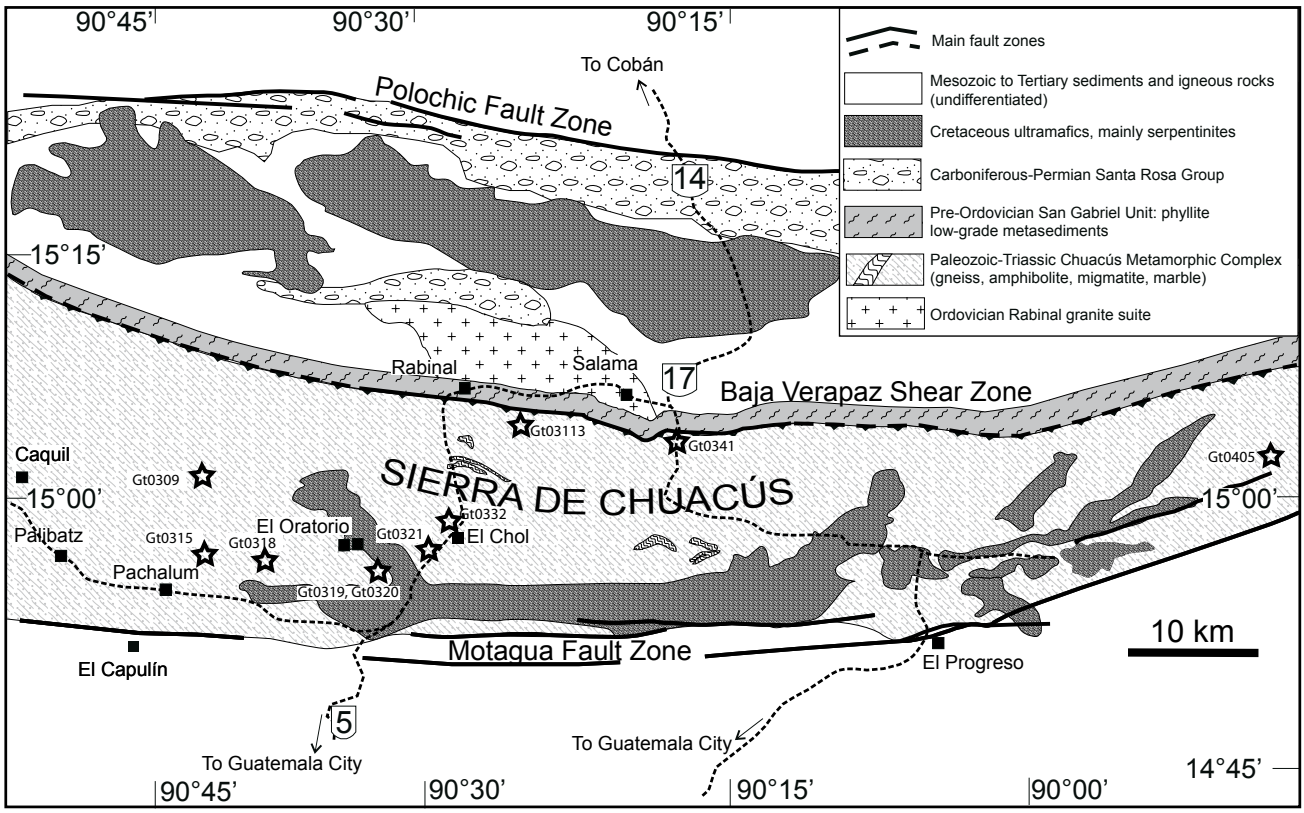

FIGURE 2 | **Simplified geologic map of the Sierra de Chuacús area, Central Guatemala. Modified from Ortega-Gutiérrez et al. (2004). Sampled localities are indicated.**

characteristics of the Chuacús Metamorphic Complex as studied at its type-area, the Sierra Chuacús between Granados and Salamá in central Guatemala. Based on detailed petrographic studies of representative samples, actual and relict evidence for high-pressure metamorphism may be found in most metapelitic, quartzofeldspathic, calcareous, and mafic lithologies of the Chuacús Complex in its type-area. The metapelites (see Table 1 for representative Wavelength Dispersive X-Ray Spectrometry (WDS) chemical analyses of the main aluminous phases) include the characteristic high-pressure assemblage kyanite - garnet - rutile - phengite - quartz, with minor phases in the matrix or as inclusions inside high-pyrope garnet ($Alm_{54}Pyr_{40.5}Gr_{4.2}Spes_{1.3}$) and kinked kyanite (Fig. 3A) such as quartz, phengite, ilmenite, titanomagnetite, zoisite, tourmaline, staurolite, phlogopite/biotite, chloritoid and monazite. Rutile inclusions in kyanite and garnet are particularly abundant and commonly show non-prismatic shapes (Fig. 3D). The high-pressure assemblages in the calcareous rocks include: a) high-Mg carbonate - rutile/titanite - quartz - white mica, with zircon, pyrrhotite and apatite as minor phases (marbles), and b) amphibole (pargasite/tremolite) - zoisite - quartz - clinopyroxene - white mica - clinochlore - serpentine - titanite (calcsilicates). Energy Dispersive X-R ay Spectrometry (EDS) analyses of high relief grains detected inclusions of corundum in some reddish pleochroic titanites, and lamellar rutile needles up to 32x0.25μm (Fig. 3B) that may be oriented in three different crystallographic planes in the cores of some zoisites. The composite association tremolite - zoisite - titanite/rutile (S1) overprinted by jadeite - lawsonite - albite - quartz - carbonate (S2) (see Fig. 3F) locally refl ects two high-pressure events verified at contrasting higher and lower temperatures. Lawsonite and jadeite were not verified by chemical analyses, but both phases display their distinctive optical properties (Ortega-Gutiérrez et al., 2004).

Quartzo-feldspathic rocks are characterized by assemblages with quartz - garnet - albite - phengite - biotite - zoisite - rutile - subcalcic amphibole, with accessory potassium feldspar, carbonates and rare green clinopyroxene (probably omphacite) included in albite porphyroblasts, indicating relict high-pressure conditions. Common rounded zircons suggest an original sedimentary protolith. Mafic rocks contain hydrous and anhydrous eclogitic remnants with the typical assemblage omphacite - garnet - rutile - quartz accompanied by variable and comm only la rge amounts of amphibole (barroisite and taramite), phengite and zoisite/epidote. The eclogitic lithologies sometimes preserved radial cracking of garnet around quartz inclusions, as well as lamellar inclusions of rutile along 3-4 crystallographic directions and polycrystalline quartz - potassium feldspar inclusions.

TABLE 1 | **Chuacús Metamorphic Complex metapelite Wavelength Dispersive X-Ray Spectrometry (WDS) mineral chemistry. Methodology described in Ortega-Gutiérrez et al., 2004**

Oxide	St	St	St	St	Ky	Ky	Grt	Phe
SiO_2	28.02	28.03	28.10	27.95	36.13	36.83	41.17	50.49
TiO_2	0.46	0.43	0.42	0.37	0.00	0.00	0.00	0.12
Al_2O_3	52.31	52.44	52.82	52.83	61.96	62.97	24.15	26.61
Cr_2O_3	0.03	0.05	0.00	0.00	0.05	0.02	0.00	0.00
FeO	14.21	14.13	13.62	13.46	0.84	0.80	22.78	4.48
MnO	0.08	0.00	0.04	0.01	0.02	0.02	0.53	0.02
MgO	1.57	1.57	1.49	1.51	0.00	0.00	9.59	2.96
CaO	0.00	0.01	0.00	0.00	0.00	0.02	1.39	0.01
Na_2O	0.15	0.00	0.00	0.13	0.00	0.00	0.00	0.21
K_2O	0.00	0.00	0.00	0.00	0.00	0.00	0.00	11.63
Total	96.83	96.66	96.49	96.26	99.00	100.66	99.61	96.53
Oxygens	46	46	46	46	5	5	12	11
Cations								
Si	7.88	7.88	7.89	7.86	0.99	0.92	3.08	3.39
Ti	0.10	0.09	0.09	0.08	-	-	-	0.01
Al	17.33	17.37	17.48	17.52	2.00	2.00	2.13	2.10
Cr	0.02	0.03	-	-	0.01	-	-	
Fe	3.34	3.32	3.20	3.17	0.02	0.02	1.43	0.25
Mn	0.02	-	0.01	0.00	-	-	0.03	-
Mg	0.66	0.66	0.62	0.63	-	-	1.07	0.30
Ca	-	0.00	-	-	-	0.00	0.11	-
Na	0.08	-	-	-	-	-	-	0.03
K	-	-	-	-	-	-	-	0.99
Sum	29.42	29.35	29.29	29.26	3.02	2.94	7.85	7.07

St: staurolite; Ky: kyanite; Grt: garnet; Phe: phengite

The polymetamorphic evolution of the Chuacús Metamorphic Complex is evident in the wide variety of reaction (prograde and retrograde) textures that characterize most rocks, particularly the eclogitic units. Prograde coronas include garnet on omphacite (Fig. 3E), or on biotite, plagioclase, chlorite and apatite, as well as occasional rims of clinopyroxene on garnet followed by amphibole - plagioclase symplectites (Fig. 3C) that suggest alternating metamorphic episodes of hydration and dehydration. Retrograde or decompression coronitic textures are characterized by symplectites of amphibole-plagioclase and clinopyroxene - albite on omphacite, subcalcic amphibole and garnet, epidote on garnet, apatite on allanite, biotite on phengite, albite on white mica and garnet, titanite on ilmenite and rutile, epidote on zoisite, green on brown biotite, and chlorite on garnet.

ANALYTICAL METHODS

Geochemistry

Major and trace element analyses were performed at Actlabs (Ancaster, Canada). Major elements were determined by X-ray fluorescence, whereas trace elements were measured by ICP-MS employing lithium metaborate/tetraborate fusions. Sm-Nd isotopic ratios were measured by Thermal Ionization Mass Spectrometry (TIMS) at the Laboratorio Universitario de Geoquímica Isotópica of the Universidad Nacional Autónoma de México (UNAM), using a Finnigan MAT 262 system equipped with eight

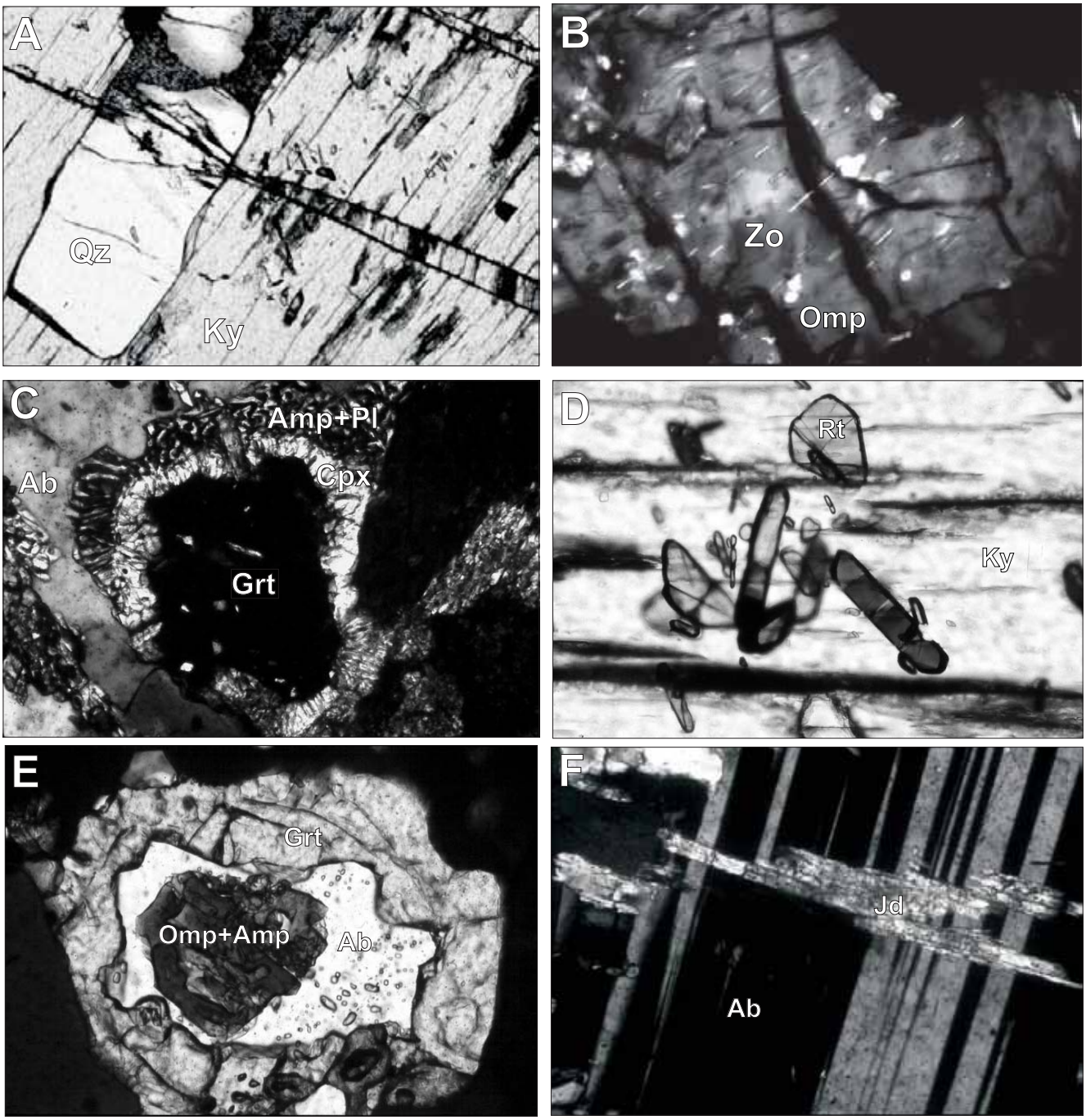

FIGURE 3 | **Some representative photomicrographs of petrographic features described in the text. A) Kink bands nucleated on an elongate quartz inclusion in kyanite. Plane polarized light, field of view is 560µm. B) Lamellar inclusions of rutile (bright needles) in zoisite in a high-pressure calc-silicate. Crossed polarized light, field of view is 220µm. C) Multiple coronas formed by retrogression of mafic eclogites; garnet appears rimmed by clinopyroxene, then by a symplectite of amphibole-plagioclase, and finally by an albite-rich matrix. Crossed polarized light, field of view is 2,240µm. D) Rutile inclusions in kyanite, many crystals show a peculiar "butterfly" shape and may be reddened by exsolution of hematite. Crossed polarized light, field of view is 220µm. E) Composite coronitic texture formed by a central zone of clinopyroxene-amphibole symplectite, rimmed by a wide band of albite followed by a band of garnet with rutile/titanite inclusions; this garnet forms a large inclusion in subcalcic amphibole. Plane polarized light, field of view is 2,240µm. F) Euhedral jadeite (optically determined by extinction angle, birefringence and relief) grown across an albite porphyroblast. Crossed polarized light, field of view is 220µm.**

Faraday cups. Sample preparation and measurement procedures for isotopic analyses have been described by Schaaf et al. (2005). $^{143}Nd/^{144}Nd$ ratios were normalized to $^{146}Nd/^{144}Nd=0.72190$ and corrected to a La Jolla standard value of $^{143}Nd/^{144}Nd=0.511860$. The long term reproducibility of La Jolla standard at Laboratorio Universitario de Geoquímica Isotópica ($^{143}Nd/^{144}Nd$) is 0.511875±22 (2σ, n=152). Geochemical results are reported in Table 2.

Geochronology

The samples selected for geochronology, (3 to 5kg) were crushed and the minerals separated following common techniques such as jaw crushing, milling, Wifley separation, Frantz magnetic separation, and heavy liquids (see also Solari et al., 2007). The zircon concentrates were carefully observed under a binocular microscope. Between 500 and 150 crystals were carefully selected from each sample, in order to obtain all the variations in morphology, shape and color. They were mounted in epoxy resin, ground to expose roughly half of the crystal, and then imaged by cathodolominescence using an ELM 3R luminoscope (Marshall, 1988).

LA-ICPMS U-Pb analyses were performed at Laboratorio de Estudios Isotópicos (LEI), Centro de Geociencias, UNAM, using a Resonetics "Resolution M50" 193nm excimer laser workstation coupled with Thermo Xii Series quadrupole mass spectrometry. Details of the analytical setup employed during this study are described in Solari et al. (2010b). 25s of gas background acquisition was followed by 30s of ablation, carried out in He atmosphere, employing 160mj laser energy, corresponding to an on-target fluence of 8J/cm^2, 34μm diameter spot and a repetition rate of 5Hz, generating a drill rate of ~0.7μm/s. The background average was subtracted from net intensities measured for each isotope. Acquisition involved an alternance of 2 analyses of Plešovice reference zircon (~337Ma, Sláma et al., 2008), NIST 610 standard glasses and 5 unknown zircons, using standard-unknown bracketing method (e.g. Solari et al., 2010b) to allow down-hole fractionation corrections to be performed using an in-house developed software (Tanner and Solari, 2009). NIST 610 glass standard is used to recalculate the concentrations of interest, for instance U and Th, by normalizing such elements with ^{29}Si. Other isotopes are observed during analysis; such as P, Ti, REE; to monitor the presence of inclusions (and in due case discard it) and to produce zircon REE patterns, which can be helpful to interpret the calculated ages. REE zircon patterns were normalized to chondrite values of McDonough and Sun (1995). Recalculated values are available in Table I (Electronic Appendix in www.geologica-acta.com). An estimation of the zircon crystallization temperature is calculated by the Ti content, according to the Ti-in thermometer of Watson et al. (2006). Precision on measured $^{207}Pb/^{206}Pb$, $^{206}Pb/^{238}U$ and $^{208}Pb/^{232}Th$ ratios typically was ~0.7% 1σ relative standard deviation. Replicate analyses of the Plešovice zircon indicate an external reproducibility of 0.8%, 0.7% and 1.6% on the measured $^{207}Pb/^{206}Pb$, $^{206}Pb/^{238}U$ and $^{208}Pb/^{232}Th$ ratios, respectively. These errors are quadratically included in the quoted uncertainties for individual analyses of the analyzed zircons. ^{204}Pb is not monitored during these analyses, because its signal is swamped by the ^{204}Hg contained in the carrier gases. Common Pb correction was thus performed employing the algebraic method of Andersen (2002). A filter was then applied to ensure the quality of selected analyses, consisting in evaluation of the concordance. For grains with ages of <1000Ma, the analysis was considered concordant if the $^{206}Pb/^{238}U$ and $^{207}Pb/^{235}U$ ages differed by less than 10%. For the grains with ages >1000Ma, the same test was carried out considering $^{206}Pb/^{238}U$ and $^{207}Pb/^{206}Pb$ ages. The concordia, probability density distribution and histogram plots, as well as age-error calculations are performed using Isoplot v. 3.70 (Ludwig, 2008). The Tuff-Zirc algorithm (Ludwig and Mundil, 2002) contained in the same software was used to calculate the mean $^{206}Pb/^{238}U$ ages and their errors, as well as to filter for outliers, which are preferred for grains younger than 1000Ma. Details of analyzed zircons, for each samples, are reported in Table II of the Electronic Appendix (www.geologica-acta.com).

RESULTS

Geochemistry

Most of the samples studied here underwent high-grade metamorphism, and therefore geochemical classifications and interpretations must be taken with caution. Nevertheless, comparisons of relatively immobile element concentrations and ratios of the studied rocks with those found in unaltered volcanic rocks can provide insights into the sources and processes that lead to their formation.

In terms of geochemistry and petrography, rocks from the Chuacús Metamorphic Complex can be divided in three different groups: tholeiitic metabasalts (amphibolites), calc-alkaline orthogneisses and pelitic gneisses. Migmatitic gneisses are also present, but they will be described separately for simplicity.

Amphibolites are found as metamorphosed lenses, or deformed dikes in orthogneisses and migmatites (e.g. samples Gt0322, Gt0327, Gt0329, Gt0334 in Table 2). They are fairly homogeneous in terms of their major elements, and show enrichment in Fe_2O_3 and TiO_2 when compared to the rest of the sequences (AFM diagram of Fig. 4A). Even though the MgO contents are not what would be expected

TABLE 2 | **Representative analyses of serpentine from antigorite serpentinites (normslized to 10 O and 8 OH)**

	Chuacús Metamorphic Complex																	
SAMPLE	Gt0303	Gt0309	Gt0314	Gt0319	Gt0320	Gt0321	Gt0322	Gt0327	Gt0329	Gt0333	Gt0334	Gt0341	GT0340	Gt03113	EC01	Gt0360	Gt0394	Gt03117
	Arc orthogneiss	Metasediment	Metasediment	Arc orthogneiss	Arc orthogneiss	Arc orthogneiss	MORB	MORB	MORB	Migmatite Leucosome	Migmatite Melanosome	Rabinal	Rabinal	Rabinal	MORB	Metasediment	MORB	MORB
SiO_2	50,72	74,81	71,91	52,90	46,78	69,43	48,15	47,65	49,60	73,02	46,55	64,35	73,45	75,84	48,44	52,25	48,13	47,56
Al_2O_3	16,05	13,45	13,81	16,24	12,04	14,90	13,78	13,76	13,19	15,34	15,47	15,45	13,05	13,17	13,55	22,65	13,91	14,29
Fe_2O_3	9,84	2,46	2,88	9,50	9,47	2,82	12,82	14,54	10,89	1,13	13,81	4,05	1,87	1,00	13,24	9,30	14,12	12,68
MnO	0,159	0,019	0,023	0,155	0,175	0,060	0,284	0,354	0,237	0,012	0,199	0,067	0,062	0,005	0,263	0,122	0,178	0,129
MgO	6,71	0,29	0,69	4,54	14,10	0,76	6,76	6,84	6,82	0,32	6,33	1,27	0,34	0,03	7,03	2,32	7,09	8,15
CaO	5,80	0,76	1,74	7,60	10,76	1,88	9,61	9,23	10,09	2,08	9,19	3,86	0,83	0,25	10,35	0,34	10,49	10,90
Na_2O	5,34	5,12	5,00	4,24	2,86	4,67	4,05	3,69	3,26	5,38	3,76	5,20	3,45	3,88	3,29	0,77	2,57	2,50
K_2O	1,42	2,19	1,98	1,58	0,62	3,66	1,14	0,66	2,80	1,50	1,24	2,04	4,97	5,51	0,15	5,48	0,29	0,23
TiO_2	1,828	0,280	0,582	1,622	1,231	0,483	2,300	2,594	1,560	0,132	2,507	0,723	0,271	0,026	1,931	1,022	1,470	1,322
P_2O_5	0,63	0,08	0,19	0,43	0,25	0,19	0,26	0,30	0,14	0,04	0,32	0,26	0,07	0,02	0,17	0,18	0,10	0,11
LOI	1,86	0,80	1,51	1,42	1,96	1,01	0,82	0,69	1,71	0,82	0,62	2,74	0,58	0,35	0,65	4,36	1,27	2,23
TOTAL	100,36	100,26	100,32	100,23	100,25	99,87	99,97	100,31	100,30	99,78	100,00	100,01	98,95	100,08	99,07	98,79	99,60	100,11
Sc	20	2	9	21	40	5	41	42	36	2	25	11	3	1	47	26	42	42
Be	2	2	1	2	1	2	2	2	2	1	1	2	5	2	1	5	BDL	BDL
V	134	13	27	200	172	28	381	370	270	13	245	65	18	5	423	104	337	325
Cr	111	BDL	BDL	28	1.020	BDL	213	122	189	BDL	67	BDL	BDL	50	209	79	173	251
Co	33	3	6	30	54	4	40	39	38	2	46	9	2	BDL	44	20	47	48
Ni	91	BDL	BDL	36	326	BDL	85	100	124	BDL	112	BDL	BDL	BDL	103	42	102	113
Cu	15	BDL	BDL	BDL	117	BDL	70	85	64	10	30	53	BDL	BDL	38	BDL	73	183
Zn	107	34	BDL	80	97	42	174	559	134	BDL	133	43	BDL	BDL	95	173	118	118
Ga	18	21	19	18	13	16	19	18	17	16	19	16	16	19	19	33	18	18
Ge	1,8	1,0	0,7	1,3	1,3	1,2	1,4	1,7	1,2	0,5	0,9	1,0	1,5	1,0	1,5	2,6	2,1	2,2
Rb	24	103	39	34	3	66	24	4	61	22	15	66	176	123	2	212	2	5
Sr	628	98	243	508	214	224	76	112	65	774	139	641	124	59	105	128	380	225
Y	36,3	17,1	31,4	28,7	21,8	25,2	49,6	59,9	40,6	1,1	29,5	15,5	27,9	11,7	50,9	76,5	23,5	22,2
Zr	237	210	436	206	126	230	156	160	83	75	158	321	180	85	141	157	80	75
Nb	8,6	6,3	13,7	13,6	12,0	17,8	10,8	8,2	8,8	4,6	14,3	14,5	28,1	6,4	3,2	26,9	7,3	5,6
Cs	0,3	0,2	0,2	0,7	-0,1	0,5	0,2	-0,1	0,6	-0,1	0,2	0,7	1,2	BDL	BDL	2,4	BDL	BDL
Ba	548	379	745	363	29	750	189	25	696	1.030	270	623	600	457	57	795	10	38
La	31,3	40,3	95,2	31,5	14,5	44,6	6,51	7,15	2,97	4,63	18,0	119	48,2	8,69	8,71	125	5,80	5,64
Ce	64,3	65,3	175	58,3	30,4	77,9	17,7	20,3	8,60	9,07	36,6	198	86,3	14,8	17,6	234	15,1	14,2
Pr	8,51	7,40	21,2	7,00	3,93	8,69	2,96	3,47	1,47	1,10	4,71	21,6	8,85	2,15	3,38	29,0	2,27	2,12
Nd	35,1	26,6	77,9	26,4	16,3	30,4	15,2	18,9	7,88	4,17	19,9	72,2	29,4	8,18	18,4	108	11,4	10,7
Sm	8,02	5,59	15,0	5,55	3,91	5,45	5,34	6,75	3,10	0,71	4,81	10,6	5,16	1,70	5,62	20,6	3,67	3,38
Eu	2,60	1,40	3,39	1,75	1,33	1,35	1,92	2,39	1,03	0,239	1,50	2,11	0,819	0,277	1,83	3,34	1,36	1,28
Gd	7,38	4,74	11,2	5,25	3,78	4,62	7,12	8,80	4,48	0,43	4,87	7,09	3,79	1,61	7,43	17,2	4,32	3,99
Tb	1,09	0,68	1,44	0,81	0,62	0,69	1,25	1,58	0,90	0,04	0,78	0,74	0,76	0,29	1,40	2,77	0,82	0,78
Dy	6,48	3,85	7,57	4,88	3,74	4,31	8,53	10,8	6,52	0,21	5,22	3,60	4,56	1,72	8,99	14,9	4,68	4,34
Ho	1,33	0,73	1,33	1,03	0,78	0,87	1,79	2,24	1,46	0,04	1,03	0,57	0,92	0,37	1,93	2,90	0,92	0,87
Er	3,52	1,81	3,11	2,80	2,08	2,51	5,20	6,43	4,26	0,10	2,92	1,37	2,94	1,22	5,94	9,07	2,76	2,58
Tm	0,532	0,245	0,404	0,428	0,305	0,414	0,847	1,02	0,708	0,014	0,448	0,159	0,549	0,196	0,884	1,35	0,388	0,372
Yb	3,46	1,48	2,32	2,72	1,96	2,72	5,28	6,38	4,38	0,11	2,67	1,10	3,40	1,34	5,53	8,02	2,38	2,27
Lu	0,513	0,210	0,310	0,410	0,288	0,432	0,785	0,951	0,676	0,022	0,389	0,173	0,533	0,223	0,811	1,21	0,358	0,329
Hf	5,5	6,6	11,8	4,7	2,8	5,9	4,6	5,0	2,8	2,5	4,3	8,3	5,5	3,4	4,1	4,6	2,4	2,5
Ta	0,56	0,10	0,48	0,83	0,48	0,96	0,26	0,25	0,28	BDL	0,90	0,40	2,99	0,63	0,12	1,25	0,25	0,21
W	0,8	BDL	BDL	BDL	BDL	BDL	0,6	0,6	BDL	BDL	0,9	BDL	0,6	0,8	BDL	BDL	BDL	BDL
Tl	0,14	0,47	0,18	0,21	BDL	0,29	0,13	0,08	0,26	0,09	0,06	0,28	0,87	1,04	0,07	2,12	BDL	0,10
Pb	9	BDL	BDL	BDL	BDL	8	BDL	BDL	BDL	10	BDL	12	13	7	BDL	8	BDL	BDL
Bi	BDL	BDL	BDL	BDL	BDL	BDL	BDL	BDL	BDL	-0,1	BDL	BDL	BDL	3,0	0,5	BDL	BDL	BDL
Th	3,08	2,81	2,56	3,05	1,31	6,15	0,38	0,39	0,20	0,34	1,08	23,1	20,8	4,91	0,26	29,0	0,43	0,42
U	0,73	1,35	0,67	0,69	0,38	1,35	0,31	0,44	0,21	0,15	0,25	2,56	4,68	2,64	0,10	3,52	0,12	0,12
$^{147}Sm/^{144}Nd$	0,125	0,115	0,103	0,115	0,132	0,107	0,196	0,202	0,221	0,092	0,139	0,062	0,104	-	-	-	-	-
$^{143}Nd/^{144}Nd$	0.512519 (19)	0.512033 (19)	0.511985 (18)	0.512603 (16)	0.512708 (20)	0.512406 (20)	0.513093 (16)	0.513055 (19)	0.512779 (19)	0.512206 (18)	0.512626 (19)	0.512166 (12)	0.512245 (18)	-	-	-	-	-
eNd	-2,32	-11,80	-12,74	-0,68	1,37	-4,53	8,88	8,13	2,75	-8,43	-0,23	-9,21	-7,67	-	-	-	-	-

Major elements expressed as wt%. Trace elements expressed as ppm

-: not determined

BLD: below than detection limits

*: last two digits in parentheses in the 143Nd/144Nd ratios refer to the 2 sigma absolute error

DOI: 10.1344/105.000001695

for pristine mantle-derived melts (Langmuir and Hanson, 1980), they have compositions that are typical of slightly differentiated tholeiitic basalts. Despite major element homogeneity, the REE patterns of these rocks are variable. Three samples have the typically depleted LREE and flat HREE pattern of normal mid-ocean ridge basalts (N-MORB) and display small negative Eu anomalies, whereas two samples have relatively flat LREE and depleted HREE without Eu anomalies (Fig. 5A). Extended incompatible trace element patterns are also similar to MORB, although fluid mobile elements (Cs, Rb, Ba, U) have been likely perturbed by weathering since they resemble the enrichments that are often observed in altered-oceanic crust (Staudigel et al., 1996; Fig 5A). In

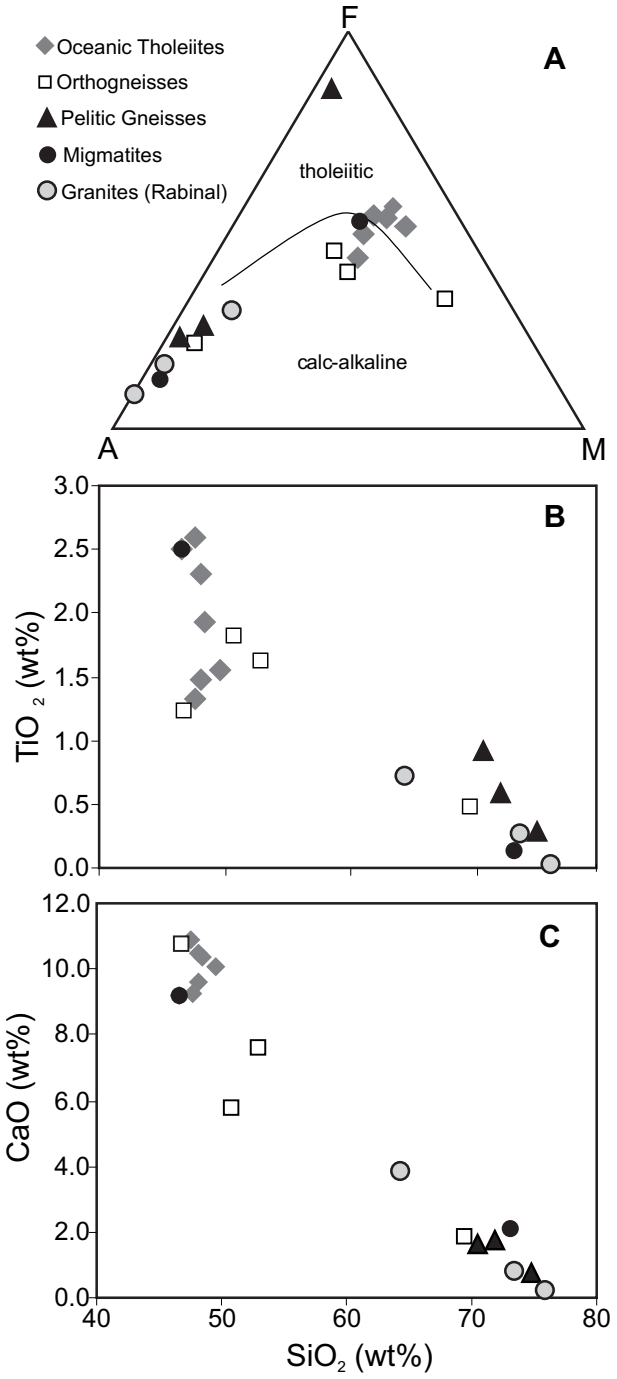

FIGURE 4 | **Major element compositions of rock suites from Chuacús Complex. A) AFM diagram after Irvine and Baragar (1971). B) TiO_2 vs SiO_2. C) CaO vs SiO_2.**

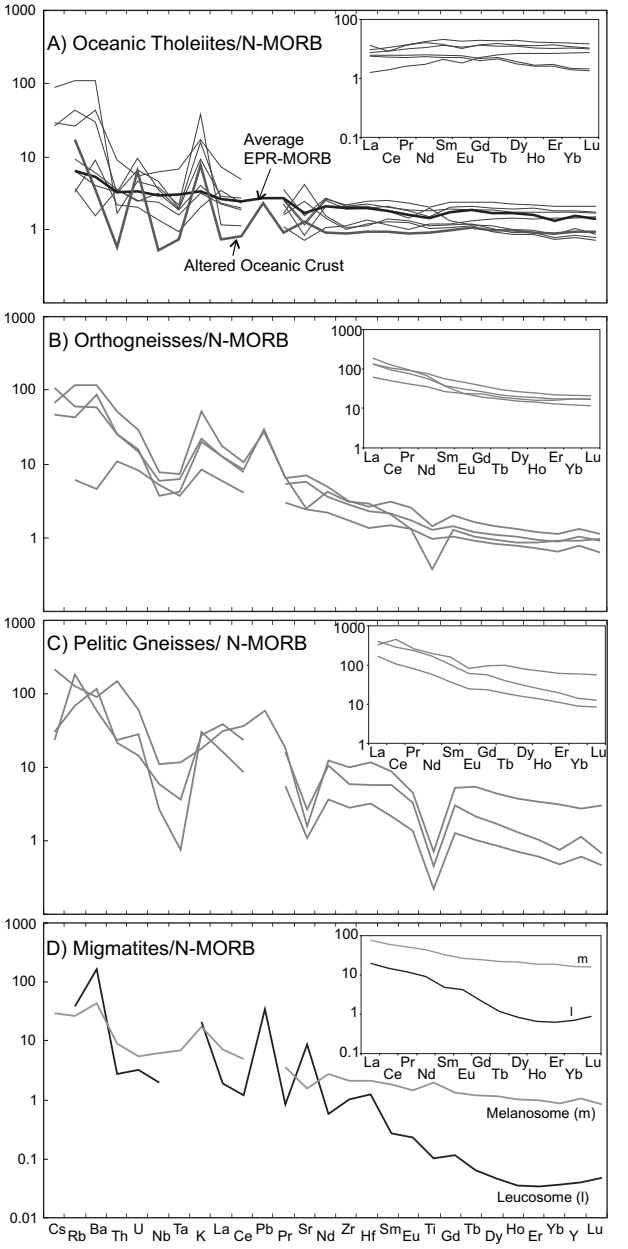

FIGURE 5 | **Trace element geochemical composition of rock suites from Chuacús Complex, normalized to the N-MORB values of Sun and McDonough (1989). REE elements normalized to the chondrite values of McDonough and Sun (1995). Also shown for comparison is the composition of an average EPR-MORB (Lehnert et al., 2000), and of a typically altered oceanic crust (Staudigel et al., 1996).**

fluid immobile elemental ratios (Th/Nd, La/Nd, Sr/Nd, Nd/Yb), these rocks display end-member compositions with values that overlap a typical Pacific MORB. Nonetheless, Nb/Ta ratios (up to 40) are much higher than in MORB, probably suggesting that an element like Ta did not remain completely immobile during high-grade metamorphism.

Orthogneisses (e.g., samples Gt0303, Gt0319, Gt0320, Gt0321 in Table 2) have variable compositions that range from gabbroic to granitic and display a systematic decrease in MgO, F_2O_3, and TiO_2 with increasing SiO_2, Na_2O and K_2O, characteristics that are typical of calc-alkaline magmas worldwide (Fig. 4A). Chondrite-normalized REE patterns show enrichment in LREE and slightly depleted HREE that are in contrast to what is observed in the tholeiitic amphibolites (Fig. 5B). A small negative Eu anomaly is only observed in a relatively evolved granite. Extended N-MORB normalized trace element patterns also display features that are typical of arc magmas, such as Large Ion Lithophile Elements (LILE) enrichment relative to the High Field Strength Elements (HFSE). It is possible that fluid mobile elements like Cs, Rb, and Ba were perturbed by weathering and/or metamorphism; but high LILE/High Field Strength Elements ratios are also coupled with relative enrichment in Th (i.e. high Th/Nb ratios), which are considered as fluid immobile. This suggests that the "arc-like" geochemical signatures of these magmas were likely acquired by crustal inputs, either in the form of subducted sediments or by crustal contamination during ascent. Yet the Th/Nb ratios of the least evolved calc-alkaline orthogneisses are higher than those of similarly evolved tholeiitic metabasalts, strongly suggesting a primary origin in a magmatic arc environment.

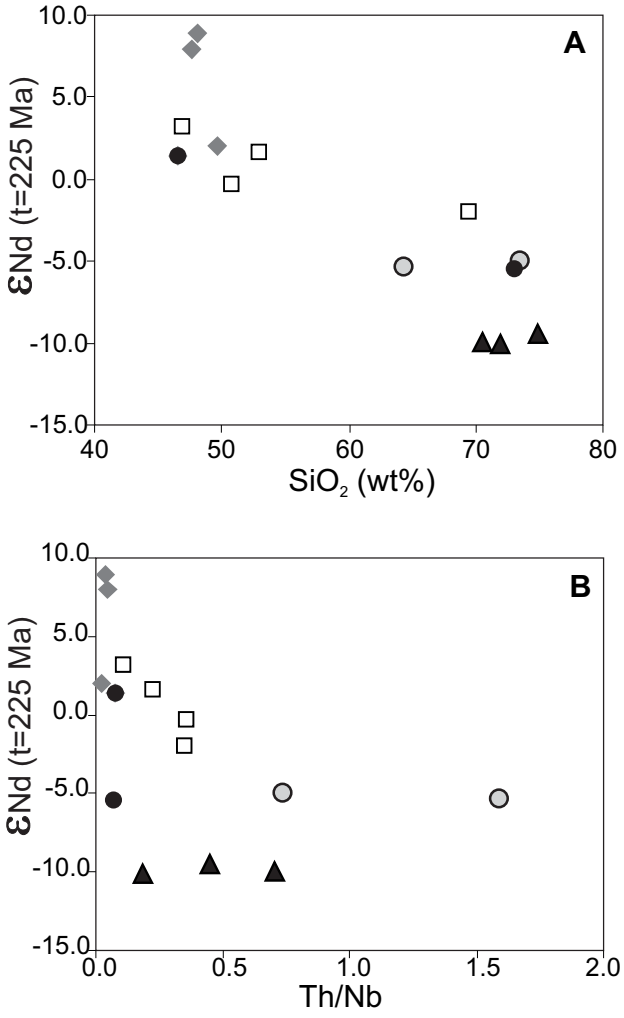

FIGURE 6 | **Initial Nd isotopic compositions calculated to 225Ma for the Chuacús Metamorphic Complex correlate inversely with A) SiO_2 contents and B) Th/Nb ratios.**

Pelitic gneisses are silica and potassium-rich and have overall chemical characteristics that are typical of hemipelagic sedimentation (e.g. samples Gt0309, Gt0314, Gt0360 in Table 2). They are LREE enriched, with either flat or depleted HREE, and usually display negative Eu anomalies. Incompatible trace element patterns also display mature upper crustal features, with highly enriched LILE/High Field Strength Elements ratios that are coupled with negative Sr and TiO_2 anomalies (Fig. 5C). Interestingly, Nb/Ta ratios are also unusually high for upper crustal lithologies (up to ~60), probably indicating a preferential mobilization of Ta during metamorphism.

Distinct magmatic phases from El Chol migmatites have different compositions. A sample taken from the melanosome (Gt0334, Table 2) has the chemical character of an enriched oceanic basalt, with relatively high Nb-Ta contents and fractionated REE patterns. In contrast, the leucosome (Gt0333) is silica-rich and trondhjemitic (K_2O/Na_2O=0.3). The incompatible trace element pattern of the leucosome displays strong positive anomalies in LILE, K_2O, Pb and Sr that are not accompanied by equivalent enrichments in elements like Th and U. Y and the HREE are strongly depleted when compared to the LREE, but the trondhjemitic leucosome also displays a distinctive concave upward pattern in which elements like Ho and Er have the lowest relative concentrations (Fig. 5D). Also noteworthy is that Zr and Hf are enriched when compared to their nearest neighbors, and form a distinctive positive anomaly. These chemical characteristic are indicative of melting under garnet amphibolite facies conditions (Foley et al., 2002).

Nd isotopic compositions were recalculated to 225Ma in accordance to the most important magmatic and recrystallization event recorded by U-Th/Pb geochronology (see below). All amphibolites have positive εNd (up to ~10) values that are close to those of the calculated depleted upper mantle for that age. In contrast, orthogneisses are less radiogenic (εNd=3.23 to -1.95), with isotopic values that correlate negatively

with SiO_2 and Th/Nb ratios (Fig. 6A, B). As it is commonly observed in ancient upper crustal lithologies, pelitic gneisses have very negative εNd (εNd=-10), with values that are even less radiogenic than the Ordovician Rabinal Granite. Interestingly, the melanosome at El Chol has a positive εNd whereas the trondhjemitic leucosome displays a very negative value, indicating that both components are genetically unrelated and that additional crustal lithologies underwent partial melting.

Geochronology

Gt 0315

Sample Gt0315 is a pegmatite which intrudes a gabbroic boudin neck in the locality of Quebrada Honda. Zircons separated from this pegmatite are colorless to pale pink, quite large (up to 280μm in length) and range in shape from large prismatic to stubby. Under cathodoluminescence they are mostly unzoned and characterized by low luminescence, although some show a faint sector-zoned to patchy-zoned cores, sometimes surrounded by moderately luminescent, faintly oscillatory-zoned rims (examples in Fig. 7). A total of 30 analyses were performed on 30 zircons belonging to this sample. The cores have an average age of 982±12Ma (Fig. 8A), as well as high Th/U ratios and typical REE anomalies indicative of igneous origin (e.g., Rubatto, 2002 and Fig. 9A). The overgrowths, as well as those zircons which show a uniform cathodoluminescence, have very low Th/U ratios of less than 0.01, and show LREE depletion compared to HREE (Fig. 9B). The mean $^{206}Pb/^{238}U$ age of 74+3/-1Ma obtained on such overgrowths

FIGURE 7 | **Cathodoluminescence image of some representative zircons analyzed in this work. The circles represent the 34µm LA-ICPMS analyzed spot.**

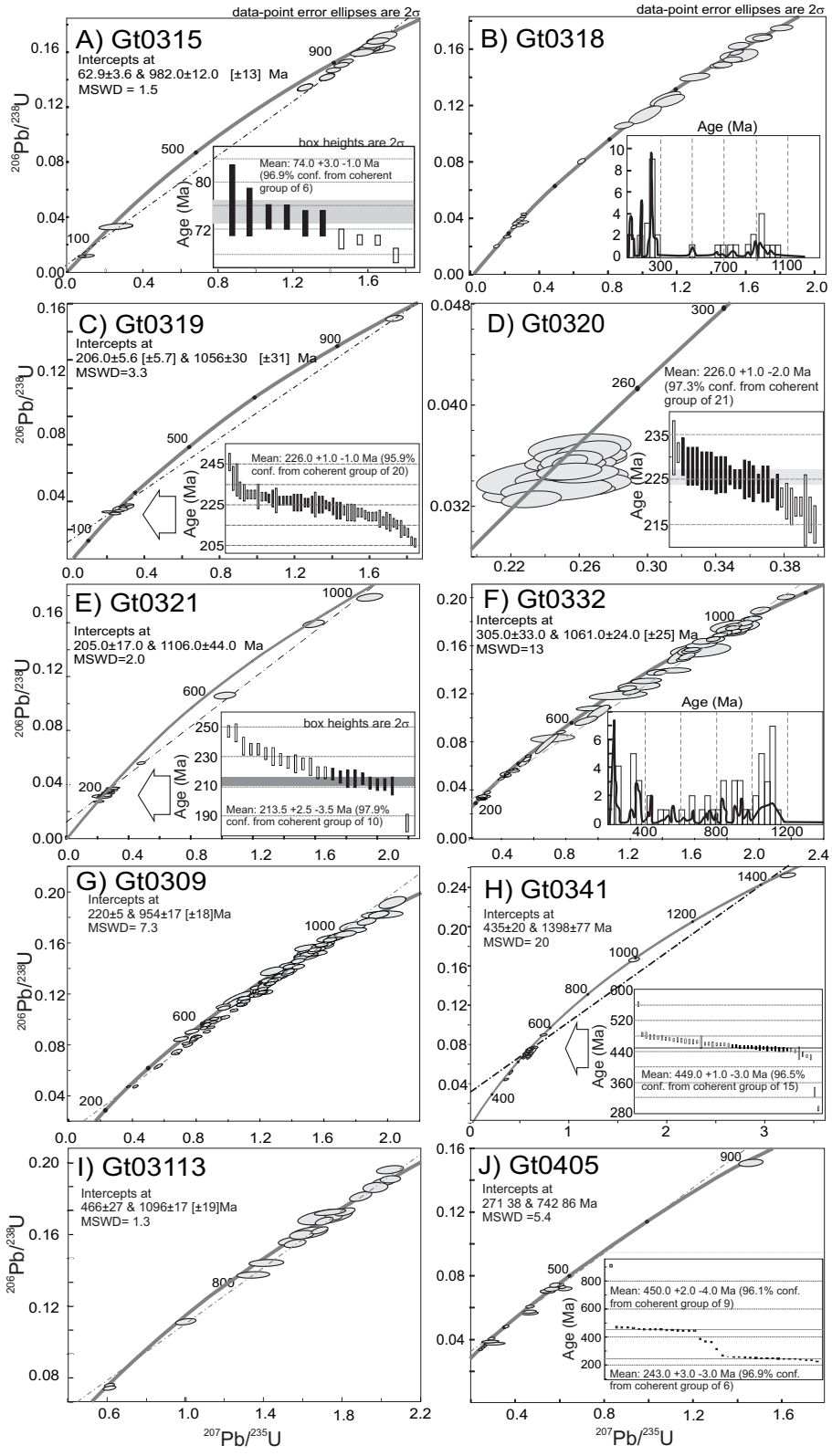

FIGURE 8 | **U-Pb concordia diagrams of the samples dated by LA-ICPMS. Concordia, ages and errors are calculated using Isoplot 3.7 (Ludwig, 2008). The mean $^{206}Pb/^{238}U$ ages in the insets, 2-sigma errors and outlier filtering are calculated with the *TuffZirc* algorithm of Ludwig and Mundil (2002). For those samples containing abundant detrital zircons, i.e. A, C, G, and I, the inset diagrams are combined histograms and probability density plots. Preferred ages are common-Pb corrected using the algebraic method of Andersen (2002). $^{206}Pb/^{238}U$ ages are used if <1000Ma, whereas $^{207}Pb/^{206}Pb$ are used if >1000Ma. See text for further explanations.**

is interpreted as indicating the recrystallization under high-grade metamorphic conditions (concordia of Fig. 8A).

Gt 0318

This sample is a high-grade metasedimentary rock cropping out in Los Altos, northeast of Pachalum (Fig. 2). It is made up of garnet, relic omphacite, white mica, hornblende and interstitial plagioclase. Rutile is present as an accessory mineral, often surrounded by titanite rims. We performed 45 U-Pb analyses on 45 zircons separated from this sample, 9 of which were discarded due to their large discordance. Zircons are in general elongated to ovoidal in shape, with polished terminations typical of sedimentary transport. Under cathodoluminescence they show complex zoning, with presence of inherited cores surrounded by variably luminescent overgrowths (examples in Fig. 7). The dated zircons yield a main cluster at 245Ma followed by other minor ones at 182, 895, 930, and concordant zircons at 125, 505, and several others between 606 and 1007Ma (concordia of Fig. 8B). Although the main provenance is thus Triassic, the few Jurassic to Cretaceous zircons indicate a young episode of sedimentation in the southern Sierra de Chuacús, postdated by high-grade metamorphism.

Gt 0319

This is a foliated gabbro cropping out in Los Limones locality, principally composed of clinopyroxene, garnet, plagioclase, minor biotite, titanite and opaque minerals. We dated 60 crystals by LA-ICPMS, 6 of which were discarded because their discordance was more than 10%. Under cathodoluminescence, the imaged zircons show a predominance of oscillatory (i.e., igneous) growth, with only minor bright overgrowths developed on some of the crystals (Fig. 7). Both oscillatory-zoned cores, as well as overgrowths, show an almost indistinguishable age pattern with a mean $^{206}Pb/^{238}U$ age of 226±1Ma. This age is interpreted as indicating the crystallization of the gabbroic protolith (concordia of Fig. 8C).

Gt 0320

Gt 0320 is an intermediate igneous rock composed of plagioclase, clinopyroxene, hornblende, opaque minerals, biotite, titanite, cropping out nearby sample Gt 0319. Cathodoluminscence shows the ubiquitous presence of oscillatory zoning, with eventual thin, high-luminescent rims developed around cores (Fig. 7). We dated 41 crystals belonging to this sample. Five analyses were omitted because of having >10% discordance. There is no inheritance in any of the dated crystals and therefore the mean $^{206}Pb/^{238}U$ age of 226+1/-2Ma is interpreted as an indication the crystallization of this sample (Fig. 8D).

Gt 0321

This is a granodioritic orthogneiss, intensely foliated, cropping out in the Barranca Agua Caliente. Leucocratic bands, such as the one dated, contain mafic pods up to 30cm in size, which were recognized as retrogressed eclogites (cf. Ortega-Gutiérrez et al., 2004). Zircons separated from this sample are up to 350μm in size and pale yellow to dark red in color. Under cathodoluminescence, they show a frequent presence of oscillatory-zoned cores, surrounded by variably developed zones of oscillatory overgrowths. Of the 50 analyses which were performed on 50 zircons belonging to this sample, 17 were discarded because they were highly (17-42%) discordant, probably as a consequence of partial Pb loss. The other analyses yield a poorly defined Grenvillian upper intercept (1106±44Ma) and a cluster of concordant to slightly discordant analyses corresponding to the lower intercept (Fig. 8E). Such analyses, showing an igneous Th/U ratio well above 0.05, yield a $^{206}Pb/^{238}U$ weighed mean age of 213.5+2.5/-3.5Ma, which is regarded as the best approximation of the crystallization age of this granodiorite.

Gt 0332

This sample belongs to a leucosome migmatitic orthogneiss of El Chol (Fig. 2). The poly-deformed leucocratic bands are interlayered, and some still preserve relict eclogitic assemblages. Previous U-Pb TIMS dating of zircons belonging to this sample yielded discordant results, with a lower intercept of 302±52Ma and an upper intercept of 1024±78Ma (Ortega-Gutiérrez et al., 2004). The lower intercept was interpreted as the age of migmatization.

The zircons selected for LA-ICPMS are of variable size, between 80 and 350μm. They are stubby to multifaceted and prismatic, and show a light pink to red color. Under cathodoluminescence they generally present one or two episodes of variably luminescent overgrowths, developed around more or less preserved relict cores. The cores often show oscillatory zoning (Fig. 7). U-Pb dating stresses the extreme complexity of such samples, and the record of several distinct events. The inherited cores are generally concordant, and broadly Grenvillian in age, ranging between ~900 to ~1100Ma (Fig. 8F). Their Th/U ratios (>>0.01) as well as the REE pattern, with marked positive Ce and negative Eu anomalies, strongly confirm the igneous nature of the protolith (Fig. 9C and Table I (electronic appendix in www.geologica-acta.com), (e.g. Hoskin and Schaltegger, 2003). The data obtained on the overgrowth analyses indicate the presence of at least two different events. A first recrystallization event occurred during the Mississippian (324-348Ma). The second overgrowth developed during the Triassic - Latest Permian

(218-253Ma), generating thin oscillatory bands under CL (Fig. 7). In all the overgrowth episodes the corresponding Th/U ratios are lower than igneous cores, and their REE patterns indicate an overall depletion in LREE (La to Eu) with respect to HREE (Gd to Lu), indicating the possible interaction with high-grade metamorphic fluids (Fig. 9D).

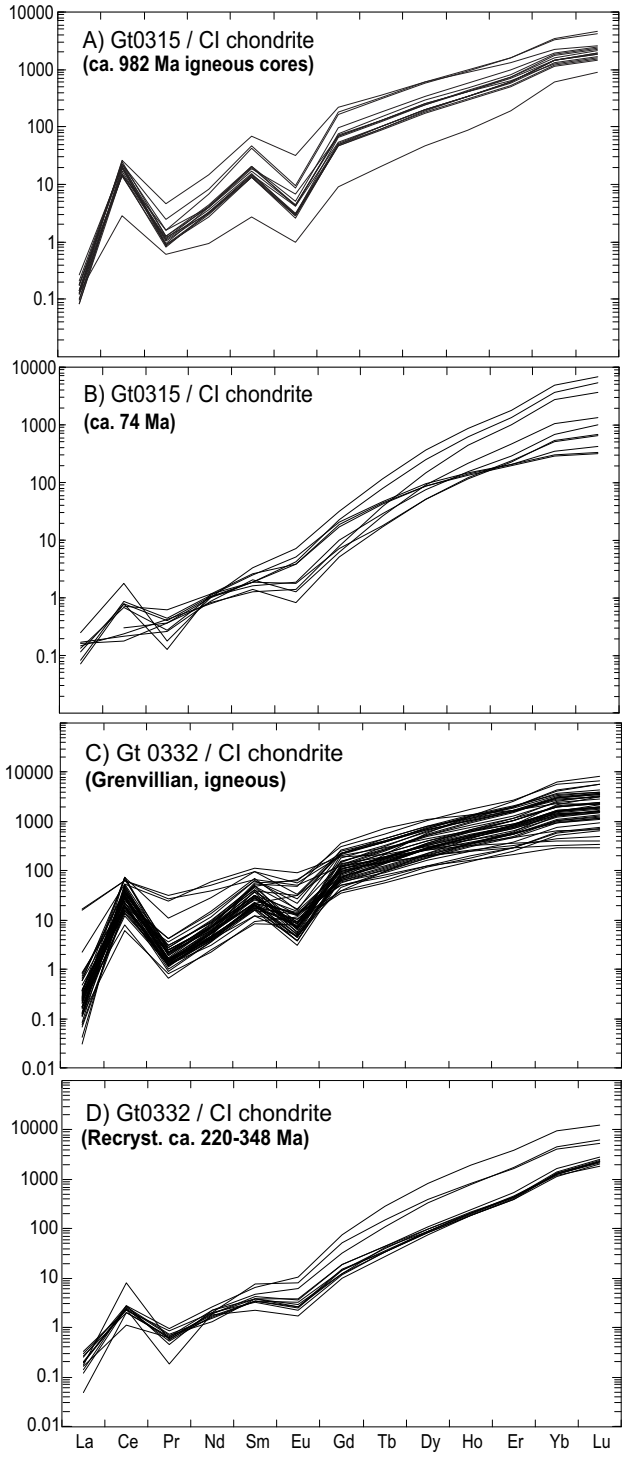

FIGURE 9 | **ircon REE elements patterns normalized to the chondrite values of McDonough and Sun (1995), obtained by LA-ICPMS on the same spot analyzed for U-Pb geochronology. A) ~982Ma igneous cores, pegmatite sample Gt0315; B) ~74Ma metamorphic zircons, pegmatite sample Gt0315; C) Grenvillian igneous zircons, sample Gt0332; D) 220-348Ma recrystallized metamorphic rims, sample Gt0332.**

Gt 0309

This sample is a pelitic metasedimentary rock made up of garnet, kyanite, phengite, quartz, biotite, plagioclase and abundant rutile. It crops out in the southern Sierra de Chuacús (Fig. 2), north of the unpaved road which connects Pachalúm with Caquíl. Separated zircons range between 40 and 320μm in size. They show different colors, varying between dark to pale red, and colorless to amber. They also show a different degree of roundness. One hundred crystals were analyzed, one analysis each, and 6 of them were discarded due to >10% discordance. Of the remaining grains, several yield Proterozoic frequency maximums at 915, 941, 961, and 1106Ma (Fig. 8G). Some younger grains are also concordant (e.g. between ~690 to ~702Ma), however the vast majority are slightly discordant. The lower intercept of such discordant grains is 220±5Ma. We interpret this lower intercept as indicative of the thermal event responsible for metamorphism and deformation of the sedimentary protholith, as well as for Pb loss in the variably discordant zircons.

Gt 0341

This orthogneiss crops out along the paved road which connects El Rancho with Cobán, near the turn off to Salamá (Fig. 2). It is made up of quartz, plagioclase, k-feldspar augens mantled by biotite and minor white mica. Pyrite is quite abundant as an opaque mineral. The concentrated zircons are colorless to pale colored, with yellow to orange tonalities. A total of 50 analyses were performed on 50 crystals and only one was discarded because of having >10% discordance. The remaining crystals define a principal cluster around 440Ma (concordia of Fig. 8H), with a weighted $^{206}Pb/^{238}U$ mean of 449+1/-3Ma, which is interpreted as the crystallization age of this sample (Fig. 8H inset). Few zircons are inherited from the source, and only two yield younger discordant ages, probably as a result of Pb loss.

Gt 03113

Sample Gt03113 is a granitic dike that cuts across high-grade metamorphic rocks (garnet+amphibole) in the northern Chuacús Complex (Fig. 2). Few zircons were concentrated from this sample. They are dark red, short prismatic, and in general show abundant cracks and inclusions. Only 30 analyses were performed on 30 selected crystals, 3 of which were discarded because of >10% discordance. The remaining analyses define a

well constrained upper intercept at 1096±17Ma, several variably discordant grains younger than 1100Ma and also a well constrained lower intercept at 466±27Ma, underlined by two analyses of crystal rims (Fig. 8I). Two interpretations are possible: either the upper intercept defines the crystallization age of the pegmatite, and the lower is coincident with a tectonothermal disturbance, or the upper intercept represents the inheritance from the protolith, and the lower intercept is the true crystallization age. Several features suggest that the last interpretation is correct: 1) all the analyzed grains have a high Th/U ratio, indicative of igneous crystallization; 2) the pegmatite is undeformed and does not show any metamorphism; and 3) its outcrop is in close vicinity with sample Gt0341, which has a similar age, and with the Rabinal granite suite, which also yielded Ordovician crystallization ages (e.g. Ortega-Obregón et al., 2008).

Gt 0405

This is a migmatitic gneiss which crops out in the southern Sierra de Las Minas, which has been considered as the eastern continuation of the Chuacús Metamorphic Complex. It is exposed along the Pasabien River, 5km northwest of Río Hondo. The gneiss is made up of up to 20cm thick leucocratic bands (quartz - plagioclase feldspar - biotite ± muscovite) alternated with garnet - amphibole - biotite pla gioclase horizons. Abundant zircons were separated from this sample. They range from 40 to 350μm in size, and are colorless to intensely red-amber colored. A total of 55 LA-ICPMS analyses were performed on 55 selected grains, 14 of which were rejected because of more than 10% discordance (Table I, electronic appendix in www.geologica-acta.com). The remaining analyses define a bimodal distribution in the concordia diagram of Fig. 8L, with two principal peaks at 450+2/-4Ma and 243±3Ma. Whereas the older age group corresponding to igneous cores (see cathodoluminescence images of Fig. 7) is readily interpreted as indicating an Ordovician magmatic event, the younger age group is more complex, being characterized by a series of 17 analyses straddling concordia between 255 and 220Ma. Moreover, those analyses are probably a mix of different zircons: igneous zircons characterized by Th/U ratios >0.1 and a mean $^{206}Pb/^{238}U$ age of 249.5±2Ma and dark red, high-U, metamict zircons with a Th/U ratio <0.02 and $^{206}Pb/^{238}U$ ages comprised between 243 and 220Ma. These last ages reflect a high-grade event maybe coincident with migmatization, which is responsible for the variable Pb loss in some of the analyzed zircons.

DISCUSSION

The new data presented in this paper on the Chuacús Metamorphic Complex allow a better definition of the tectonothermal events that affected it, as well as its possible paleogeographic settings. Three main events are discussed: 1) Ordovician magmatism, 2) Triassic magmatism and metamorphism and its tectonic implications, and 3) Late Cretaceous magmatism and metamorphism. The autochthonous vs. allochthonous nature of the Chuacús Metamorphic Complex with respect to the Maya Block will be discussed at the end of this chapter.

Ordovician magmatism

Although Grenvillian and other Mesoproterozoic inherited ages are present in most rocks, they are in general overprinted, or reworked by Ordovician magmatism at the southern edge of the Maya Block, as previously reported for the Rabinal-Salamá area of central Guatemala by Ortega-Obregón et al. (2008) who dated S-type granites between 455-462Ma. Ordovician bodies are also present nearby the Chiapas Massif of SE México, where Pompa-Mera et al. (2008) dated an S-type granite at 482±3Ma and an amphibolite at 456±14Ma (U-Pb, single-grain zircons), as well as in the Altos Cuchumatanes, where Solari et al. (2010a) reported an undeformed granite whose crystallization age was dated at 461+6/-3Ma. In Belize the magmatism is mainly Silurian, dated at ~410Ma (Martens et al., 2010). In the northern Sierra de Chuacús Ordovician magmatism is represented by orthogneisses and pegmatitic dikes (samples Gt0341 and Gt03113, respectively), which intrude greenschist facies metasediments belonging either to the San Gabriel unit or the Chuacús Metamorphic Complex (cf. Solari et al., 2009). Bimodal magmatism is widespread in the Acatlán Complex of southern México and associated to rifting of the Rheic Ocean (e.g. Miller et al., 2007; Ortega-Obregón et al., 2009). In northwestern México the Río Fuerte Formation (Late Ordovician) contains magmatic zircons of both Ordovician and Cambrian age (Vega-Granillo et al., 2008). Ordovician magmatism has been documented as well all around the Rheic Ocean realm, generally represented by continental, within-plate tholeiites and as felsic magmas originated by crustal melting of Neoproterozoic and Mesoproterozoic basement (Murphy et al., 2009, 2010, and references therein). Thus, the presence of some Ordovician rocks in the northernmost Chuacús Metamorphic Complex (sample Gt0341), as well as in the nearby Sierra de Las Minas (sample Gt0405) cannot be used as conclusive evidence to establish its autochthony relative to the Maya Block *sensu strictu* (cf. Ortega-Gutiérrez et al., 2007; Ortega-Obregón et al., 2008).

Upper Triassic magmatism and metamorphism

Ordovician magmatism was not recognized in the higher grade central and southern Sierra de Chuacús, where the main magmatic event is Upper Triassic (218-

226Ma, samples Gt0319, Gt0320, Gt0321) and has an arc-like geochemical signature. This magmatic event is also coincident with the tectonothermal event responsible for migmatization in El Chol (sample Gt0332) and Sierra de Las Minas (sample Gt0405). Because remnants of eclogite-facies mafic rocks are present within these deformed migmatites, and are also recognized as deformed lenses nearby the felsic orthogneisses (sample Gt0321, 218Ma) of Agua Caliente River (cf. Ortega-Gutiérrez et al., 2004), we interpret such Upper Triassic ages to be younger than the eclogite-facies metamorphism of the Chuacús Metamorphic Complex. It is interesting to note that none of the S-type Ordovician granites cropping out north of the Sierra de Chuacús (Rabinal-Salamá area), along the Baja Verapaz shear zone of Ortega-Obregón et al. (2008) contain xenoliths of eclogite-facies mafic rocks. This suggests that the eclogite facies metamorphism is constrained between the age of emplacement of the Ordovician granites and the Triassic arc magmas.

Late Cretaceous magmatism and metamorphism

Late Cretaceous metamorphic overprint is present in many of the Chuacús Metamorphic Complex rocks (e.g., Ortega-Gutiérrez et al., 2004, and references therein; Martens et al., 2007; Raschbacher et al., 2009). Some pegmatites were also generated by high-grade metamorphism during the Late Cretaceous, and sample Gt0315 is a clear example of this. Late Cretaceous metamorphism was also reported in the San Gabriel unit (Ortega-Obregón et al., 2008), along the Baja Verapaz Shear Zone, during overthrusting of the Chuacús Metamorphic Complex on top of the southern Maya Block edge. High-pressure metamorphism is also evidenced in several Ar-Ar ages calculated in phengites belonging to the Motagua mélange, which yielded 77-65Ma (Harlow et al., 2004) and were interpreted as the result of the Late Cretaceous collision of the Nicaragua Rise with the southern edge of the Maya Block. Tectonic convergence between the northern Caribbean and the southern North American plates caused subduction of the Chuacús Metamorphic Complex and HP-HT conditions followed by its exhumation, as well as by the northward obduction of El Tambor ophiolites and closure of the Proto-Caribbean Ocean along the paleo Motagua Suture Zone (e.g. Brueckner et al., 2009; see also García-Casco et al., 2008 for correlation with the Antilles).

Allochthony vs. autochthony of the Chuacús Metamorphic Complex with respect to the Maya Block

The Chuacús Metamorphic Complex constitutes the highest-grade metamorphic complex of all Central America. Major faults bound the complex to the north (Baja Verapaz) and south (Motagua fault system), and no similar rocks occur beyond those faults. Although the Chuacús Metamorphic Complex occurs next to typical Maya cover and basement units of pre-Jurassic age, its youngest cover is of Neogene age, and thus, in principle, it should be considered a suspect tectonostratigraphic unit presently located between the Maya and Chortís blocks. At least three points must be considered to further evaluate the allochthonous versus autochthonous nature of the Chuacús Metamorphic Complex with respect to the Maya Block.

The Maya Block north of the Baja Verapaz Shear Zone and, furthermore, north of the Polochic fault, does not record many of the tectonothermal events that have been recognized in the Chuacús Metamorphic Complex. These include HP metamorphism (e.g. Ortega-Gutiérrez et al., 2004; Ratschbacher et al., 2009, and this paper), Triassic magmatism and deformation/migmatization (Ratschbacher et al., 2009, and this paper), and widespread presence of Late Cretaceous, amphibolite facies reworking and magmatism (McBirney, 1963; Ortega-Gutiérrez et al., 2004; Martens et al., 2007; Martens, 2009; Ratschbacher et al., 2009, and this paper).

No other basement outcrop within the Maya Block (Guichicovi, Chiapas Massif, Maya Mountains) shares geological similarities with the Chuacús Metamorphic Complex. For instance the Guichicovi Complex is composed of Grenvillian (1000-1300Ma, Weber and Kohler, 1999) granulites, only affected by Permian intrusions; whereas the Chiapas Massif is made up of high temperature gneisses, intruded by Late Permian granites metamorphosed at 250-254Ma (Weber et al., 2005), and later covered by Jurassic red beds (Blair, 1988). The Maya Mountains are constituted by Silurian plutons, Devonian (and older) strata, covered by Early Devonian volcanics and sedimentary rocks of late Paleozoic age (Martens et al., 2010). None of the aforementioned units contain high pressure rocks. Furthermore the Chuacús Metamorphic Complex is characterized by the absence of Devonian and Permian ages, as well as by the absence of any sedimentary cover older than the Cenozoic.

The voluminous Late Permian granitic magmatism, recently dated by Schaaf et al. (2002) and Weber et al. (2005) in the Chiapas Massif, as well as by Solari et al. (2010a) in the Altos Cuchumatanes, is not represented by detrital zircon ages in any of the more than 500 zircons dated in this work. Furthermore, volcanic units in the Jurassic Todos Santos Formation, cropping out in Chiapas state, and farther to west, in the Cuicateco terrane of southern México, were recently dated by Godínez-Urban et al. (2011) and Pérez-Gutiérrez et al. (2009), respectively, and yet none of the dated samples show the presence of Middle-Upper Triassic zircons,

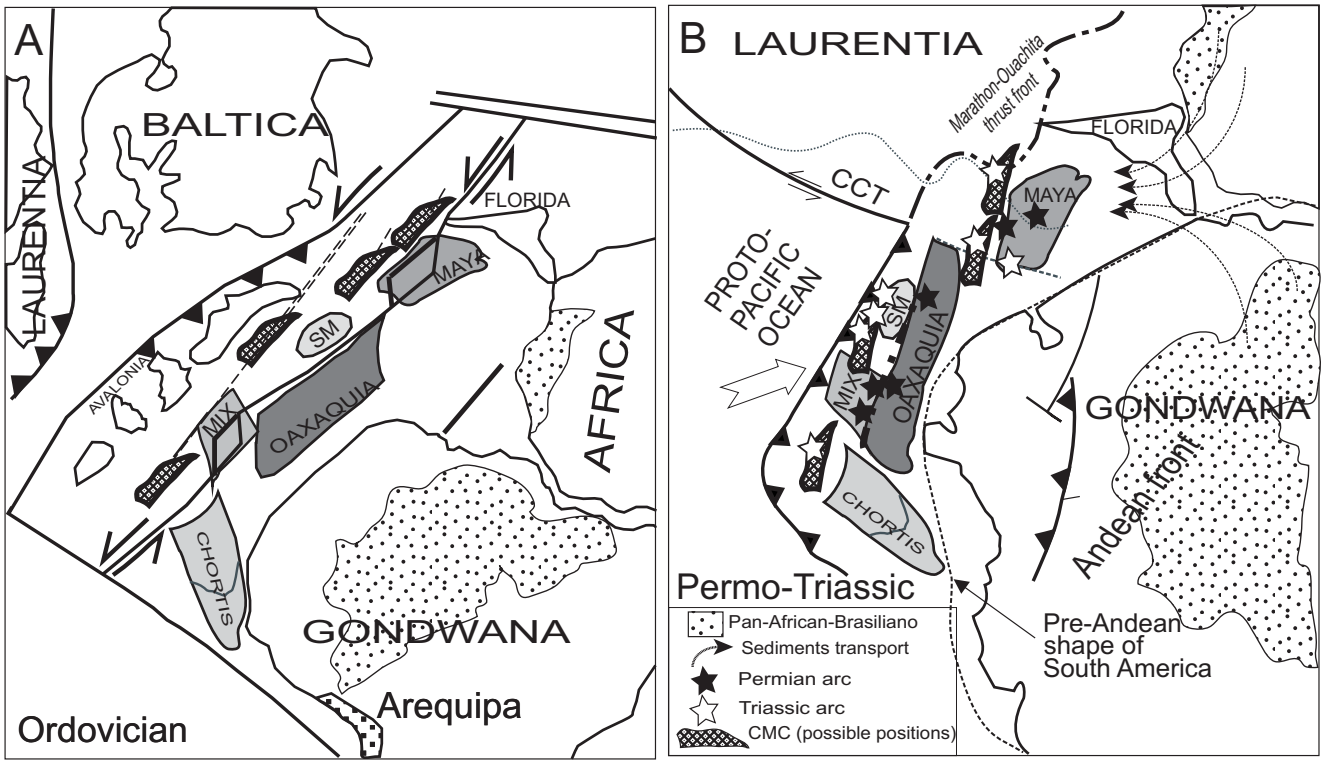

FIGURE 10 | **Paleogeographic models for the Ordovician A) and the Permo-Triassic B) Modified from Dickinson and Lawton (2001), Ortega-Obregón et al. (2008), Nance and Linnemann (2008), Weber et al. (2008), and Solari et al. (in press). MIX: Mixteco terrane; SM: Sierra Madre terrane; CCT: California-Coahuila Transform.**

such as those dated (213-226Ma) in this work. Although these features may not be considered as conclusive and further studies will be needed, they strongly support the allochthony of the Chuacús Metamorphic Complex with respect to the Maya Block.

On the other hand, correlation of the Chuacús Metamorphic Complex with the Chortís Block to the south of the major Guatemalan faults may be also discarded because the Chortís Black lies in on a different plate (the Caribbean plate, which is considered a far traveled unit originated in the Pacific). Moreover basement units in this block that are most proximal to the Chuacús Metamorphic Complex radically differ in fundamental geologic aspects, such as protoliths and contrasting metamorphic conditions (HP/HT in the Chuacús Metamorphic Complex, versus HT/LP in Las Ovejas Complex, or very low grade metamorphism of the pre-Mesozoic San Diego phyllite, Solari et al., 2009; Ratschbacher et al., 2009, and references therein).

Paleozoic-Triassic paleogeographic reconstructions

Paleogeographic reconstructions for the Late Ordovician–Early Silurian and Permo-Carboniferous suggest that the present southern edge of the Maya Block was located adjacent to northeastern México (e.g., Dickinson and Lawton, 2001; Keppie et al., 2006, 2008a; Weber et al., 2008) (Fig. 10A). These interpretations also agree with the Permian paleomagnetic data of Steiner (2005).

In these models, Paleozoic rocks of the Rabinal-Salamá area, just north of our studied area, would have lain close to NE México, north of Oaxaquia and near the Mixteco terrane, where megacrystic granites intruded a passive-margin sedimentary sequence older than ~460Ma (e.g., Nance et al., 2006). Those terranes would have been located close to northwestern Gondwana until the closure of the Rheic Ocean accompanying the amalgamation of Pangea in the late Carboniferous-Permian (e.g., Nance and Linnemann, 2008). The S-type granites cropping out to the north of the studied area could have been produced by partial crustal melting during the Cambro-Ordovician rifting episode coincident with the initial stages of the opening of the Rheic Ocean and the separation of Avalonia from Gondwana (e.g., Murphy et al., 2004).

This suggestion is in agreement with the zipper tectonics model invoked by Martens et al. (2010), which would explain the Silurian-Devonian shifting of magmatism to the Maya Mountains of Belize during subsequent extension related to the opening of the Rheic Ocean. From the Early Pennsylvanian to Permian, the oblique

convergence between Laurentia and Gondwana apparently caused the development of an E-dipping subduction zone with the onset of a new phase of magmatism in the Altos Cuchumatanes (312-317Ma, Solari et al., 2009), and thereafter in northwestern and eastern México (e.g. Torres et al., 1999), the Mixteco terrane (~288Ma, Yañez et al., 1991), the Oaxacan Complex (~275Ma, Solari et al., 2001), and in the Chiapas Massif (~272Ma, Weber et al., 2007).

In this scenario, the Chuacús Metamorphic Complex protoliths could have been deposited in a marginal basin receiving minor input of Ordovician zircons during the Silurian, as demonstrated by their presence in one metasedimentary sample dated by Solari et al. (2009) in the northernmost Sierra de Chuacús (Fig. 10A).

The proposed time constraint on HP metamorphism in the Chuacús Metamorphic Complex (Mid Ordovician to Upper Triassic) is roughly coincident with HP metamorphism reported in the Acatlán Complex of southern México, which was dated as Devonian and was exhumed during the Mississippian (e.g., Keppie et al., 2008). In this view, the Chuacús Metamorphic Complex would have been subducted during the Devonian and metamorphosed at high-grade conditions during the closure of the Rheic Ocean in the late Paleozoic. Exhumation would have taken place causing decompression melting, magmatism and migmatization in the Late Triassic (218-226Ma, Fig. 10B). The Triassic ages in the Chuacús Metamorphic Complex are only slightly younger than those of the Permo-Triassic arc of Chiapas (e.g. Weber et al., 2007), and this can be explained by an easternmost position for the Chuacús Metamorphic Complex in the evolving E-directed, proto-Pacific magmatic arc active since the Permo-Triassic (Fig. 10B).

CONCLUDING REMARKS

The discovery of high-grade metamorphic conditions in the Chuacús Metamorphic Complex of central Guatemala (Ortega-Gutiérrez et al., 2004) has awoken interest and appreciation as a key element for the geologic evolution of the Caribbean region. This contribution presents new geochronologic and geochemical data of some of the most distinctive lithologies of the complex, and provide important constraints to understand this formerly neglected piece of the Caribbean-North America tectonic realm. Indeed, the new results appear to be inconsistent with previous tectonic interpretations that considered the Chuacús Metamorphic Complex to be related to the Chortís-Maya collision, and instead support an independent evolution and an allochthonous provenance. Nevertheless we recognize that further research must be dedicated to address some other important questions that are still poorly understood, or that remained largely unexplored: Among those we can suggest the following:

The existence of ultrahigh pressure metamorphism (UHP) once suggested by (Ortega-Guitérrez et al., 2004) for the Chuacús Metamorphic Complex has yet to be confirmed. Nevertheless, intriguing minerals and peculiar textural features, coupled with thermobarometric calculations that approach such conditions, keep this possibility open for future petrologic work in the eclogitic domains that resisted retrogression inside the high-pressure gneisses.

It is still uncertain if the Chuacús Metamorphic Complex experienced only one eclogite-facies metamorphic event. Although there is clear evidence for a mid-late Paleozoic tectonothermal event, a pervasive Late Triassic magmatism and metamorphism as well as an intense Cretaceous tectonothermal overprint throughout most of the sequence; further and more detailed studies are needed to elucidate the kinematic history of its protracted tectonic evolution. In particular, the structural and kinematic history of the Chuacús Metamorphic Complex has remained almost unattended, despite its basic importance.

Finally, the lithotectonic nature of Chuacús Metamorphic Complex protoliths, as preliminary described in this work, should in the near future be an attractive target to unravel what is, perhaps, the most important question that has not been satisfactorily answered: Where does the Chuacús Metamorphic Complex come from, and which were its connections to the now adjacent Maya and Chortís blocks?

ACKNOWLEDGMENTS

We want to acknowledge several people who contributed to this work: U. Martens and S. Morán-Ical who introduced us to the Sierra de Chuacús and its fascinating rocks; O. Pérez-Arvizu, G. Solís-Pichardo, J.J. Morales, M.S. Hernández-Bernal, P. Schaaf who helped with some of the lab work; B. Martiny who kindly revised the English; and in general, the organizers and participants of the 2007 IGCP 546 excursion in central Guatemala, whose field discussions and suggestions helped to refine some of the models. CONACyT grant 54559 and PAPIIT-DGAPA grant 101407 to LAS covered some of the analytical costs. We also want to acknowledge the thoughtful reviews by U. Martens, V. Valencia and an anonymous reviewer, which greatly helped to improve the manuscript, as well as the editorial handling and suggestions of A. García-Casco.

REFERENCES

Andersen, T., 2002, Correction of common lead in U–Pb analyses that do not report 204Pb. Chemical Geology, 192, 59-79.

Brueckner, H.K., Avé Lallemant, H.G., Sisson, V.B., Harlow, G.E., Hemming, S.R., Martens, U., Tsujimori, T., Sorensen, S.S., 2009. Metamorphic reworking of a high pressure–low temperature mélange along the Motagua fault, Guatemala: A record of Neocomian and Maastrichtian transpressional tectonics. Earth and Planetary Sciences Letters, 284(1-2), 228-235. doi:10.1016/j.epsl.2009.04.032

Carswell, D.A., Wilson, R.N., Zhai, M., 1996. Ultra-high pressure aluminous titanites in carbonate-bearing eclogites at Shuanghe in Dabieshan, central China. Mineralogical Magazine, 60, 461-471.

Dengo, G., 1969. Problems of tectonic relations between Central America and the Caribbean. Transactions Gulf Coast Association Geological Society, 19, 311-320.

Dickinson, W.R., Lawton, T.F., 2001. Carboniferous to Cretaceous assembly and fragmentation of México. Geological Society of America Bulletin, 113(9), 1142-1160.

Foley, S., Tiepolo, M., Vannucci, R., 2002. Growth of early continental crust controlled by melting of amphibolite in subduction zones. Nature, 417, 837-840.

García-Casco, A., Iturralde-Vinent, M.A., Pindell, J., 2008. Latest Cretaceous collision/accretion between the Caribbean Plate and Caribeana: Origin of metamorphic terranes in the Greater Antilles. International Geology Review, 50, 781-809.

Giunta, G., Beccaluva, L., Siena, F., 2006. Caribbean plate margin evolution: constraints and current problems. Geologica Acta, 4(1-2), 265-277.

Godinez-Urbán, A., Lawton, T.F., Molina-Garza, R.S., Iriondo, A., Weber, B., López-Martínez, M., 2011. Jurassic volcanic and sedimentary rocks of the La Silla and Todos Santos Formations, Chiapas: Record of Nazas arc magmatism and rift-basin formation prior to opening of the Gulf of México. Geosphere, 7(1), 1-24.

Gomberg, D.M., Banks, P.O., McBirney, A.R., 1968. Guatemala: preliminary zircon ages from Central cordillera. Science, 162, 121-122.

Harlow, G.E., Hemming, S.R., Avé-Lallemant, H.G., Sisson, V.B., Sorensen, S.S., 2004. Two high-pressure-low temperature serpentinite-matrix mélange belts, Motagua fault zone, Guatemala: A record of Aptian and Maastrichtian collisions. Geology, 32, 17-20.

Hoskin, P.W.O, Schaltegger, U, 2003. The composition of zircon and igneous and metamorphic petrogenesis. Reviews in Mineralogy and Geochemistry, 53(1), 27-62.

Hwang, S.L., Shen, P., Chu, H.T., Yui, T.F., 2000. Nanometer-Size-PbO_2-Type TiO_2 in Garnet: A Thermobarometer for Ultrahigh-Pressure Metamorphism. Science, 288(5464), 321-324.

Irvine, T.N., Baragar, W.R.A., 1971. A guide to the chemical classification of the common volcanic rocks. Canadian Journal of Earth Sciences, 8, 523-548.

Keppie, J.D., Nance, R.D., Fernández-Suárez, J., Storey, C.D., Jeffries, T.E., Murphy, J.B., 2006. Detrital zircon data from the eastern Mixteca Terrane, southern México: evidence for an Ordovician-Mississippian continental rise and a Permo-Triassic clastic wedge adjacent to Oaxaquia. International Geology Review, 48, 97-111.

Keppie, J.D., Dostal, J., Murphy, J.B., Nance, R.D., 2008a. Synthesis and tectonic interpretation of the westernmost Paleozoic Variscan orogen in southern México: From rifted Rheic margin to active Pacific margin. Tectonophysics, 461(1-4), 277-290.

Keppie, J.D., Dostal, J., Miller, B.V., Ramos-Arias, M., Morales-Gámez, M., Nance, R.D., Murphy, J.B., Ortega-Rivera, A., Lee, J.K.W., Housh, T., 2008b. Ordovician–earliest Silurian rift tholeiites in the Acatlán Complex, southern México: Evidence of rifting on the southern margin of the Rheic Ocean. Tectonophysics, 461(1-4), 130-156.

Kesler, S.E., Josey, W.L., Collins, E.M., 1970. Basement rocks of western nuclear Central America: the western Chuacús Group, Guatemala. Geological Society of America Bulletin, 81, 3307-3322.

Langmuir, C., Hanson, G., 1980. An evaluation of major element heterogeneity in the mantle sources of basalts. Philosophical Transactions of the Royal Society London, A297, 383-407.

Lehnert, K., Su, Y., Langmuir, C., Sarbas, B., Nohl, U., 2000. A global geochemical database structure for rocks. Geochemistry Geophysics Geosystems, 1, 1012. doi:10.1029/1999GC000026, www.petdb.org.

Lenze, A., Stöckhert, B., Wirth, R., 2005. Grain scale deformation in ultra-high-pressure metamorphic rocks—an indicator of rapid phase transformation. Earth and Planetary Science Letters, 229, 217-230.

Ludwig, K.L., 2008. Isoplot 3.70. A geochronological toolkit for Microsoft Excel. Berkeley Geochronology Center, 4 (Special Publications), August 26, 1-77.

Ludwig, K.L., Mundil, R., 2002. Extracting reliable U-Pb ages and errors from complex populations of zircons from Phanerozoic tuffs. Davos (Switzerland), 12th Goldschmidt Conference, Journal of Conference Abstracts, A-463.

Manton, W.I., 1996. The Grenville of Honduras. Geological Society of America, Denver, Abstracts with Programs, A-493.

Marshall, D.J., 1988. Cathodoluminescence of geological materials. Boston, Sydney, Wellington, Unwin Hyman, 146pp.

Martens, U., 2009. Geologic evolution of the Maya Block (southern edge of the North American plate): an example of terrane transferral and crustal recycling. Doctoral Thesis. United States of America, Stanford University, 166pp.

Martens, U., Ratschbacher, L., McWilliams, M., 2005. U-Pb geochronology of the Maya Block, Guatemala. American Geophysical Union (AGU), Eos Transactions, Fall Meeting Supplement, 86(52), T51D-1387.

Martens, U., Mattinson, C.G., Wooden, J., Liou, J.G., 2007. Protolith and metamorphic ages of gneiss hosting eclogite in the Chuacús complex, Central Guatemala. American Geophysical Union (AGU), EOS Transactions, 88(23), Joint Assembly Supplement, Abstract, U53A-08.

Martens, U., Weber, B., Valencia, V.A., 2010. U/Pb geochronology of Devonian and older Paleozoic beds in the

southwestern Maya Block, Central America: its affinity with Peri-Gondwanan terranes. Geological Society of America Bulletin, 122, 815-829.

Massonne, H-J., Nasdala, L., 2003. Characterization of an early metamorphic stage through inclusions in zircon of a diamondiferous quartzofeldspathic rock from the Erzgebirge, Germany. American Mineralogist, 88, 883-889.

McBirney, A.R., 1963. Geology of a part of the central Guatemalan cordillera. California University Publications in Geological Sciences, 38, 177-242.

McDonough, W.F., Sun, S.S., 1995. Composition of the Earth. Chemical Geology, 120, 223-253. doi: 10.1016/0009-2541(94)00140-4.

Miller, B.V., Dostal, J., Keppie, J.D., Nance, R.D., Ortega-Rivera, A., Lee, J.W.K., 2007. Ordovician calc-alkaline granitoids in the Acatlán Complex, southern México: geochemical and geochronologic data and implications for tectonics of the Gondwanan margin of the Rheic Ocean. In: Linnemann, U., Nance, R.D., Zulaf, G., Kraft, P. (eds.). The Geology of Peri-Gondwana: The Avalonian-Cadomian Belt, Adjoining Cratons and the Rheic Ocean. Geological Society of America, 423 (Special Paper), 465-475. doi: 10.1130/2007.2423(23).

Murphy, J.B., Fernández-Suárez, J., Keppie, J.D., Jeffries, T.E., 2004. Contiguous rather than discrete Paleozoic histories for the Avalon and Meguma terranes based on detrital zircon data. Geology, 32, 585-588.

Murphy, J.B., Gutiérrez-Alonso, G., Nance, R.D., Fernández-Suárez, J., Keppie, J.D., Quesada, C., Dostal, J., Braid, J.A., 2009. Rheic ocean mafic complexes: overview and synthesis. In: Murphy, J.B., Keppie, J.D., Hynes, A.J. (eds.). Ancient orogens and modern analogues. Geological Society, London, 327 (Special Publications), 343-369.

Murphy, J.B., Keppie, J.D., Nance, R.D., Dostal, J., 2010, Comparative evolution of the Iapetus and Rheic Oceans: A North America perspective. Gondwana Research, 17, 482-499. doi:10.1016/j.gr.2009.08.009

Nance, R.D., Miller, B.V., Keppie, J.D., Murphy, J.B., Dostal, J., 2006. Acatlán Complex, southern México: Record spanning the assembly and breakup of Pangea. Geology, 34(10), 857-860.

Nance, R.D., Linnemann, U., 2008. The Rheic Ocean: Origin, evolution, and significance. GSA Today, 18(12), 4-12.

Ortega-Gutiérrez, F., Solari, L.A., Solé, J., Martens, U., Gómez-Tuena, A., Morán-Ical, S., Reyes-Salas, M., Ortega-Obregón, C., 2004. High Pressure eclogite facies Metamorphism in the Chuacús Complex, Sierra de Chuacús, Central Guatemala: Petrology, Geochronology, and Tectonic implications. International Geology Review, 46, 445-470.

Ortega-Gutiérrez, F., Solari, L.A., Ortega-Obregón, C., Elías-Herrera, M., Morán-Ical, S., Chiquín, M., Keppie, J.D., Torres de León, R., Schaaf, P., 2007. The Maya-Chortís boundary: a tectonostratigraphic approach. International Geology Review, 449, 996-1024.

Ortega-Obregón, C., Solari L.A., Keppie, J.D., Ortega-Gutiérrez, F., Solé, J., Morán-Ical, S., 2008. Middle – Late Ordovician magmatism and Late Cretaceous collision in the southern Maya block, Rabinal - Salamá area, central Guatemala: implications for North America-Caribbean plate tectonics. Geological Society of America Bulletin, 120, 556-570.

Ortega-Obregón, C., Keppie, J.D., Murphy, J.B., Lee, J.K.W., Ortega-Rivera, A., 2009. Geology and geochronology of Paleozoic rocks in western Acatlán Complex, southern México: Evidence for contiguity across an extruded high-pressure belt and constraints on Paleozoic reconstructions. Geological Society of America Bulletin, 121, 1678-1694.

Pérez-Gutiérrez, R., Solari, L.A., Gómez-Tuena, A., Valencia, V.A., 2009. El terreno Cuicateco: ¿una cuenca oceánica con influencia de subducción del Cretácico Superior en el sur de México? Nuevos datos estructurales, geoquímicos y geocronológicos. Revista Mexicana de Ciencias Geológicas, 26, 222-242.

Pindell, J., Kennan, L., Stanek, K.P., Maresch, W.V., Draper, G., 2006. Foundations of Gulf of México and Caribbean evolution: eight controversies resolved. Geologica Acta, 4(1-2), 303-341.

Pindell, J.L., Barret, S.F., 1990. Geological evolution of the Caribbean region; a plate-tectonic perspective. In: Dengo, G., Case, J.E. (eds.). The Geology of North America, The Caribbean Region. Boulder (Colorado), Geological Society of America, II, 405-432.

Pindell, J., Kennan, L., 2009. Tectonic evolution of the Gulf of México, Caribbean and northern South America in the mantle reference frame: an update. In: James, K., Lorente, M.A., Pindell, J. (eds.). The geology and evolution of the Caribbean Plate. Geological Society of London, 328 (Special Publications), 1-55.

Pompa-Mera, V., Schaaf, P., Weber, B., Solís-Pichardo, G., Hernández-Treviño, T., Ortega-Gutiérrez, F., 2008. Devonian-Ordovician Magmatism in Chiapas Massif, Southern Maya Block, México. American Geophysical Union (AGU), Eos Transactions, 89(53), Fall Meeting Supplement, Abstract, V31B-2138.

Ratschbacher, L., Franz, L., Min, M., Bachmenn, R., Martens, U., Stanek, K., Stubner, K., Nelson, B.K., Herrmann, U., Weber, B., López-Martínez, M., Jonckheere, R., Sperner, B., Tichomirowa, M., McWilliams, M.O., Gordon, M., Meschede, M., Bock, P., 2009. The North American–Caribbean plate boundary in México–Guatemala–Honduras. In: James, K.H., Lorente, M.A., Pindell, J.L. (eds.). The origin and Evolution of the Caribbean Plate. Geological Society of London, 328 (Special Publications), 219-293.

Rogers, R.D., Mann, P., Emmet, P.A., 2007. Tectonic terranes of the Chortis block based on integration of regional aeromagnetic and geologic data. In: Mann, P. (ed.). Geologic and tectonic development of the Caribbean plate in northern Central America. Geological Society of America, 428 (Special Paper), 65-88.

Rubatto, D., 2002. Zircon trace element geochemistry: partitioning with garnet and the link between U - Pb ages and metamorphism. Chemical Geology, 184, 123-138.

Schaaf, P., Weber, B., Weis, P., Gross, A., Ortega-Gutiérrez, F., Kohler, H, 2002. The Chiapas Massif (México) revised: new

geologic and isotopic data and basement characteristics. Neues Jahrbuch fur Geologie und Palaontologie Abhandlungen, 225, 1-23.

Schaaf, P., Stimac, J., Siebe, C., Macías, J.L., 2005. Geochemical Evidence for Mantle Origin and Crustal Processes in Volcanic Rocks from Popocatépetl and Surrounding Monogenetic Volcanoes, Central México. Journal of Petrology, 46(6), 1243-1282.

Sedlock, R., Ortega-Gutiérrez, F., Speed, R., 1993. Tectonostratigraphic terranes and tectonic evolution of México. Geological Society of America, 278 (Special Paper), 153.

Sláma, J., Košler, J., Condon, D.J., Crowley, J.L., Gerdes, A., Hanchar, J.M., Horstwood, M.S.A., Morris, G.A., Nasdala, L., Norberg, N., Schaltegger, U., Schoene, B., Tubrett, M.N., Whitehouse, M.J., 2008. Plešovice zircon - A new natural reference material for U-Pb and Hf isotopic microanalysis. Chemical Geology, 249, 1-35.

Solari, L.A., Dostal, J., Ortega-Gutiérrez, F., Keppie, J.D., 2001. The 275 Ma arc-related La Carbonera stock in the northern Oaxacan Complex of southern México: U-Pb geochronology and geochemistry. Revista Mexicana de Ciencias Geológicas, 18(2), 149-161.

Solari, L.A., Torres de León, R., Hernández-Pineda, G., Solé, J., Henández-Treviño, T., Solis, G., 2007. Tectonic significance of Cretaceous Tertiary magmatic and structural evolution of the northern margin of the Xolapa Complex, Tierra Colorada area, southern México. Geological Society of America Bulletin, 119, 1265-1279.

Solari, L.A., Ortega-Gutiérrez, F., Elías-Herrera, M., Schaaf, P., Norman, M., Torres De León, R., Ortega-Obregon, C., Chiquin, M., Morán-Ical, S., 2009. U-Pb zircon geochronology of Paleozoic units in Western and Central Guatemala: insights into the tectonic evolution of Middle America. In: James, K., Lorente, M.A., Pindell, J. (eds.). Origin and evolution of the Caribbean Plate. Geological Society of London, 328 (Special Publications), 293-311.

Solari, L.A., Ortega-Gutiérrez, F., Elías-Herrera, M., Gómez-Tuena, A., Schaaf, P., 2010a. Refining the age of magmatism in the Altos Cuchumatanes, western Guatemala, by LA-ICPMS, and tectonic implications. International Geology Review.

Solari, L.A., Gómez-Tuena, A., Bernal, J.P., Pérez-Arvizu, O., Tanner, M., 2010b. U-Pb zircon geochronology by an integrated LA-ICPMS microanalytical workstation: achievements in precision and accuracy. Geostandards and Geoanalytical Research, 34(1), 5-18.

Staudigel, H., Plank, T., White, B., Schmincke, H.-U., 1996. Geochemical fluxes during seafloor alteration of the basaltic upper oceanic crust: DSDP Sites 417-417. In: Bebout, G., Scholl, D., Kirby, S., Platt, J. (eds.). Subduction Top to Bottom. American Geophysical Union, Washington DC, Geophysical Monograph Series, 19-38.

Steiner, M.B., Walker, J.D., 1996. Late Silurian plutons in Yucatan. Journal of Geophysical Research, 101, 17,727-17,735.

Steiner, M.B., 2005. Pangean reconstruction of the Yucatan Block: Its Permian, Triassic, and Jurassic geologic and tectonic history. In: Anderson, T.H., Nourse, J.A., McKee, J.W., Steiner, M.B. (eds.). The Mojave-Sonora megashear hypothesis: Development, assessment, and alternatives. Geological Society of America, 393 (Special Paper), 457-480. doi: 10.1130/2005.2393(17).

Sun, S.S., McDonough, W.F., 1989. Chemical and isotopic systematics of oceanic basalts: implications for mantle composition and processes. In: Saunders, A.D., Norry, M.J. (eds.). Magmatism in the ocean basins. Geological Society of London, 42 (Special Publications), 313-345.

Tanner, M., Solari, L.A., 2009. Fast reduction of U-Pb data using R. Geochimica et Cosmochimica Acta, 1 (Supplement), 73-13, A1313.

Torres, R., Ruíz, J., Patchett, P.J., Grajales-Nishimura, J.M., 1999. Permo-Triassic continental arc in eastern México; tectonic implications for reconstructions of southern North America. In: Bartolini, C., Wilson, J.L., Lawton, T.F. (eds.). Mesozoic sedimentary and tectonic history of north-central México. Geological Society of America, 340 (Special Paper), 191-196.

Vega-Granillo, R., Talavera-Mendoza, O., Meza-Figueroa, D., Ruiz, J., Gehrels, G.E., López-Martínez, M., De La Cruz-Vargas, J.C., 2007. Pressure-temperature-time evolution of Paleozoic high-pressure rocks of the Acatlán Complex (southern México): Implications for the evolution of the Iapetus and Rheic Oceans. Geological Society of America Bulletin, 119(9), 1249-1264.

Vega-Granillo, R., Salgado-Souto, S., Herrera-Urbina, S., Valencia, V., Ruiz, J., Meza-Figueroa, D., Talavera-Mendoza, O., 2008. U-Pb detrital zircon data of the Rio Fuerte Formation (NW México): Its peri-Gondwanan provenance and exotic nature in relation to southwestern North America. Journal of South American Earth Sciences, 26, 343-354.

Watson, E.B., Wark, D.A., Thomas, J.B., 2006. Crystallization thermometers for zircon and rutile. Contributions to Mineralogy and Petrology, 151, 413-433.

Weber, B., Köhler, H., 1999. Sm-Nd, Rb-Sr and U-Pb geochronology of a Grenville terrane in southern México: origin and geologic history of the Guichicovi Complex. Precambrian Research, 96, 245-262.

Weber, B., Cameron, K., Osorio, M., Schaaf, P., 2005. A Late Permian Tectonothermal Event in Grenville Crust of the Southern Maya Terrane: U-Pb Zircon Ages from the Chiapas Massif, Southeastern México. International Geology Review, 47, 509-529.

Weber, B., Valencia, V.A., Iriondo, A., Ortega-Gutiérrez, F., 2006. Provenance ages of Late Peleozoic sandstones (Santa Rosa Formation) from the Maya block, SE México - implications on the tectonic evolution of western Pangea. Revista Mexicana de Ciencias Geológicas, 23, 262-276.

Weber, B., Iriondo, A., Premo, W.R., Hecht, L., Schaaf, P., 2007. New insights into the history and origin of the southern Maya

block, SE México: U-Pb-SHRIMP zircon geochronology from metamorphic rocks of the Chiapas massif. International Journal of Earth Sciences, 96(2), 253-269.

Weber, B., Valencia, V.A., Schaaf, P., Pompa-Mera, V., Ruiz, J., 2008. Significance of provenance ages from the Chiapas massif Complex (Southeastern México): redefining the Paleozoic basement of the Maya Block and its evolution in a Peri-Gondwanan Realm. The Journal of Geology, 116, 619-639.

Weber, B., Valencia, V.A., Schaaf, P., Ortega-Gutiérrez, F., 2009. Detrital zircon ages from the Lower Santa Rosa Formation, Chiapas: implications on regional Paleozoic stratigraphy. Revista Mexicana de Ciencias Geológicas, 26(1), 260-276.

Yañez, P., Ruíz, J., Patchett, P.J., Ortega-Gutiérrez, F., Gehrels, G., 1991. Isotopic studies of the Acatlan Complex, southern México: Implications for Paleozoic North American tectonics. Geological Society of America Bulletin, 103, 817-828.

Zhang, L.S., Ellis, D.J., Williams, S., Jiang, W., 2003. Ultrahigh-pressure metamorphism in eclogites from the western Tianshan, China-Reply. American Mineralogist, 88(7), 1157-1160.

Manuscript received November 2010;
revision accepted May 2011;
published Online June 2011.

ELECTRONIC APPENDIX

TABLE I | **Trace and REE concentrations of the selected zircons of Figure 9**

Sample number	P	Ti	Y	Nb	La	Ce	Pr	Nd	Sm	Eu	Gd	Tb	Dy	Ho	Er	Yb	Lu	Hf	Th	U	Log(Ti)	T°C
Gt0315, pegmatite																						
14°58'15.49"																						
90°43'29.88"																						
Gt0315 002	6	bdl	250	1.44	0.03	0.49	0.01	0.52	0.38	0.22	3.78	1.6	21	7	31	47	8	15449	0.07	54	bdl	
Gt0315 003	4	13	268	1.56	0.02	0.54	0.04	0.51	0.37	0.28	4.10	1.7	23	8	33	49	8	15998	0.06	57	1.103199066	762
Gt0315 004	70	bdl	1462	13.6	0.06	1.08	0.02	0.45	0.48	0.41	6.43	4.2	88	46	290	778	171	18943	0.14	945	bdl	
Gt0315 005	6	2	245	1.57	bdl	0.44	0.06	0.52	0.27	0.21	3.42	1.5	21	7	32	57	10	16040	0.05	52	0.396018219	632
Gt0315 007	bdl	6	423	2.93	0.04	0.13	0.02	0.40	0.30	0.07	1.21	0.9	23	12	74	167	33	18434	0.02	168	0.763894393	695
Gt0315 008	93	2	1078	4.53	0.02	0.49	0.04	0.49	0.27	0.24	4.43	2.8	61	33	213	594	131	18351	0.11	688	0.211118804	603
Gt0315 009	4	bdl	235	1.32	0.03	0.14	0.04	0.36	0.21	0.05	1.00	0.6	13	7	38	82	16	17691	0.01	33	bdl	
Gt0315 010	73	18	562	4.12	0.02	10.6	0.10	1.48	2.20	0.23	10.8	3.7	49	19	94	211	42	13183	71	189	1.243679001	793
Gt0315 011	47	25	502	4.52	0.03	8.95	0.07	1.48	2.11	0.16	10.0	3.4	45	17	83	189	37	13579	13	121	1.389978264	827
Gt0315 013	bdl	3	829	7.94	0.04	0.11	0.03	0.39	0.19	0.08	1.57	1.4	36	24	163	431	89	20941	0.01	82	0.521366919	653
Gt0315 014	80	19	690	4.16	0.02	9.18	0.15	1.81	2.48	0.25	13.9	4.6	61	23	116	259	51	13735	29	88	1.271995867	799
Gt0315 015	119	10	1600	6.39	0.04	13.9	0.23	3.71	6.98	0.53	36	11.9	151	54	259	538	103	13842	60	100	0.984846748	738
Gt0315 016	114	10	798	8.00	0.04	12.8	0.12	2.00	3.01	0.24	15.3	5.4	72	27	133	295	58	13892	36	76	1.010989262	743
Gt0315 017	13	3	275	1.74	0.03	0.41	0.03	0.47	0.24	0.11	1.98	1.1	19	8	46	111	24	16572	0.02	59	0.454141414	641
Gt0315 018	62	23	565	5.80	0.06	12.5	0.08	1.24	2.00	0.16	9.50	3.3	48	18	98	232	47	15266	257	1009	1.360248977	820
Gt0315 019	107	14	732	2.56	7.98	30	1.87	7.77	3.65	0.61	16.8	5.4	69	25	119	229	43	11723	86	191	1.151753091	773
Gt0315 020	67	7	657	3.78	0.03	8.78	0.10	1.91	2.86	0.25	14.2	4.6	62	23	112	235	44	13904	3.05	30	0.843004284	710
Gt0315 021	18	2	215	1.08	bdl	0.18	0.03	0.46	0.28	0.10	1.42	0.7	12	6	37	85	17	17363	0.02	45	0.339636339	623
Gt0315 022	93	20	462	4.14	0.04	8.61	0.08	1.40	1.95	0.16	9.18	3.2	43	16	79	182	35	14119	21	90	1.291892951	804
Gt0315 023	72	19	575	5.46	0.03	9.68	0.11	1.44	2.19	0.17	10.2	3.7	49	19	96	233	47	14421	151	397	1.286472869	802
Gt0315 024	123	25	1618	6.39	0.03	13.9	0.15	3.03	6.40	0.48	33	11.0	144	52	259	566	111	14055	392	706	1.405922792	830
Gt0315 025	48	24	562	5.65	0.02	12.0	0.08	1.37	1.97	0.15	9.58	3.6	48	18	95	228	46	13917	285	901	1.381290362	824
Gt0315 026	73	bdl	162	3.43	0.03	1.74	0.06	0.44	0.41	0.05	1.77	0.7	11	5	31	96	21	15183	34	390	bdl	
Gt0315 027	72	24	706	5.75	0.02	11.4	0.10	1.63	2.33	0.16	12.8	4.5	60	23	118	277	55	14155	302	901	1.379728486	824
Gt0315 028	100	13	966	5.16	0.03	15.3	0.12	1.80	3.04	0.28	19.4	6.5	85	32	157	310	59	13086	199	469	1.114091374	765
Gt0315 029	127	28	1390	2.22	0.03	15.9	0.43	6.82	10.3	1.79	45	12.9	149	48	213	355	65	10947	115	186	1.440732925	839
Gt0315 030	99	16	639	2.54	0.05	13.8	0.09	1.80	2.82	0.39	13.9	4.6	61	22	103	202	39	11737	71	169	1.199154779	783
Gt0319, deformed diorite																						
14°57'56.9"																						
90°32'49"																						
Gt0319 001	88	20	1651	2.06	0.05	30	0.32	4.05	6.05	2.45	30	10	139	52	271	568	112	9578	221	204	1.295550897	805
Gt0319 003	58	bdl	724	1.29	0.01	12	0.17	2.02	2.69	1.18	12	4	58	23	124	304	68	10035	184	203	bdl	
Gt0319 004	32	8.95	649	1.19	0.01	14	0.06	1.02	1.55	0.77	9	3	47	19	108	284	67	12442	165	238	0.951763132	731
Gt0319 005	64	bdl	896	2.00	0.06	18	0.33	3.47	4.32	2.13	16	5	68	27	147	371	83	8458	282	234	bdl	
Gt0319 006	173	bdl	2516	5.77	0.19	50	0.72	8.84	11.16	6.19	49	16	206	76	397	924	192	7752	991	549	bdl	
Gt0319 007	185	10	2039	3.63	0.19	31	0.74	10.39	12.52	6.06	47	14	176	64	322	709	146	6812	316	184	0.982921036	738
Gt0319 008	64	1.19	456	1.02	0.02	9.38	0.09	1.34	1.31	0.62	5.87	2.16	30	13	78	226	55	8655	79	99	0.077303038	583
Gt0319 009	48	bdl	190	0.62	0.01	4.06	0.05	0.82	0.63	0.26	2.49	0.85	13	6	35	113	29	8004	15	39	bdl	
Gt0319 010	148	4.53	1996	4.27	0.13	40	0.64	8.63	11.09	4.89	42	13	171	62	318	710	149	7812	470	280	0.656560103	676
Gt0319 011	62	3.28	542	1.00	0.03	9.71	0.24	2.65	2.63	1.13	10	3	42	16	88	229	51	7199	72	69	0.515478469	652
Gt0319 012	69	bdl	491	1.13	0.00	10.4	0.06	1.15	1.50	0.69	8	3	37	15	83	205	45	10755	95	113	bdl	
Gt0319 014	16	5.65	239	1.08	bld	6.56	0.03	0.64	0.54	0.22	2	0.98	15	7	43	134	32	11627	31	87	0.752050631	693
Gt0319 015	19	bdl	663	1.08	0.03	11.7	0.09	1.57	2.35	1.08	12	4	54	21	111	252	54	10338	193	204	bdl	
Gt0319 016	42	17	817	2.09	0.03	14.8	0.14	1.85	2.24	0.97	12	4	64	25	140	338	73	9560	247	294	1.240889137	792
Gt0319 017	104	8.82	1053	2.67	0.10	25	0.35	4.36	4.67	2.32	19	6	82	32	171	429	93	8463	344	259	0.945369276	730
Gt0319 018	34	6.60	526	1.14	0.02	8.97	0.06	1.23	1.38	0.70	7	3	37	16	90	243	61	10957	128	232	0.819354015	706
Gt0319 019	24	bdl	470	1.07	0.04	9.01	0.05	1.13	1.47	0.76	7	3	35	15	80	206	47	10977	131	169	bdl	
Gt0319 021	93	bdl	831	2.18	0.08	19.6	0.23	2.33	2.83	1.42	11	4	58	24	141	389	89	8269	250	247	bdl	
Gt0319 022	30	bdl	41	0.46	0.01	1.54	0.04	0.49	0.24	0.03	0.34	0.12	2.03	1.14	8	36	11	11556	3	43	bdl	
Gt0319 023	124	7.05	2233	3.61	0.07	59	0.38	5.26	8.38	3.52	44	15	196	72	362	690	133	10077	506	293	0.84829666	711
Gt0319 024	161	32	2044	3.03	0.04	20	0.40	5.39	7.70	3.13	40	14	182	68	334	651	128	8495	119	103	1.498371018	853

TABLE I | **Continued**

Sample number	P	Ti	Y	Nb	La	Ce	Pr	Nd	Sm	Eu	Gd	Tb	Dy	Ho	Er	Yb	Lu	Hf	Th	U	Log(Ti)	T°C
Gt0319 025	192	7.65	839	2.13	0.00	11.3	0.08	1.30	2.07	0.90	12	4	65	26	144	322	66	8386	28	44	0.883559191	718
Gt0319 026	150	8.93	1784	3.77	0.15	23	0.49	5.12	7.14	3.91	35	11	144	54	284	686	147	7112	463	292	0.950930639	731
Gt0319 027	115	bdl	572	1.53	0.00	11.4	0.05	0.90	1.27	0.48	7	3	41	18	103	267	61	10293	145	228	bdl	
Gt0319 028	16	5.80	125	1.03	0.03	6	0.05	0.58	0.24	0.10	1.27	0.49	8	4	23	71	18	11740	80	207	0.763214558	695
Gt0319 029	103	5.66	1616	3.09	0.08	16	0.25	3.78	5.26	2.42	30	10	140	53	265	535	106	8024	86	81	0.752565659	693
Gt0319 030	187	8.87	2536	9.27	0.02	38	0.28	3.94	6.79	2.55	37	14	200	82	435	907	182	8523	164	170	0.947703735	730
Gt0319 031	63	bdl	1014	2.01	0.05	16	0.19	2.72	3.30	1.07	19	7	88	33	172	362	74	9949	188	185	bdl	
Gt0319 033	146	1.42	1077	2.32	0.03	26	0.12	1.72	2.55	1.17	14	6	82	33	186	428	90	9270	166	180	0.153732124	594
Gt0319 034	87	6.10	899	2.27	0.08	16	0.21	2.43	3.42	1.84	16	5	69	27	145	384	83	7580	225	174	0.785504443	699
Gt0319 037	99	bdl	1379	1.87	0.04	15	0.23	3.72	5.82	2.40	28	9	123	45	228	448	87	8719	66	63	bdl	
Gt0319 038	72	bdl	873	1.45	0.07	16	0.29	3.67	3.44	1.70	16	5.29	69	26	140	350	75	8042	188	175	bdl	
Gt0319 039	37	3.59	951	1.65	0.02	18	0.20	2.45	3.34	1.85	16	5.33	75	29	162	401	90	10617	323	322	0.55558113	658
Gt0319 040	42	3.87	351	0.87	0.06	7.1	0.09	1.31	1.07	0.55	5	1.74	25	10	60	172	41	8855	51	72	0.588209591	664
Gt0319 041	49	11	675	1.24	0.07	13	0.29	3.30	3.43	1.43	13	4.08	54	20	110	274	59	7633	119	110	1.02155217	745
Gt0319 042	10	bdl	180	0.70	0.02	4.52	0.05	0.67	0.40	0.18	1.74	0.70	11	5	32	93	24	12253	56	97	bdl	
Gt0319 043	88	340	956	1.43	0.07	8.23	0.26	2.91	3.82	2.01	19	6	80	30	154	344	74	6633	151	135	2.530947298	1187
Gt0319 044	68	9.48	1212	2.43	0.10	21.17	0.37	4.23	5.24	2.70	22	7	98	37	196	468	100	7581	273	214	0.976713284	736
Gt0319 045	100	bdl	1766	2.24	0.05	16.44	0.33	5.41	7.75	2.83	36	12	159	58	289	560	109	7963	91	82	bdl	
Gt0319 046	120	5.43	1861	3.47	0.13	34	0.55	6.65	8.35	3.83	37	12	155	57	298	682	139	7454	407	294	0.734849388	690
Gt0319 047	48	bdl	805	1.73	0.07	12.89	0.21	2.73	2.92	1.51	14	5	63	25	131	328	71	9237	217	170	bdl	
Gt0319 048	68	12	462	1.27	0.03	8.93	0.14	1.64	1.58	0.63	6	2.31	33	14	78	207	47	7612	63	68	1.069009689	755
Gt0319 049	47	bdl	437	0.94	0.05	8.64	0.07	1.14	1.25	0.63	6	2.13	32	13	78	215	50	9933	86	126	bdl	
Gt0319 050	172	1.40	2148	2.90	0.07	17.49	0.43	6.03	9.02	3.56	44	15	198	72	358	669	132	7801	124	93	0.147002165	593
Gt0319 051	203	bdl	1407	3.88	0.03	30	0.17	2.47	3.28	1.68	18	7	103	43	241	591	126	7712	322	292	bdl	
Gt0319 053	20	bdl	180	0.75	0.05	4.27	0.06	0.76	0.71	0.28	3	0.95	13	5	32	93	23	9607	53	70	bdl	
Gt0319 054	123	6.16	1707	3.91	0.15	31	0.49	6.35	8.40	4.12	35	11	141	52	271	645	135	7897	497	305	0.789745011	700
Gt0319 055	36	5.10	1010	1.76	0.08	17	0.30	3.31	3.59	1.69	17	6	78	31	166	395	91	8902	279	248	0.707723998	685
Gt0319 056	81	bdl	1366	1.68	0.10	13	0.35	3.89	5.38	2.66	26	9	115	43	221	509	108	7901	263	228	bdl	
Gt0319 057	68	bdl	1276	1.30	0.01	22	0.20	3.12	4.49	2.10	23	8	108	42	209	436	89	10451	201	198	bdl	
Gt0319 058	23	bdl	525	1.09	0.06	11.28	0.06	0.86	1.43	0.79	9	2.96	41	17	90	217	48	11704	110	144	bdl	
Gt0319 059	134	7.97	2173	4.47	0.10	39	0.56	6.19	8.28	4.46	43	14	184	68	350	762	153	9058	560	410	0.901251809	721
Gt0319 060	80	10	766	1.42	0.10	12.2	0.37	3.79	3.81	1.95	15	5	62	23	127	311	67	7068	103	86	1.000299154	741
Gt0320, deformed gabbro																						
14°57'56.9"																						
90°32'49"																						
Gt0320 001	524	7.70	1756	2.98	0.06	19.27	0.36	4.92	7.50	3.38	39.02	12.09	158	58	271	595	107	7433	349	268	0.886218314	718
Gt0320 002	578	9.91	1391	2.28	0.14	16.54	0.37	4.41	5.79	2.84	30.80	9.47	121	45	212	468	88	7353	249	204	0.995998407	740
Gt0320 003	412	10.50	1117	6.45	0.05	23.12	0.14	1.81	1.92	1.12	12.64	4.88	75	34	192	517	103	11243	270	404	1.021189916	745
Gt0320 006	41	bdl	130	0.58	0.03	4.02	0.07	1.29	0.62	0.12	1.62	0.53	8	4	23	78	19	10373	31	58	bdl	
Gt0320 008	315	7.87	431	1.46	0.08	10.72	0.13	1.21	1.19	0.63	6.33	2.29	33	13	71	186	37	10434	44	60	0.896249179	720
Gt0320 009	564	0.64	1639	2.63	0.13	24.07	0.43	6.08	8.41	3.68	36.95	11.59	143	53	248	502	90	7519	256	199	-0.19603029	546
Gt0320 010	849	7.80	2218	4.46	0.11	35.60	0.57	7.05	10.23	4.47	49.97	15.72	197	71	336	680	124	6935	398	295	0.892123547	720
Gt0320 011	554	0.86	1924	2.97	bdl	24.32	0.39	6.18	8.62	3.40	43.31	13.33	173	62	295	562	100	9388	167	140	-0.0659347	563
Gt0320 012	664	1.28	2326	3.96	0.08	28.89	0.46	7.74	9.35	3.81	50.07	16.17	205	76	358	697	121	9447	224	181	0.105606177	587
Gt0320 013	247	7.39	664	2.66	0.07	11.49	0.10	1.57	1.69	0.73	8.43	3.16	45	20	114	308	66	8907	100	155	0.868745364	715
Gt0320 014	460	bdl	689	2.58	0.02	11.42	0.12	1.48	1.86	0.73	8.11	3.07	47	21	116	314	66	8476	95	140	bdl	
Gt0320 016	770	11.66	2478	4.17	0.06	29.20	0.44	6.10	8.63	3.82	47.82	16.43	214	82	382	774	133	8700	378	289	1.066725496	755
Gt0320 018	158	2.22	402	1.85	0.02	9.51	0.10	1.63	1.30	0.55	6.66	2.21	31	13	68	186	37	9413	41	88	0.346833695	624
Gt0320 020	967	3.30	1477	7.11	0.00	27.02	0.08	1.67	2.90	1.13	19.37	7.13	108	47	246	622	117	12343	193	281	0.517857267	652
Gt0320 021	244	5.77	1061	2.04	0.05	13.79	0.22	3.47	4.52	2.13	22.08	6.91	90	35	171	399	74	9554	209	194	0.761329923	695
Gt0320 022	196	bdl	414	0.88	bdl	5.69	0.15	1.79	1.55	0.51	6.28	1.99	31	13	75	235	49	10468	85	178	bdl	
Gt0320 023	356	6.06	637	2.92	0.03	10.94	0.13	1.70	1.75	0.81	8.79	3.15	46	20	108	295	59	9583	119	191	0.782565847	699
Gt0320 025	250	0.51	610	1.14	0.05	9.70	0.13	2.10	2.27	1.10	11.99	3.73	49	20	96	233	45	9216	123	135	-0.293224655	533
Gt0320 026	480	14.25	654	2.45	0.07	13.08	0.15	1.90	2.17	0.86	10.33	3.55	50	21	111	282	55	9652	130	185	1.153810115	773
Gt0320 027	378	bdl	852	2.11	0.11	16.75	0.38	4.55	4.89	2.26	20.44	6.40	78	28	131	287	50	7860	192	150	bdl	
Gt0320 028	818	4.08	1164	2.71	0.07	17.81	0.19	2.58	3.85	1.57	19.84	6.85	93	37	187	432	79	7164	121	131	0.610500573	668
Gt0320 029	149	10.04	216	0.84	0.07	4.98	0.08	1.32	1.05	0.44	4.54	1.45	19	7	35	82	15	7640	53	66	1.001905299	741

DOI: 10.1344/105.000001695

TABLE I | **Continued**

Sample number	P	Ti	Y	Nb	La	Ce	Pr	Nd	Sm	Eu	Gd	Tb	Dy	Ho	Er	Yb	Lu	Hf	Th	U	Log(Ti)	T°C
Gt0320 030	130	bdl	296	0.76	0.03	5.94	0.10	1.10	1.11	0.63	5.54	1.83	25	10	48	113	21	7954	88	99	bdl	
Gt0320 032	369	6.90	962	2.18	0.09	15.65	0.31	3.83	4.89	2.23	20.47	6.42	84	30	149	350	64	7961	162	139	0.839158302	709
Gt0320 033	327	2.09	676	1.16	0.06	9.26	0.21	2.50	2.85	1.39	12.38	4.22	54	21	110	282	55	8407	103	117	0.320630029	620
Gt0320 034	441	4.23	517	2.13	0.07	11.16	0.10	1.31	1.44	0.56	7.15	2.44	38	16	88	246	49	8373	74	160	0.62597851	671
Gt0320 035	187	7.00	378	1.32	0.02	6.34	0.11	1.59	1.64	0.65	6.50	2.15	31	12	64	177	35	8130	51	79	0.844869035	711
Gt0320 036	388	6.88	947	2.37	0.02	14.36	0.21	3.02	2.89	1.58	14.34	5.33	73	30	160	413	86	10503	330	382	0.837443497	709
Gt0320 037	547	1.79	472	1.22	0.01	8.24	0.10	1.26	1.31	0.74	6.46	2.42	36	15	80	227	47	9303	103	148	0.25242783	609
Gt0320 038	1052	6.33	3483	7.64	0.22	57.42	0.82	11.28	15.94	6.87	83.92	25.90	326	116	531	1047	178	8457	534	323	0.801597915	702
Gt0320 039	543	7.70	1409	2.73	bdl	24.79	0.18	2.36	3.92	1.86	25.42	8.70	118	47	233	526	97	13112	464	450	0.886220897	718
Gt0320 040	443	bdl	1673	3.36	0.04	24.84	0.21	3.26	5.84	2.67	31.32	10.66	145	55	271	604	111	12329	539	464	bdl	
Gt0320 041	383	3.29	639	3.20	0.00	16.22	0.09	1.23	1.52	0.72	8.09	2.96	44	20	112	311	63	12069	234	359	0.517786085	652
Gt0320 042	430	2.58	1199	3.03	0.09	16.41	0.31	4.11	5.22	2.61	27.54	8.27	107	39	186	421	73	7530	293	216	0.411205829	634
Gt0320 043	748	2.08	1260	3.66	0.00	20.40	0.15	2.18	3.44	1.49	17.83	6.89	98	41	213	552	106	10944	328	371	0.318707321	620
Gt0320 044	471	5.72	811	1.50	0.04	9.71	0.23	2.84	3.51	1.58	16.81	5.55	72	27	129	295	53	7938	119	122	0.757695036	694
Gt0321, Agua Caliente River felsic orthogneiss																						
14°56'07.8"																						
90°30'10.9"																						
Gt0321 006	-	5.5	2375	-	0.07	58	-	-	5.5	1.33	-	-	183	-	-	-	175	12389	226	440	0.743273313	692
Gt0321 007	-	7.6	1082	-	0.44	37	-	-	3.0	0.91	-	-	82	-	-	-	87	12656	98	182	0.882269836	718
Gt0321 009	-	bdl	881	-	0.01	32	-	-	2.4	0.57	-	-	71	-	-	-	67	12170	47	75	bdl	
Gt0321 010	-	0.85	1609	-	0.05	49	-	-	2.5	0.56	-	-	95	-	-	-	187	15203	753	955	-0.072605499	562
Gt0321 013	-	5.6	2491	-	0.06	61	-	-	7.1	1.79	-	-	202	-	-	-	146	12472	159	197	0.74612956	692
Gt0321 016	-	10	2500	-	0.10	59	-	-	7.4	1.84	-	-	203	-	-	-	159	10133	176	168	1.00441451	742
Gt0321 019	-	5.4	1800	-	0.11	51	-	-	3.9	1.02	-	-	135	-	-	-	139	12884	189	266	0.729411984	689
Gt0321 020	-	1.1	1967	-	0.06	62	-	-	3.8	0.89	-	-	152	-	-	-	155	14318	594	649	0.033785807	577
Gt0321 021	-	7.4	4358	-	1.3	113	-	-	12	2.86	-	-	356	-	-	-	269	12918	694	774	0.867115224	715
Gt0321 022	-	9.9	1416	-	0.05	57	-	-	3.1	1.0	-	-	112	-	-	-	105	12360	183	221	0.994758068	740
Gt0321 027	-	13	2666	-	39	153	-	-	26	8.12	-	-	217	-	-	-	185	10969	172	220	1.116793241	765
Gt0321 030	-	7.2	580	-	0.11	21	-	-	1.2	0.36	-	-	45	-	-	-	52	13687	53	92	0.857475871	713
Gt0321 033	-	8.0	1392	-	0.54	38	-	-	3.2	0.42	-	-	108	-	-	-	118	15678	307	474	0.900545554	721
Gt0321 034	-	4.1	1464	-	0.24	32	-	-	4.3	0.77	-	-	120	-	-	-	96	14191	156	386	0.617962445	669
Gt0321 037	-	3.6	1478	-	1.7	61	-	-	5.5	1.65	-	-	119	-	-	-	101	12309	204	206	0.5559389	658
Gt0321 044	-	7.1	1816	-	0.05	60	-	-	2.6	0.71	-	-	106	-	-	-	215	15017	986	1181	0.849242039	711
Gt0321 045	-	2.7	1734	-	3.7	84	-	-	4.2	1.07	-	-	126	-	-	-	148	11944	522	505	0.429099049	637
Gt0321 048	-	8.1	3083	-	0.30	59	-	-	11	3.48	-	-	260	-	-	-	197	11192	206	208	0.910885653	723
Gt0321 049	-	4.1	928	-	0.04	38	-	-	2.5	0.70	-	-	74	-	-	-	76	14300	120	189	0.611383906	668
Gt0321 051	-	5.8	1334	-	0.03	46	-	-	2.4	0.65	-	-	93	-	-	-	124	13930	378	460	0.761619418	695
Gt0321 052	-	11	2001	-	3.0	81	-	-	6.9	2.47	-	-	151	-	-	-	168	9694	221	298	1.038444237	749
Gt0321 055	-	6.6	2022	-	0.08	81	-	-	3.9	0.92	-	-	138	-	-	-	189	13765	764	777	0.817890144	705
Gt0321 056	-	bdl	2346	-	0.10	69	-	-	3.9	0.69	-	-	176	-	-	-	187	13721	330	499	bdl	
Gt0321 057	-	bdl	1594	-	19	95	-	-	5.2	1.05	-	-	110	-	-	-	146	13885	799	725	bdl	
Gt0321 058	-	bdl	1720	-	16	92	-	-	11	2.96	-	-	120	-	-	-	165	14579	517	660	bdl	
Gt0321 060	-	8.9	1279	-	8.3	63	-	-	4.6	0.97	-	-	102	-	-	-	99	13504	159	229	0.951678187	731
Gt0321 061	-	5.5	1180	-	0.14	34	-	-	3.7	0.43	-	-	101	-	-	-	81	14964	105	238	0.741255368	691
Gt0321 062	-	13.9	2190	-	7.2	93	-	-	5.8	1.46	-	-	134	-	-	-	210	14194	1619	1339	1.143553907	771
Gt0321 064	-	4.7	657	-	12.9	58	-	-	16	6.65	-	-	60	-	-	-	54	15921	55	187	0.670117775	678
Gt0332, El Chol migmatite leucosome																						
14°57'53.6"																						
90°29'12.5"																						
Gt0332 001	83	bdl	1914	3	0.05	11	0.09	1.6	3.2	1.8	29	11	158	64	318	697	140	13353	20	204	bdl	
Gt0332 002	4	22	2081	2	0.11	10	0.21	3.6	7.2	3.6	44	15	182	69	323	657	141	11779	20	195	1.337857028	814
Gt0332 004	49	6	573	3	0.05	11	0.14	2.4	3.1	0.29	13	4.1	50	19	93	210	42	15460	77	382	0.775688502	698
Gt0332 005	86	9	807	5	0.02	11	0.15	2.1	2.7	0.48	15	5.4	73	28	133	277	50	13974	7.3	133	0.941255496	729
Gt0332 006	20	bdl	2297	13	0.03	3.7	0.08	1.0	1.4	0.63	14	7.8	147	72	403	1005	199	17048	5.2	392	bdl	
Gt0332 007	bdl	bdl	412	1.4	0.06	1.3	0.06	0.89	0.64	0.21	4	1.6	24	12	72	225	63	16311	1.6	132	bdl	
Gt0332 008	116	bld	1620	4.6	0.20	13	0.24	3.0	4.2	0.32	27	10	136	54	258	499	90	13121	135	460	bdl	

DOI: 10.1344/105.000001695

TABLE I | **Continued**

Sample number	P	Ti	Y	Nb	La	Ce	Pr	Nd	Sm	Eu	Gd	Tb	Dy	Ho	Er	Yb	Lu	Hf	Th	U	Log(Ti)	T°C
Gt0332 009	144	13	3548	55	0.06	1.8	0.09	1.2	1.0	0.60	15	10	210	109	624	1536	314	23711	5.1	1465	1.111469047	764
Gt0332 011	176	6	1204	3.8	0.14	12	0.29	4.0	6.6	0.50	30	10	119	43	184	326	58	13412	21	107	0.776792954	698
Gt0332 012	83	8	2772	8.6	0.04	17	0.16	3.3	8.2	3.5	60	20	255	95	438	896	166	16607	106	562	0.882341149	718
Gt0332 013	88	bld	761	4.2	0.08	8.8	0.13	1.9	2.9	0.25	15	5.4	69	26	123	247	45	13655	50	176	bdl	
Gt0332 014	77	bld	1918	20	0.04	4.6	0.07	1.4	1.5	0.41	13	7.1	126	62	342	822	171	18907	17	462	bdl	
Gt0332 015	62	15	537	3.7	0.07	24	0.14	2.6	3.1	0.52	13	4.2	53	19	87	167	32	13272	37	67	1.184900596	780
Gt0332 016	20	2	461	4.6	0.06	22	0.25	4.5	7.0	1.0	28	6.8	65	17	58	65	10	14261	16	77	0.298330495	616
Gt0332 017	80	bdl	1390	3.1	0.04	5.0	0.05	0.93	1.1	0.46	10	5.4	95	46	262	667	131	16816	11	369	bdl	
Gt0332 018	50	bdl	358	1.9	0.08	1.4	0.08	0.91	0.5	0.13	2	1.2	22	12	70	199	45	16861	1.6	108	bdl	
Gt0332 020	21	17	760	3.6	0.06	4.9	0.06	1.2	1.3	0.44	8	3.4	54	24	132	347	77	15350	25	440	1.223226465	788
Gt0332 021	65	3.1	756	3.2	0.02	10	0.11	1.8	2.5	0.21	14	5.1	67	27	125	264	50	13618	54	237	0.496733833	648
Gt0332 022	9.1	6.5	323	1.9	0.04	0.7	0.06	0.85	0.33	0.10	2	1.0	19	10	64	218	56	18353	1.3	125	0.81329298	705
Gt0332 023	42	bdl	1488	5.5	bdl	6.0	0.07	1.0	1.2	0.5	12	5.9	103	48	261	652	131	16780	24	307	bdl	
Gt0332 024	bdl	bdl	413	1.5	0.04	1.3	0.08	0.79	0.54	0.20	3	1.4	25	13	73	222	63	17270	1.7	136	bdl	
Gt0332 025	125	1.0	1802	3.1	bdl	18	0.10	2.2	5.7	1.8	44	16	193	64	270	524	93	18142	44	453	0.016169753	575
Gt0332 026	125	8.0	891	4.5	0.02	31	0.15	2.8	4.6	0.4	24	8.0	97	34	146	238	40	14652	25	96	0.903888331	722
Gt0332 027	123	1.8	814	3.9	0.03	33	0.23	3.2	4.6	0.4	21	6.6	81	29	132	251	47	14014	77	68	0.265789719	611
Gt0332 028	153	11	1609	7.1	0.07	13	0.39	6.7	10	0.9	46	14	168	59	254	451	79	13858	117	361	1.04310827	750
Gt0332 029	156	9.1	2157	8.5	0.03	28	0.13	2.6	7.9	2.7	71	25	271	76	266	372	54	19179	244	696	0.959636191	733
Gt0332 030	73	18	256	1.5	0.04	8	0.13	2.1	2.6	0.7	10	2.9	31	9.1	33	47	7.3	12003	0.50	7.1	1.253629001	795
Gt0332 031	106	6.2	686	2.0	0.06	45	0.23	3.2	4.6	0.8	20	5.5	67	24	106	199	37	13144	115	111	0.789716169	700
Gt0332 033	91	5.3	819	3.0	0.07	11	0.12	2.4	4.0	0.7	21	6.8	84	30	129	230	40	13460	24	96	0.728288268	689
Gt0332 034	967	39	7108	24	4.6	34	2.2	15	11	4.2	63	30	493	223	1266	3611	696	33329	44	4137	1.59212312	877
Gt0332 035	118	14	778	8.8	0.01	30	0.18	3.1	4.7	0.5	22	6.8	79	28	124	219	40	15717	108	290	1.157080809	774
Gt0332 036	2929	17	1878	11	3.8	39	2.9	23	14	1.9	50	14	177	67	306	533	95	13870	195	438	1.232525512	790
Gt0332 037	56	bdl	302	1.2	0.09	21	0.20	2.8	3.2	0.7	10	2.7	31	11	48	96	18	11363	17	18	bdl	
Gt0332 038	4754	5.0	635	1.2	0.53	33	2.3	28	17	5.0	38	7.8	74	23	93	154	27	10533	47	38	0.694706402	683
Gt0332 039	95	2.5	537	6.8	0.03	22	0.23	3.3	5.5	0.3	23	6.6	68	20	75	103	17	14927	19	135	0.39315191	631
Gt0332 040	145	11	1658	13	0.08	22	0.20	3.9	6.1	0.4	36	12	154	59	273	494	88	14381	193	406	1.052586702	752
Gt0332 041	50	151	374	5.8	0.15	24	0.20	3.4	5.5	0.7	22	5.4	49	14	52	72	12	14819	13	132	2.178634801	1053
Gt0332 042	33	18	366	5.4	0.05	18	0.19	3.3	4.7	0.4	20	5.3	51	14	46	52	8	15096	16	168	1.261846578	797
Gt0332 043	194	11	2081	5.2	0.20	15	0.39	6.2	9.4	1.2	51	16	202	74	327	563	99	12659	114	218	1.058710446	753
Gt0332 044	117	5.3	972	9.5	0.07	16	0.11	1.7	2.7	0.2	17	6.4	85	34	165	332	61	15647	106	370	0.726617297	689
Gt0332 045	92	22	976	5.8	0.09	12	0.12	1.9	3.0	0.4	19	6.6	88	35	164	324	59	14811	69	247	1.338619267	814
Gt0332 046	153	12	1592	3.5	0.06	9	0.33	5.4	9.4	1.5	46	14	165	58	251	428	77	12165	38	72	1.095834104	761
Gt0332 047	192	64	1089	11	0.09	18	0.14	2.0	3.1	0.2	17	6.3	89	37	187	414	81	15475	247	698	1.804898427	935
Gt0332 048	130	3.2	1474	8.8	0.03	19	0.14	2.4	4.4	0.3	26	9.2	128	51	245	487	89	15351	195	464	0.506379204	650
Gt0332 049	87	22	239	1.3	0.04	20	0.15	1.8	1.8	0.5	7	2.1	23	8.3	39	83	16	12113	5.2	13	1.334855881	814
Gt0332 051	74	6	454	2.7	0.05	27	0.14	2.1	2.9	0.6	13	3.7	45	17	75	152	28	12896	37	63	0.749366097	693
Gt0332 052	129	bdl	956	2.1	0.08	44	1.0	13	14	3.2	41	11	109	35	145	259	45	11846	95	80	bdl	
Gt0332 053	73	19	379	1.3	0.06	21	0.20	2.8	3.2	0.82	12	3.4	40	14	62	124	23	10248	10	10	1.269906469	799
Gt0332 055	109	7.0	779	8.4	0.04	14	0.09	1.7	2.4	0.17	13	5.1	68	27	132	271	49	15701	80	282	0.845070784	711
Gt0332 056	147	7.0	708	5.3	0.06	12	0.12	1.8	2.9	0.26	16	5.5	72	26	119	209	38	14217	17	65	0.845419222	711
Gt0332 057	196	23	1996	30	0.14	40	0.26	4.3	7.5	0.37	42	14	188	71	324	603	106	14402	315	655	1.36165927	820
Gt0332 058	101	7	1303	11	0.17	25	0.29	4.1	6.2	0.36	30	10	127	47	211	386	69	14869	182	467	0.86014947	713
Gt0332 059	88	19	715	8.6	0.06	19	0.13	2.4	3.5	0.25	18	5.8	72	26	116	218	39	15180	62	250	1.284174333	802
Gt0332 060	93	7.7	1041	6.2	0.04	12	0.15	2.7	4.2	0.47	24	7.9	101	37	171	316	56	14114	54	101	0.885497713	718
Gt0332 061	bdl	bdl	1381	16	0.01	1.2	0.06	1.1	0.69	0.34	6.5	4.1	85	44	280	741	156	19846	2.9	305	bdl	
Gt0332 062	41	19	365	1.3	0.07	1.5	0.05	0.79	0.52	0.18	2.9	1.3	22	11	69	202	54	17636	2.0	174	1.280145715	801
Gt0332 063	64	bdl	375	1.6	0.05	1.4	0.06	0.74	0.52	0.14	2.9	1.5	24	11	74	210	56	18693	2.3	171	bdl	
Gt0332 064	31	bdl	326	1.2	0.05	1.6	0.07	0.71	0.53	0.15	3.1	1.3	21	10	63	187	51	18171	2.6	264	bdl	
Gt0332 065	54	171	336	1.4	0.03	1.7	0.04	1.0	0.56	0.15	2.5	1.2	21	10	68	211	58	19682	1.9	279	2.232300797	1072
Gt0332 066	bdl	bdl	437	1.3	0.05	1.5	0.02	0.88	0.58	0.22	3.7	1.6	27	14	86	263	71	19842	1.6	181	bdl	
Gt0332 067	bdl	bdl	362	1.1	0.03	1.5	0.06	0.63	0.57	0.17	2.5	1.5	22	11	72	208	57	17884	1.8	141	bdl	
Gt0405 migmatite Rio Pasabien 15°02'21.4" 89°41'02.4"																						

DOI: 10.1344/105.000001695

TABLE I | **Continued**

Sample number	P	Ti	Y	Nb	La	Ce	Pr	Nd	Sm	Eu	Gd	Tb	Dy	Ho	Er	Yb	Lu	Hf	Th	U	Log(Ti)	T°C
Gt0405 002	-	5.99	1026	6.4	0.02	16	0.07	1.5	3.4	0.78	19	6.8	87	34	157	315	61	12295	160	460	0.777501147	698
Gt0405 003	-	10	1032	1.5	0.00	3.2	0.09	1.6	3.4	0.16	21	7.1	93	35	156	280	54	12666	38	112	1.006260193	742
Gt0405 004	-	13	870	1.5	0.02	9.4	0.12	1.7	3.3	0.50	17	5.7	74	29	135	275	56	11596	98	171	1.116968356	765
Gt0405 005	-	16	781	1.8	0.03	5.9	0.08	1.4	2.3	0.18	13	4.9	69	26	126	245	49	11986	78	201	1.207314235	785
Gt0405 006	-	21	1236	1.6	0.05	3.9	0.18	2.7	5.3	0.31	26	8.9	115	43	190	354	68	10483	78	193	1.325347534	811
Gt0405 007	-	14	1095	4.3	0.26	14	0.18	1.9	3.1	0.15	19	7.0	94	37	177	348	67	13022	204	531	1.139556347	770
Gt0405 008	-	bdl	625	1.7	0.01	9.4	0.04	1.0	1.6	0.15	11	3.9	54	21	102	210	41	11412	56	150	bdl	
Gt0405 011	-	bdl	812	2.4	0.03	9.3	0.08	1.3	2.2	0.24	14	5.1	70	28	129	258	50	11798	80	222	bdl	
Gt0405 012	-	5.86	1260	5.7	0.34	15	0.34	4.0	5.0	0.27	24	8.6	113	43	203	395	76	13094	224	637	0.767977955	696
Gt0405 014	-	12.6	1507	3.1	0.34	18	0.41	4.7	7.6	1.2	38	12	141	50	225	417	79	11634	327	674	1.100910944	762
Gt0405 015	-	bdl	1890	9.3	0.70	14	0.38	3.4	5.0	0.57	29	12	165	64	310	676	132	13640	386	2792	bdl	
Gt0405 017	-	7.98	1277	4.7	0.04	24	0.18	3.3	6.1	0.98	32	9.6	120	44	193	369	71	11760	334	650	0.901998803	722
Gt0405 018	-	63	1091	3.9	0.05	13	0.12	1.9	3.8	0.25	21	7.5	100	38	172	333	63	12019	115	250	1.802549922	934
Gt0405 019	-	12	2435	4.0	61	194	24	120	38	3.3	89	22	248	84	350	611	114	12264	585	870	1.092074453	760
Gt0405 020	-	1.11	1090	5.1	0.03	16	0.10	1.7	3.6	0.60	21	7.2	93	36	174	375	76	12309	221	794	0.043410358	578
Gt0405 021	-	bdl	996	3.7	0.01	15	0.11	1.5	3.1	0.15	19	6.5	88	34	158	312	60	11693	147	359	bdl	
Gt0405 023	-	12	1067	2.1	5.7	24	1.8	10.0	5.6	0.51	24	7.6	98	37	166	319	61	10494	86	174	1.066278244	755
Gt0405 024	-	3.66	727	11	0.14	2.8	0.08	0.82	0.95	0.12	7.1	3.0	51	23	133	386	83	14260	41	1681	0.563937352	660
Gt0405 025	-	bdl	673	2.2	0.03	12	0.06	0.93	1.3	0.26	10	3.6	53	22	112	278	59	13447	165	492	bdl	
Gt0405 026	-	bdl	618	3.3	0.02	4.4	0.07	1.05	1.2	0.22	9.4	3.2	49	21	108	277	61	12576	56	608	bdl	
Gt0405 028	-	5.34	1858	2.5	0.02	12	0.30	5.00	9.5	1.4	49	16	190	69	298	524	99	10135	207	437	0.727853861	689
Gt0405 029	-	2.29	1198	5.1	2.87	11	1.01	5.41	2.7	0.15	14	5.9	91	39	198	476	96	15684	130	1802	0.359597789	626
Gt0405 030	-	10	1610	2.7	1.91	25	0.89	7.95	10	1.6	44	14	153	54	235	412	79	11647	344	481	1.017094093	744
Gt0405 031	-	8.22	1108	2.0	6.87	27	2.75	15.41	7.3	0.63	26	8.3	103	39	174	326	63	9735	112	215	0.914636804	724
Gt0405 034	-	1.08	833	5.8	0.03	42	0.09	1.09	1.8	0.45	11	3.8	56	25	135	382	89	12054	464	670	0.03361381	577
Gt0405 035	-	2.48	2237	2.9	0.07	25	0.28	4.61	8.7	1.8	51	17	218	81	361	650	124	10592	157	211	0.3939897	632
Gt0405 036	-	3.31	2141	8.8	0.36	2.2	0.17	1.49	2.0	0.48	16	8.6	151	69	381	954	200	19038	88	5406	0.520450964	652
Gt0405 038	-	7.11	2866	12.6	0.32	1.7	0.19	1.67	2.4	0.53	23	13	214	90	487	1407	294	18771	87	8019	0.851755007	712
Gt0405 039	-	bdl	2775	10.8	0.54	3.6	0.23	1.96	2.7	0.65	22	12	199	90	475	1114	226	17361	127	6488	bdl	
Gt0405 042	-	6.39	2648	10.9	0.95	3.2	0.42	3.14	3.5	0.90	27	13	200	82	427	1257	294	17651	62	5585	0.805750805	703
Gt0405 044	-	bdl	2250	7.2	0.03	1.7	0.05	0.60	1.4	0.12	17	9.5	165	76	373	692	132	16700	84	4382	bdl	
Gt0405 045	-	14.8	3148	27	225	470	56	239	79	2	126	31	318	102	463	1321	306	30804	133	3509	1.17033651	777
Gt0405 046	-	1.45	464	1.87	0.02	0.21	0.04	0.48	0.34	0.05	3	1.66	32	15	87	282	65	23831	9	1632	0.162698655	596
Gt0405 048	-	4.35	2526	10.13	0.05	2.01	0.05	0.65	1.72	0.12	17	10	178	82	442	1090	225	18507	117	6442	0.638377542	673
Gt0405 050	-	4.67	1458	4.56	0.02	1.67	0.05	0.56	0.84	0.08	9	5.7	104	48	247	528	104	17076	41	2762	0.669399534	678
Gt0405 051	-	3.62	1907	6.3	0.59	2.3	0.34	2.7	2.2	0.42	15	8.1	136	61	325	801	170	19009	60	3765	0.558921999	659
Gt0405 052	-	4.34	6890	20	18	71	5.4	30	24	12	125	47	636	227	972	1906	366	18246	243	8981	0.637967392	673
Gt0405 053	-	bdl	1255	6.5	0.21	1.22	0.10	1.10	1.12	0.24	9.1	4.8	85	40	227	642	139	19232	33	2862	bdl	

Trace and REE elemental concentrations in ppm

Elemental concetrations are calibrated relative to the analysis of NIST 610 trace element standard glass

Zircon crystallization temperature calculated according to the method and formulas of Watson et al. (2006)

bdl: below detection limits

-: not determined

DOI: 10.1344/105.000001695

TABLE II | **U-Pb data, Chuacús Complex, Central Guatemala**

				CORRECTED RATIOS[2]									CORRECTED AGES (Ma)								
Sample number	U[1] (ppm)	Th[1] (ppm)	Th/U	$^{207}Pb/^{206}Pb$	±1σ[3]	$^{207}Pb/^{235}U$	±1σ[3]	$^{206}Pb/^{238}U$	±1σ[3]	$^{208}Pb/^{232}Th$	±1σ[3]	Rho	$^{206}Pb/^{238}U$	±1σ	$^{207}Pb/^{235}U$	±1σ	$^{207}Pb/^{206}Pb$	±1σ	Best age (Ma)	±1σ	% disc
Gt0309 Metapelite. 15°01'18.3" 90°42'53.9"																					
Gt0309 001	513	169	0.33	0.07275	0.0007	1.6085	0.0169	0.16054	0.0007	0.0485	0.0006	0.4	960	4	974	7	1007	19	960	4	1.4
Gt0309 002	608	114	0.19	0.07076	0.0007	1.39806	0.0176	0.14329	0.0009	0.04344	0.0003	0.6	863	5	888	7	951	19	863	5	2.8
Gt0309 003	711	84	0.12	0.07209	0.0007	1.3886	0.0156	0.13987	0.0009	0.04342	0.0006	0.6	844	5	884	7	988	17	844	5	4.5
~~Gt0309 004~~	~~149~~	~~63~~	0.42	~~0.07434~~	~~0.0013~~	~~1.193~~	~~0.0215~~	~~0.11649~~	~~0.0007~~	~~0.05555~~	~~0.0008~~	~~0.3~~	~~710~~	~~4~~	~~797~~	~~10~~	~~1051~~	~~34~~	~~710~~	~~4~~	~~10.9~~
Gt0309 005	206	68	0.33	0.07429	0.001	1.73	0.0279	0.16889	0.001	0.05092	0.0003	0.5	1006	6	1020	10	1049	27	1049	27	4.1
Gt0309 006	1050	132	0.13	0.06966	0.0007	1.18858	0.0211	0.12374	0.0015	0.03759	0.0005	0.8	752	9	795	10	918	21	752	9	5.4
Gt0309 007	612	220	0.36	0.07094	0.0009	1.39745	0.0228	0.14286	0.0009	0.0433	0.0003	0.5	861	5	888	10	956	26	861	5	3.0
Gt0309 008	836	131	0.16	0.07062	0.0008	1.34313	0.0255	0.13793	0.0017	0.04183	0.0005	0.7	833	10	865	11	947	24	833	10	3.7
~~Gt0309 010~~	~~2026~~	~~149~~	0.07	~~0.06442~~	~~0.0006~~	~~0.65529~~	~~0.0073~~	~~0.07377~~	~~0.0004~~	~~0.02264~~	~~0.0002~~	~~0.5~~	~~459~~	~~2~~	~~512~~	~~4~~	~~756~~	~~19~~	~~459~~	~~2~~	~~10.4~~
Gt0309 011	116	46	0.40	0.07292	0.0012	1.54793	0.0288	0.15397	0.0008	0.04652	0.0003	0.3	923	5	950	11	1012	32	923	5	2.8
Gt0309 012	374	87	0.23	0.07208	0.0008	1.55972	0.0191	0.15693	0.0008	0.04747	0.0002	0.5	940	4	954	8	988	20	940	4	1.5
Gt0309 013	528	152	0.29	0.07177	0.0008	1.5127	0.0187	0.15287	0.0007	0.04627	0.0002	0.4	917	4	936	8	979	21	917	4	2.0
Gt0309 014	1052	131	0.12	0.07115	0.0007	1.20944	0.0146	0.12329	0.0008	0.03738	0.0002	0.5	749	4	805	7	962	19	749	4	7.0
Gt0309 015	1935	240	0.12	0.06482	0.0007	0.7824	0.0109	0.08754	0.0007	0.02683	0.0002	0.7	541	4	587	6	769	20	541	4	7.8
~~Gt0309 016~~	~~2333~~	~~294~~	0.13	~~0.06877~~	~~0.0006~~	~~0.91113~~	~~0.0092~~	~~0.09609~~	~~0.0004~~	~~0.02926~~	~~0.0001~~	~~0.5~~	~~591~~	~~2~~	~~658~~	~~5~~	~~892~~	~~17~~	~~591~~	~~2~~	~~10.2~~
Gt0309 017	2338	267	0.11	0.06523	0.0006	0.90328	0.0096	0.10044	0.0004	0.03074	0.0002	0.5	617	2	653	5	782	19	617	2	5.5
Gt0309 018	500	95	0.19	0.07003	0.0007	1.45129	0.0169	0.1503	0.0007	0.04561	0.0002	0.4	903	4	910	7	929	20	903	4	0.8
Gt0309 019	1989	232	0.12	0.06731	0.0006	0.86275	0.0093	0.09296	0.0004	0.02837	0.0001	0.5	573	3	632	5	847	18	573	3	9.3
Gt0309 020	~~1373~~	~~118~~	0.09	~~0.06569~~	~~0.0007~~	~~0.70301~~	~~0.0085~~	~~0.07762~~	~~0.0005~~	~~0.02377~~	~~0.0002~~	~~0.6~~	~~482~~	~~3~~	~~541~~	~~5~~	~~797~~	~~19~~	~~482~~	~~3~~	~~10.9~~
Gt0309 021	1911	441	0.23	0.06266	0.0008	0.87439	0.0125	0.1012	0.0005	0.03111	0.0002	0.4	621	3	638	7	697	25	621	3	2.7
Gt0309 022	2845	526	0.18	0.06539	0.0007	0.77848	0.0115	0.08635	0.0008	0.02644	0.0002	0.7	534	4	585	7	787	20	534	4	8.7
Gt0309 023	344	110	0.32	0.06807	0.0009	1.24584	0.0197	0.13273	0.0008	0.04041	0.0003	0.5	803	5	822	9	871	25	803	5	2.3
Gt0309 024	211	86	0.41	0.07151	0.0012	1.50035	0.0332	0.15217	0.0015	0.04607	0.0005	0.6	913	9	931	13	972	32	913	9	1.9
Gt0309 025	2263	230	0.10	0.06597	0.0007	0.80816	0.0095	0.08885	0.0005	0.02718	0.0002	0.5	549	3	601	5	805	20	549	3	8.7
Gt0309 026	324	53	0.16	0.07077	0.0008	1.4934	0.0189	0.15304	0.0008	0.04639	0.0002	0.4	918	4	928	8	951	22	918	4	1.1
Gt0309 027	223	85	0.38	0.07276	0.0009	1.237	0.0163	0.12352	0.0007	0.05038	0.0007	0.4	751	4	818	7	1007	23	751	4	8.2
Gt0309 028	1059	244	0.23	0.06491	0.0009	1.02931	0.0283	0.11502	0.0021	0.03521	0.0006	0.9	702	12	719	14	771	26	702	12	2.4
Gt0309 029	377	174	0.46	0.07313	0.0009	1.68506	0.0289	0.16713	0.0014	0.05047	0.0004	0.6	996	7	1003	11	1017	24	1017	24	2.1
Gt0309 030	2175	174	0.08	0.0709	0.0006	1.20841	0.0117	0.12362	0.0005	0.03749	0.0002	0.4	751	3	804	5	954	17	751	3	6.6
Gt0309 031	2165	611	0.28	0.06682	0.0007	1.17028	0.0144	0.12703	0.0006	0.03876	0.0002	0.5	771	4	787	7	832	20	771	4	2.0
Gt0309 032	1163	194	0.17	0.06862	0.0007	1.18335	0.0143	0.12507	0.0008	0.03806	0.0002	0.6	760	4	793	7	887	19	760	4	4.2
~~Gt0309 033~~	~~1449~~	~~81~~	0.06	~~0.06498~~	~~0.0007~~	~~0.63163~~	~~0.0106~~	~~0.0705~~	~~0.0008~~	~~0.02163~~	~~0.0003~~	~~0.8~~	~~439~~	~~5~~	~~497~~	~~7~~	~~774~~	~~21~~	~~439~~	~~5~~	~~11.7~~
Gt0309 034	1192	262	0.22	0.05999	0.0012	0.77025	0.0183	0.09312	0.0008	0.02876	0.0003	0.6	574	5	580	10	603	40	574	5	1.0
Gt0309 035	1298	73	0.06	0.05975	0.0008	0.41601	0.0071	0.0505	0.0005	0.01565	0.0002	0.6	318	3	353	5	595	27	318	3	9.9
Gt0309 036	168	102	0.61	0.07596	0.0008	1.8654	0.0237	0.1784	0.0011	0.05643	0.0008	0.5	1058	6	1069	8	1094	21	1094	21	3.3
Gt0309 037	770	173	0.22	0.07233	0.0007	1.6352	0.0167	0.16423	0.0007	0.04907	0.0006	0.4	980	4	984	6	995	18	980	4	0.4
Gt0309 038	665	127	0.19	0.07154	0.0007	1.5825	0.016	0.16056	0.0006	0.04891	0.0006	0.4	960	4	963	6	973	18	960	4	0.3
Gt0309 039	1000	160	0.16	0.06974	0.0007	1.21279	0.0129	0.12612	0.0005	0.03831	0.0002	0.4	766	3	806	6	921	18	766	3	5.0
Gt0309 040	1099	256	0.23	0.07194	0.0007	1.36868	0.0152	0.13799	0.0007	0.04177	0.0002	0.5	833	4	876	7	984	18	833	4	4.9
Gt0309 041	1284	266	0.21	0.06968	0.0007	1.19079	0.0147	0.12395	0.0008	0.03765	0.0002	0.6	753	4	796	7	919	19	753	4	5.4
Gt0309 042	3076	447	0.15	0.06126	0.0007	0.55771	0.0109	0.06603	0.0009	0.02037	0.0003	0.8	412	5	450	7	648	22	412	5	8.4
Gt0309 043	2338	249	0.11	0.06917	0.0006	1.15717	0.0124	0.12133	0.0007	0.03689	0.0002	0.5	738	4	781	6	904	17	738	4	5.5
Gt0309 044	2621	442	0.17	0.06386	0.0007	0.84272	0.0103	0.0957	0.0005	0.02936	0.0002	0.5	589	3	621	6	737	21	589	3	5.2
Gt0309 045	1821	166	0.09	0.06447	0.0006	0.67321	0.0076	0.07574	0.0003	0.02324	0.0001	0.4	471	2	523	5	757	21	471	2	9.9
Gt0309 046	239	132	0.56	0.06915	0.0011	1.37892	0.025	0.14462	0.0008	0.04395	0.0002	0.4	871	5	880	11	903	30	871	5	1.0
Gt0309 047	1195	344	0.29	0.0632	0.0008	0.85747	0.0134	0.09839	0.0006	0.03022	0.0002	0.6	605	4	629	7	715	25	605	4	3.8
Gt0309 048	1619	164	0.10	0.07074	0.0006	1.183	0.012	0.12146	0.0006	0.03703	0.0005	0.5	739	3	793	6	950	17	739	3	6.8
Gt0309 049	901	137	0.15	0.07107	0.0007	1.33183	0.0162	0.13591	0.0009	0.04119	0.0003	0.5	821	5	860	7	959	20	821	5	4.5
Gt0309 050	1721	340	0.20	0.07043	0.0007	1.29521	0.0147	0.13338	0.0007	0.04046	0.0002	0.5	807	4	844	6	941	19	807	4	4.4
Gt0309 051	128	44	0.34	0.07231	0.0011	1.58898	0.0289	0.15937	0.001	0.04819	0.0003	0.4	953	6	966	11	995	32	953	6	1.3
Gt0309 052	1976	165	0.08	0.05361	0.0007	0.37253	0.0057	0.0504	0.0003	0.01578	0.0002	0.5	317	2	322	4	355	29	317	2	1.6
Gt0309 053	219	43	0.20	0.05838	0.0013	0.70152	0.0184	0.08715	0.0008	0.027	0.0004	0.5	539	4	540	11	544	49	539	4	0.2
~~Gt0309 054~~	~~195~~	~~98~~	0.50	~~0.07673~~	~~0.0008~~	~~1.7662~~	~~0.0231~~	~~0.16728~~	~~0.0012~~	~~0.05818~~	~~0.0008~~	~~0.6~~	~~997~~	~~7~~	~~1033~~	~~8~~	~~1114~~	~~22~~	~~1114~~	~~22~~	~~10.5~~
Gt0309 055	1391	228	0.16	0.06399	0.0007	0.90895	0.0115	0.10302	0.0005	0.03159	0.0002	0.4	632	3	656	6	741	23	632	3	3.7
Gt0309 056	120	67	0.56	0.0697	0.0017	1.51657	0.0415	0.15781	0.0012	0.04791	0.0004	0.4	945	7	937	17	919	48	945	7	-0.9
Gt0309 057	421	118	0.28	0.0699	0.0009	1.46318	0.0219	0.15182	0.0008	0.04608	0.0003	0.5	911	5	915	9	925	26	911	5	0.4
Gt0309 058	781	244	0.31	0.06398	0.0012	1.05048	0.0355	0.11908	0.0022	0.03651	0.0006	0.9	725	13	729	18	741	41	725	13	0.5
Gt0309 059	1140	363	0.32	0.06707	0.0008	1.09909	0.0164	0.11884	0.0006	0.03625	0.0002	0.5	724	4	753	8	840	26	724	4	3.9

DOI: 10.1344/105.000001695

TABLE II | **Continued**

				CORRECTED RATIOS[2]									CORRECTED AGES (Ma)								
Sample number	U[1] (ppm)	Th[1] (ppm)	Th/U	$^{207}Pb/^{206}Pb$	±1σ[3]	$^{207}Pb/^{235}U$	±1σ[3]	$^{206}Pb/^{238}U$	±1σ[3]	$^{208}Pb/^{232}Th$	±1σ[3]	Rho	$^{206}Pb/^{238}U$	±1σ	$^{207}Pb/^{235}U$	±1σ	$^{207}Pb/^{206}Pb$	±1σ	Best age (Ma)	±1σ	% disc
Gt0309 062	2150	301	0.14	0.06962	0.0007	1.20089	0.0142	0.12511	0.0008	0.03801	0.0003	0.6	760	5	801	7	917	19	760	5	5.1
Gt0309 063	2891	610	0.21	0.06872	0.0007	1.10261	0.0123	0.11636	0.0006	0.03541	0.0002	0.5	710	3	755	6	890	19	710	3	6.0
Gt0309 064	69	27	0.39	0.07397	0.0013	1.7762	0.0339	0.17459	0.0015	0.0535	0.0009	0.5	1037	8	1037	12	1041	34	1041	34	0.4
Gt0309 065	834	184	0.22	0.07246	0.0007	1.6023	0.0247	0.16024	0.0019	0.05002	0.0008	0.8	958	11	971	10	999	19	958	11	1.3
Gt0309 066	418	103	0.25	0.0728	0.0007	1.6214	0.0179	0.16179	0.0008	0.0491	0.0006	0.4	967	4	979	7	1008	20	967	4	1.2
Gt0309 067	1303	99	0.08	0.06959	0.0006	1.25083	0.0134	0.13035	0.0007	0.0396	0.0002	0.5	790	4	824	6	916	19	790	4	4.1
Gt0309 068	70	38	0.54	0.07745	0.0019	1.96302	0.0532	0.18382	0.0012	0.05516	0.0003	0.3	1088	6	1103	18	1133	48	1133	48	4.0
Gt0309 069	1704	305	0.18	0.06991	0.0006	1.27777	0.0137	0.13256	0.0006	0.04025	0.0002	0.5	802	4	836	6	926	19	802	4	4.1
Gt0309 070	1061	199	0.19	0.06964	0.0007	1.37946	0.0157	0.14366	0.0008	0.04362	0.0002	0.5	865	4	880	7	918	19	865	4	1.7
~~Gt0309 072~~	~~145~~	~~57~~	0.39	~~0.07335~~	~~0.0011~~	~~1.0519~~	~~0.0176~~	~~0.10411~~	~~0.0008~~	~~0.05376~~	~~0.0008~~	~~0.4~~	~~638~~	~~4~~	~~730~~	~~9~~	~~1024~~	~~30~~	~~638~~	~~4~~	~~12.6~~
Gt0309 073	557	177	0.32	0.07272	0.0007	1.4359	0.0156	0.14339	0.0007	0.05463	0.0007	0.4	864	4	904	7	1006	20	864	4	4.4
Gt0309 074	460	117	0.25	0.0698	0.0008	1.4622	0.0206	0.15192	0.0009	0.04612	0.0003	0.5	912	5	915	8	923	24	912	5	0.3
~~Gt0309 075~~	~~206~~	~~93~~	0.45	~~0.07702~~	~~0.0008~~	~~2.2426~~	~~0.0269~~	~~0.2115~~	~~0.0014~~	~~0.06238~~	~~0.0008~~	~~0.6~~	~~1237~~	~~7~~	~~1194~~	~~8~~	~~1122~~	~~20~~	~~1122~~	~~20~~	~~-10.2~~
Gt0309 076	438	70	0.16	0.06329	0.0009	0.96965	0.0161	0.11112	0.0008	0.03411	0.0003	0.5	679	4	688	8	718	29	679	4	1.3
Gt0309 077	1024	207	0.20	0.07032	0.0007	1.43331	0.0165	0.14782	0.0007	0.04484	0.0002	0.5	889	4	903	7	938	20	889	4	1.6
Gt0309 078	305	181	0.59	0.0757	0.0011	1.79123	0.03	0.17161	0.0009	0.05163	0.0002	0.4	1021	5	1042	11	1087	28	1087	28	6.1
Gt0309 079	2298	272	0.12	0.0668	0.0006	0.88747	0.0097	0.09636	0.0005	0.02943	0.0002	0.5	593	3	645	5	831	19	593	3	8.1
Gt0309 080	1642	172	0.10	0.06342	0.0008	0.73323	0.0103	0.08385	0.0004	0.02576	0.0002	0.5	519	2	558	6	722	26	519	2	7.0
Gt0309 081	2406	585	0.24	0.07026	0.0006	1.2602	0.0124	0.13027	0.0006	0.04004	0.0005	0.5	789	3	828	6	936	18	789	3	4.7
Gt0309 082	1966	132	0.07	0.0684	0.0006	1.03396	0.0101	0.10963	0.0005	0.03338	0.0002	0.4	671	3	721	5	881	18	671	3	6.9
Gt0309 083	1469	125	0.08	0.06836	0.0006	1.07376	0.0109	0.11393	0.0005	0.03469	0.0002	0.4	696	3	741	5	879	19	696	3	6.1
Gt0309 084	138	48	0.35	0.06605	0.0012	1.27482	0.0307	0.13998	0.0014	0.04275	0.0004	0.6	845	8	835	14	808	38	845	8	-1.2
Gt0309 085	620	72	0.12	0.0657	0.0008	0.92525	0.0165	0.10214	0.001	0.03124	0.0004	0.7	627	6	665	9	797	26	627	6	5.7
Gt0309 086	1435	208	0.15	0.06441	0.0007	0.78902	0.011	0.08884	0.0006	0.02724	0.0002	0.6	549	4	591	6	755	23	549	4	7.1
Gt0309 087	539	66	0.12	0.06927	0.0009	1.24087	0.0241	0.12992	0.0017	0.03949	0.0005	0.7	787	10	819	11	907	25	787	10	3.9
Gt0309 088	929	204	0.22	0.07171	0.0007	1.5355	0.0164	0.15557	0.0008	0.04779	0.0007	0.5	932	5	945	7	978	19	932	5	1.4
Gt0309 089	1791	366	0.20	0.0681	0.0007	0.97778	0.0116	0.10413	0.0006	0.03173	0.0002	0.5	639	3	692	6	872	20	639	3	7.7
Gt0309 090	1353	143	0.11	0.06894	0.0007	1.08311	0.0129	0.11395	0.0006	0.03467	0.0002	0.5	696	3	745	6	897	21	696	3	6.6
Gt0309 091	296	89	0.30	0.06221	0.001	0.96661	0.0186	0.11269	0.0008	0.03465	0.0003	0.5	688	4	687	10	681	33	688	4	-0.1
Gt0309 092	121	78	0.65	0.07674	0.0009	1.9414	0.0263	0.18392	0.0012	0.05619	0.0008	0.5	1088	6	1095	9	1114	24	1114	24	2.3
Gt0309 093	658	115	0.17	0.07008	0.0008	1.31643	0.0172	0.13624	0.0008	0.04135	0.0003	0.5	823	5	853	8	931	22	823	5	3.5
Gt0309 094	861	170	0.20	0.07153	0.0007	1.5424	0.0158	0.15665	0.0007	0.04723	0.0006	0.4	938	4	947	6	973	19	938	4	1.0
Gt0309 095	268	19	0.07	0.06324	0.001	0.67264	0.0135	0.07715	0.0009	0.02371	0.0004	0.6	479	5	522	8	716	32	479	5	8.2
Gt0309 096	122	69	0.57	0.07116	0.0015	1.51462	0.0361	0.15438	0.001	0.04676	0.0003	0.4	925	6	936	15	962	41	925	6	1.2
Gt0309 097	1067	316	0.30	0.06754	0.0009	1.09296	0.0175	0.11737	0.0008	0.03578	0.0003	0.5	715	5	750	8	854	26	715	5	4.7
Gt0309 098	144	73	0.51	0.07628	0.0011	2.0268	0.0349	0.1933	0.0019	0.05936	0.001	0.6	1139	10	1125	12	1102	28	1102	28	-3.4
Gt0309 099	1683	163	0.10	0.06514	0.0008	0.74321	0.0114	0.08275	0.0007	0.02535	0.0003	0.6	513	4	564	7	779	24	513	4	9.0
Gt0309 100	2512	510	0.20	0.07061	0.0007	1.3206	0.0155	0.13598	0.0008	0.04188	0.0005	0.5	822	5	855	7	946	19	822	5	3.9
Gt0315, pegmatite. 14°58'15.49" 90°43'29.88"																					
~~Gt0315 001~~	~~40.4~~	~~0.67~~	~~0.0167~~	~~0.0586~~	~~0.0075~~	~~0.265~~	~~0.0366~~	~~0.0328~~	~~0.0008~~	~~0.01016~~	~~0.0032~~	~~0.4~~	~~208~~	~~5~~	~~239~~	~~29~~	~~552~~	~~266~~	~~208~~	~~5~~	~~13.0~~
Gt0315 002	45.3	0.06	0.0014	0.05629	0.0051	0.08862	0.0083	0.01142	0.0002	0.00355	0.0068	0.3	73	1	86	8	464	188	73	1	5.1
Gt0315 003	45.9	0.05	0.0012	0.05546	0.0043	0.08815	0.007	0.01153	0.0002	0.00359	0.0057	0.2	74	1	86	7	431	173	74	1	5.1
Gt0315 004	787.4	0.12	0.0002	0.04882	0.001	0.07367	0.0015	0.01097	7E-05	0.03316	0.0163	0.3	70.3	0.4	72	1	139	44	70.3	0.4	2.4
Gt0315 005	43.0	0.04	0.0010	0.06416	0.0058	0.1015	0.0095	0.01147	0.0002	0.00352	0.0033	0.3	74	1	98	9	747	179	74	1	15.7
~~Gt0315 006~~	~~37.2~~	~~0.04~~	~~0.0009~~	~~0.06058~~	~~0.0055~~	~~0.09603~~	~~0.009~~	~~0.01166~~	~~0.0003~~	~~0.34938~~	~~0.2166~~	~~0.2~~	~~75~~	~~2~~	~~93~~	~~8~~	~~624~~	~~185~~	~~75~~	~~2~~	~~19.4~~
Gt0315 007	139.0	0.01	0.0001	0.05178	0.002	0.07489	0.003	0.01054	0.0001	0.65195	0.2608	0.2	67.6	0.6	73	3	276	83	67.6	0.6	7.4
Gt0315 008	577.3	0.09	0.0002	0.04882	0.0011	0.07382	0.0018	0.01095	6E-05	0.06517	0.0287	0.3	70.2	0.4	72	2	139	50	70.2	0.4	2.5
Gt0315 009	20.9	0.01	0.0003	0.07087	0.0092	0.11384	0.0154	0.01198	0.0004	4.2841	2.0564	0.3	77	3	109	14	954	255	77	3	15.8
Gt0315 010	157.8	60.15	0.3811	0.07311	0.0009	1.622	0.0213	0.16095	0.0009	0.04788	0.0008	0.4	962	5	979	8	1017	24	962	5	1.7
Gt0315 011	100.6	11.39	0.1132	0.07225	0.0009	1.6325	0.0232	0.16385	0.0009	0.04699	0.0011	0.4	978	5	983	9	993	26	978	5	0.5
~~Gt0315 012~~	~~36.4~~	~~0.04~~	~~0.0010~~	~~0.05784~~	~~0.0035~~	~~0.09493~~	~~0.006~~	~~0.01201~~	~~0.0002~~	~~0.17545~~	~~0.1456~~	~~0.3~~	~~77~~	~~1~~	~~92~~	~~6~~	~~524~~	~~133~~	~~77~~	~~1~~	~~16.3~~
Gt0315 013	68.5	0.01	0.0001	0.05505	0.0029	0.08345	0.0045	0.01098	0.0001	0.9008	0.4684	0.2	70.4	0.8	81	4	414	116	70.4	0.8	7.5
Gt0315 014	73.1	24.81	0.3392	0.07299	0.0012	1.6273	0.0286	0.16157	0.0012	0.04731	0.001	0.4	965	6	981	11	1014	32	965	6	1.6
Gt0315 015	82.9	50.34	0.6071	0.07247	0.0009	1.6642	0.0234	0.16667	0.0009	0.04811	0.0009	0.4	994	5	995	9	999	26	994	5	0.1
Gt0315 016	64.0	30.13	0.4708	0.07235	0.0011	1.5771	0.0255	0.15818	0.001	0.04595	0.0009	0.4	947	5	961	10	996	30	947	5	1.5
Gt0315 017	49.3	0.02	0.0004	0.05231	0.0059	0.08262	0.0095	0.01146	0.0002	0.0036	0.1502	0.2	73	1	81	9	299	233	73	1	9.9
Gt0315 018	840.8	215.91	0.2568	0.07165	0.0007	1.39	0.0173	0.14059	0.0011	0.04331	0.0008	0.6	848	6	885	7	976	20	848	6	4.2
Gt0315 019	158.8	72.51	0.4565	0.07237	0.0009	1.6101	0.0215	0.16143	0.0009	0.0474	0.0008	0.4	965	5	974	8	996	24	965	5	0.9
Gt0315 020	24.6	2.57	0.1044	0.07468	0.0017	1.6513	0.0401	0.16075	0.0013	0.04808	0.0018	0.3	961	7	990	15	1060	46	1060	46	9.3
Gt0315 021	37.8	0.02	0.0004	0.05942	0.0065	0.0925	0.0105	0.01167	0.0003	1.0194	0.3364	0.2	75	2	90	10	583	226	75	2	3.8
Gt0315 022	73.8	17.69	0.2397	0.0724	0.001	1.6983	0.0272	0.17012	0.0013	0.0518	0.001	0.5	1013	7	1008	10	997	28	997	28	-0.5
Gt0315 023	329.9	127.26	0.3857	0.07219	0.0008	1.6278	0.0202	0.16345	0.0009	0.04831	0.0008	0.5	976	5	981	8	991	22	976	5	0.5
Gt0315 024	585.9	329.42	0.5622	0.07171	0.0007	1.6004	0.0181	0.16177	0.0009	0.04673	0.0008	0.5	967	5	970	7	978	20	967	5	0.3
~~Gt0315 025~~	~~746~~	~~239~~	0.32	~~0.07135~~	~~0.0007~~	~~1.4909~~	~~0.0166~~	~~0.1515~~	~~0.0008~~	~~0.04452~~	~~0.0008~~	~~0.5~~	~~909~~	~~5~~	~~927~~	~~7~~	~~967~~	~~20~~	~~909~~	~~5~~	~~1.9~~

DOI: 10.1344/105.000001695

TABLE II | **Continued**

				CORRECTED RATIOS[2]									CORRECTED AGES (Ma)								
Sample number	U[1] (ppm)	Th[1] (ppm)	Th/U	$^{207}Pb/^{206}Pb$	±1σ[3]	$^{207}Pb/^{235}U$	±1σ[3]	$^{206}Pb/^{238}U$	±1σ[3]	$^{208}Pb/^{232}Th$	±1σ[3]	Rho	$^{206}Pb/^{238}U$	±1σ	$^{207}Pb/^{235}U$	±1σ	$^{207}Pb/^{206}Pb$	±1σ	Best age (Ma)	±1σ	% disc
Gt0315 026	325.9	28.94	0.0888	0.0693	0.0007	1.27239	0.0172	0.13316	0.0011	0.04045	0.0003	0.6	806	6	833	8	908	21	806	6	3.2
Gt0315 027	752.0	255.40	0.3396	0.07097	0.0007	1.4249	0.0156	0.14563	0.0008	0.04186	0.0007	0.5	876	4	899	7	957	19	876	4	2.6
Gt0315 028	393.4	169.07	0.4297	0.07131	0.0007	1.4685	0.0164	0.14923	0.0008	0.04353	0.0007	0.5	897	4	918	7	966	20	897	4	2.3
Gt0315 029	154.2	95.55	0.6196	0.07219	0.0009	1.6024	0.0212	0.161	0.0009	0.04586	0.0008	0.4	962	5	971	8	991	24	962	5	0.9
Gt0315 030	139.9	59.93	0.4283	0.07179	0.0008	1.6533	0.0202	0.16699	0.0009	0.04836	0.0009	0.4	996	5	991	8	980	21	996	5	-0.5
Gt0318, High pressure arkose. 14°54'56.01" 90°37'54.62"																					
Gt0318 002	44	17	0.38	0.07184	0.0012	1.5254	0.0278	0.1544	0.001	0.04742	0.0008	0.4	926	6	941	11	981	33	926	6	1.6
~~Gt0318 003~~	~~118~~	~~3~~	0.03	~~0.06103~~	~~0.0018~~	~~0.16126~~	~~0.005~~	~~0.01912~~	~~0.0002~~	~~0.03933~~	~~0.0016~~	~~0.3~~	~~122~~	~~1~~	~~152~~	~~4~~	~~640~~	~~59~~	~~122~~	~~1~~	~~19.7~~
Gt0318 004	38	13	0.34	0.07337	0.0016	1.576	0.0395	0.15558	0.0019	0.04884	0.0009	0.5	932	10	961	16	1024	45	932	10	3.0
Gt0318 005	67	19	0.28	0.07043	0.0011	1.5083	0.0247	0.15541	0.001	0.04687	0.0007	0.4	931	6	934	10	941	31	931	6	0.3
Gt0318 006	153	3	0.02	0.0481	0.0015	0.13049	0.0041	0.01968	0.0002	0.00624	0.0012	0.3	126	1	125	4	104	70	126	1	-0.8
Gt0318 007	84	29	0.34	0.07242	0.001	1.52632	0.0238	0.15286	0.0008	0.04621	0.0002	0.4	917	4	941	10	998	29	917	4	2.6
Gt0318 008	91	30	0.33	0.06521	0.0012	1.13073	0.0365	0.12575	0.0022	0.03847	0.0006	0.8	764	13	768	17	781	41	764	13	0.5
Gt0318 009	258	45	0.17	0.05717	0.0007	0.63994	0.0098	0.08127	0.0007	0.02457	0.0005	0.5	504	4	502	6	498	29	504	4	-0.4
Gt0318 010	228	73	0.32	0.05035	0.0009	0.19844	0.0042	0.02862	0.0003	0.01172	0.0002	0.5	182	2	184	4	211	39	182	2	1.1
Gt0318 011	67	31	0.47	0.072	0.001	1.6672	0.0269	0.16831	0.0014	0.05035	0.0008	0.5	1003	7	996	10	986	26	1003	7	-1.7
~~Gt0318 012~~	~~45~~	~~9~~	0.19	~~0.07127~~	~~0.0024~~	~~0.82519~~	~~0.0441~~	~~0.08463~~	~~0.0036~~	~~0.05066~~	~~0.0039~~	~~0.8~~	~~524~~	~~21~~	~~611~~	~~25~~	~~965~~	~~62~~	~~524~~	~~21~~	~~14.2~~
Gt0318 013	127	86	0.67	0.05165	0.001	0.27432	0.0055	0.03865	0.0002	0.01244	0.0002	0.3	244	1	246	4	270	40	244	1	0.8
Gt0318 014	61	67	1.11	0.05187	0.0016	0.28999	0.0094	0.04074	0.0004	0.01267	0.0002	0.3	257	2	259	7	280	66	257	2	0.8
Gt0318 015	183	79	0.43	0.07012	0.0008	1.4349	0.0172	0.14864	0.0007	0.04746	0.0006	0.4	893	4	904	7	932	21	893	4	1.2
~~Gt0318 016~~	~~108~~	~~2~~	0.02	~~0.06483~~	~~0.0026~~	~~0.17144~~	~~0.0073~~	~~0.0196~~	~~0.0003~~	~~0.27703~~	~~0.0693~~	~~0.4~~	~~125~~	~~2~~	~~161~~	~~6~~	~~769~~	~~78~~	~~125~~	~~2~~	~~22.4~~
Gt0318 017	113	19	0.17	0.05155	0.0012	0.24863	0.0065	0.03498	0.0004	0.011	0.0001	0.4	222	2	225	5	266	49	222	2	1.3
Gt0318 018	43	42	0.97	0.05298	0.0018	0.28298	0.0099	0.0389	0.0003	0.01186	0.0002	0.2	246	2	253	8	328	73	246	2	2.8
Gt0318 019	59	8	0.14	0.065	0.0016	1.01867	0.0379	0.11367	0.0026	0.03478	0.0008	0.7	694	15	713	19	774	52	694	15	2.7
Gt0318 020	64	13	0.21	0.06064	0.0013	0.89087	0.0224	0.10654	0.0011	0.03286	0.0004	0.5	653	7	647	12	627	42	653	7	-0.9
Gt0318 021	474	102	0.21	0.07107	0.0007	1.5468	0.0165	0.15803	0.0008	0.04752	0.0006	0.5	946	5	949	7	959	18	946	5	0.3
~~Gt0318 022~~	~~3~~	~~0~~	0.01	~~0.41014~~	~~0.0357~~	~~1.8124~~	~~0.1846~~	~~0.03441~~	~~0.0018~~	~~2.4419~~	~~0.2686~~	~~0.5~~	~~218~~	~~11~~	~~1050~~	~~67~~	~~3947~~	~~134~~	~~3947~~	~~134~~	~~94.5~~
Gt0318 023	69	22	0.32	0.06952	0.001	1.5598	0.0235	0.16289	0.0009	0.0475	0.0007	0.4	973	5	954	9	914	27	973	5	-2.0
~~Gt0318 024~~	~~20~~	~~0~~	0.02	~~0.25912~~	~~0.0382~~	~~0.9964~~	~~0.1524~~	~~0.02789~~	~~0.0014~~	~~0.00742~~	~~0.0004~~	~~0.3~~	~~177~~	~~9~~	~~702~~	~~78~~	~~3241~~	~~227~~	~~3241~~	~~227~~	~~94.5~~
Gt0318 025	34	36	1.07	0.05304	0.0018	0.28224	0.0101	0.03892	0.0004	0.01167	0.0002	0.3	246	3	252	8	331	73	246	3	2.4
Gt0318 026	50	38	0.77	0.05269	0.002	0.27174	0.0119	0.0374	0.0004	0.01173	0.0001	0.4	237	3	244	10	316	82	237	3	2.9
Gt0318 027	54	45	0.83	0.05384	0.0019	0.21146	0.0076	0.02858	0.0002	0.00908	0.0002	0.2	182	1	195	6	364	75	182	1	6.7
Gt0318 028	196	74	0.38	0.05225	0.0012	0.13492	0.0032	0.01883	0.0002	0.00856	0.0001	0.4	120	1	129	3	296	48	120	1	7.0
Gt0318 029	31	25	0.81	0.05586	0.0021	0.28161	0.011	0.03699	0.0004	0.01233	0.0002	0.3	234	3	252	9	447	78	234	3	7.1
Gt0318 030	59	7	0.11	0.04914	0.0025	0.14797	0.0079	0.02165	0.0004	0.02083	0.0052	0.3	138	2	140	7	155	107	138	2	1.4
Gt0318 031	79	24	0.30	0.07475	0.0011	1.8076	0.027	0.17543	0.0009	0.049	0.0007	0.3	1042	5	1048	10	1062	27	1062	27	1.9
~~Gt0318 032~~	~~89~~	~~20~~	0.22	~~0.05641~~	~~0.0049~~	~~0.20335~~	~~0.0186~~	~~0.02614~~	~~0.0004~~	~~0.00813~~	~~0.0002~~	~~0.4~~	~~166~~	~~3~~	~~188~~	~~16~~	~~469~~	~~182~~	~~166~~	~~3~~	~~11.7~~
Gt0318 033	75	16	0.21	0.07333	0.001	1.7008	0.0241	0.1684	0.001	0.04997	0.0008	0.4	1003	5	1009	9	1023	25	1023	25	2.0
~~Gt0318 034~~	~~178~~	~~6~~	0.04	~~0.06709~~	~~0.001~~	~~0.67012~~	~~0.0142~~	~~0.07244~~	~~0.0011~~	~~0.02209~~	~~0.0004~~	~~0.8~~	~~451~~	~~7~~	~~521~~	~~9~~	~~841~~	~~28~~	~~451~~	~~7~~	~~13.4~~
Gt0318 035	82	66	0.80	0.05088	0.0011	0.30734	0.0068	0.04399	0.0003	0.01325	0.0002	0.3	278	2	272	5	235	46	278	2	-2.2
Gt0318 037	48	40	0.82	0.05452	0.0032	0.29172	0.0183	0.03881	0.0004	0.01212	0.0001	0.2	245	2	260	14	393	126	245	2	5.8
Gt0318 038	71	69	0.96	0.05143	0.0012	0.28315	0.0072	0.04001	0.0003	0.01249	0.0002	0.3	253	2	253	6	260	52	253	2	0.0
Gt0318 039	131	81	0.62	0.05194	0.001	0.30048	0.0063	0.04198	0.0002	0.01342	0.0002	0.3	265	1	267	5	283	43	265	1	0.7
~~Gt0318 040~~	~~135~~	~~41~~	0.31	~~0.06567~~	~~0.0017~~	~~0.20833~~	~~0.0057~~	~~0.02308~~	~~0.0002~~	~~0.01522~~	~~0.0003~~	~~0.3~~	~~147~~	~~1~~	~~192~~	~~5~~	~~796~~	~~52~~	~~147~~	~~1~~	~~23.4~~
Gt0318 041	47	32	0.69	0.07168	0.001	1.4735	0.0222	0.14927	0.0008	0.04616	0.0007	0.4	897	5	920	9	977	27	897	5	2.5
Gt0318 042	35	13	0.37	0.06799	0.0016	1.16322	0.036	0.12408	0.0018	0.03778	0.0005	0.6	754	10	783	17	868	45	754	10	3.7
~~Gt0318 043~~	~~29~~	~~11~~	0.36	~~0.06969~~	~~0.0018~~	~~0.83151~~	~~0.0232~~	~~0.08693~~	~~0.0009~~	~~0.03859~~	~~0.0008~~	~~0.4~~	~~537~~	~~5~~	~~614~~	~~13~~	~~919~~	~~51~~	~~537~~	~~5~~	~~12.5~~
Gt0318 044	25	10	0.40	0.06737	0.0016	1.30853	0.0361	0.14087	0.0013	0.04293	0.0004	0.4	850	7	849	16	849	47	850	7	-0.1
Gt0318 045	112	127	1.13	0.05096	0.001	0.26984	0.0056	0.03845	0.0002	0.01186	0.0002	0.3	243	1	243	5	239	47	243	1	0.0
Gt0318 046	214	139	0.65	0.05306	0.0008	0.28424	0.0045	0.03892	0.0002	0.01214	0.0002	0.3	246	1	254	4	331	35	246	1	3.1
Gt0318 047	130	96	0.74	0.05107	0.0016	0.2644	0.009	0.03755	0.0002	0.01182	7E-05	0.3	238	1	238	7	244	73	238	1	0.0
Gt0319, deformed diorite. 14°57'56.9" 90°32'49"																					
Gt0319 001	174	190	1.10	0.05289	0.0013	0.24357	0.0061	0.03347	0.0002	0.01064	0.0002	0.3	212	1	221	5	324	52	212	1	4.1
~~Gt0319 002~~	~~115~~	~~80~~	0.70	~~0.05611~~	~~0.0033~~	~~0.21867~~	~~0.0128~~	~~0.02816~~	~~0.0003~~	~~0.00956~~	~~0.0002~~	~~0.2~~	~~179~~	~~2~~	~~201~~	~~11~~	~~457~~	~~124~~	~~179~~	~~2~~	~~10.9~~
Gt0319 003	152	130	0.85	0.05278	0.0029	0.26072	0.0158	0.03583	0.0004	0.01123	0.0001	0.3	227	3	235	13	319	121	227	3	3.4
Gt0319 004	193	137	0.71	0.05156	0.0014	0.23067	0.0071	0.03245	0.0002	0.0102	6E-05	0.3	206	1	211	6	266	62	206	1	2.4
Gt0319 005	193	236	1.22	0.05357	0.001	0.26817	0.0053	0.03628	0.0002	0.01145	0.0002	0.3	230	1	241	4	353	41	230	1	4.6
Gt0319 006	454	836	1.84	0.05139	0.0008	0.24465	0.0039	0.03455	0.0002	0.01056	0.0001	0.3	219	1	222	3	258	33	219	1	1.4
Gt0319 007	155	266	1.72	0.05448	0.0012	0.25889	0.0059	0.03454	0.0002	0.01079	0.0001	0.3	219	1	234	5	391	47	219	1	6.4
Gt0319 008	88	74	0.84	0.05705	0.0014	0.26964	0.0071	0.03432	0.0003	0.01086	0.0002	0.3	218	2	242	6	494	53	218	2	9.9
Gt0319 009	33	12	0.37	0.05327	0.0022	0.26483	0.0116	0.03623	0.0004	0.01115	0.0004	0.3	229	3	239	9	340	92	229	3	4.2
~~Gt0319 010~~	~~235~~	~~396~~	1.68	~~0.05158~~	~~0.0011~~	~~0.24375~~	~~0.0056~~	~~0.0343~~	~~0.0002~~	~~0.01052~~	~~0.0001~~	~~0.3~~	~~217~~	~~1~~	~~221~~	~~5~~	~~267~~	~~48~~	~~217~~	~~1~~	~~1.8~~

DOI: 10.1344/105.000001695

TABLE II | **Continued**

				CORRECTED RATIOS[2]									CORRECTED AGES (Ma)								
Sample number	U[1] (ppm)	Th[1] (ppm)	Th/U	$^{207}Pb/^{206}Pb$	±1σ[3]	$^{207}Pb/^{235}U$	±1σ[3]	$^{206}Pb/^{238}U$	±1σ[3]	$^{208}Pb/^{232}Th$	±1σ[3]	Rho	$^{206}Pb/^{238}U$	±1σ	$^{207}Pb/^{235}U$	±1σ	$^{207}Pb/^{206}Pb$	±1σ	Best age (Ma)	±1σ	% disc
Gt0319 011	52	56	1.07	0.05677	0.0031	0.29136	0.0165	0.0374	0.0006	0.0116	0.0003	0.3	237	4	260	13	483	115	237	4	8.8
Gt0319 012	94	81	0.86	0.05524	0.0021	0.26562	0.0109	0.03488	0.0003	0.01088	9E-05	0.3	221	2	239	9	422	80	221	2	7.5
~~Gt0319 013~~	~~56~~	~~32~~	0.58	~~0.06762~~	~~0.0078~~	~~0.30529~~	~~0.0359~~	~~0.03274~~	~~0.0004~~	~~0.00997~~	~~0.0002~~	~~0.1~~	~~208~~	~~2~~	~~271~~	~~28~~	~~857~~	~~237~~	~~208~~	~~2~~	~~23.2~~
Gt0319 014	70	25	0.36	0.05173	0.0019	0.25589	0.0094	0.03597	0.0003	0.0124	0.0003	0.2	228	2	231	8	273	79	228	2	1.3
Gt0319 015	172	165	0.96	0.05349	0.0009	0.25762	0.0047	0.03497	0.0002	0.01103	0.0001	0.3	222	1	233	4	350	37	222	1	4.7
Gt0319 016	236	197	0.84	0.05147	0.001	0.24512	0.0051	0.03452	0.0002	0.01096	0.0002	0.3	219	1	223	4	262	44	219	1	1.8
Gt0319 017	205	265	1.29	0.0506	0.0009	0.25273	0.0045	0.03628	0.0002	0.0114	0.0002	0.3	230	1	229	4	223	38	230	1	-0.4
Gt0319 018	189	108	0.57	0.05215	0.0013	0.23961	0.0067	0.03332	0.0002	0.01046	7E-05	0.3	211	1	218	5	292	55	211	1	3.2
Gt0319 019	142	119	0.83	0.0527	0.0012	0.2614	0.006	0.0361	0.0002	0.01165	0.0002	0.3	229	1	236	5	316	48	229	1	3.0
~~Gt0319 020~~	~~103~~	~~144~~	1.41	~~0.05883~~	~~0.0015~~	~~0.28057~~	~~0.0073~~	~~0.0348~~	~~0.0003~~	~~0.01096~~	~~0.0001~~	~~0.3~~	~~221~~	~~2~~	~~251~~	~~6~~	~~561~~	~~52~~	~~221~~	~~2~~	~~12.0~~
Gt0319 021	199	203	1.02	0.05139	0.0008	0.2563	0.0044	0.03617	0.0002	0.01122	0.0002	0.4	229	1	232	4	258	35	229	1	1.3
Gt0319 022	35	12	0.34	0.05252	0.0023	0.26265	0.0119	0.03662	0.0004	0.01251	0.0009	0.2	232	2	237	10	308	96	232	2	2.1
Gt0319 023	287	538	1.88	0.05323	0.0008	0.26353	0.0043	0.03594	0.0002	0.01128	0.0002	0.4	228	1	238	3	339	33	228	1	4.2
Gt0319 024	83	96	1.16	0.04737	0.0048	0.2222	0.024	0.03402	0.0004	0.01081	0.0005	0.2	216	2	204	20	68	205	216	2	-5.9
Gt0319 025	36	23	0.64	0.05263	0.0027	0.25519	0.0134	0.03556	0.0004	0.01111	0.0003	0.2	225	3	231	11	313	111	225	3	2.6
Gt0319 026	232	365	1.57	0.05194	0.001	0.25638	0.0053	0.03581	0.0002	0.01116	0.0002	0.3	227	1	232	4	283	44	227	1	2.2
Gt0319 027	191	124	0.65	0.05074	0.001	0.25107	0.005	0.0359	0.0002	0.01077	0.0002	0.3	227	1	227	4	229	42	227	1	0.0
Gt0319 028	172	67	0.39	0.05307	0.0012	0.24866	0.0059	0.03406	0.0002	0.0112	0.0002	0.3	216	1	225	5	332	50	216	1	4.0
Gt0319 029	68	65	0.97	0.05209	0.0016	0.25531	0.008	0.03553	0.0003	0.01128	0.0002	0.3	225	2	231	6	289	66	225	2	2.6
Gt0319 030	137	133	0.97	0.05098	0.0013	0.2512	0.0065	0.03574	0.0003	0.01127	0.0002	0.3	226	2	228	5	240	55	226	2	0.9
Gt0319 031	152	155	1.02	0.05144	0.0011	0.24822	0.0057	0.03491	0.0002	0.01085	0.0002	0.3	221	1	225	5	261	48	221	1	1.8
~~Gt0319 032~~	~~28~~	~~10~~	0.36	~~0.05679~~	~~0.0029~~	~~0.24238~~	~~0.0139~~	~~0.03095~~	~~0.0005~~	~~0.00962~~	~~0.0002~~	~~0.4~~	~~197~~	~~3~~	~~220~~	~~11~~	~~484~~	~~110~~	~~197~~	~~3~~	~~10.5~~
Gt0319 033	168	171	1.02	0.0514	0.0009	0.25164	0.0048	0.03549	0.0002	0.01125	0.0002	0.3	225	1	228	4	259	40	225	1	1.3
Gt0319 034	137	161	1.17	0.05066	0.0014	0.25581	0.0077	0.03656	0.0004	0.01433	0.0003	0.4	231	2	231	6	225	62	231	2	0.0
~~Gt0319 036~~	~~466~~	~~59~~	0.13	~~0.0742~~	~~0.0007~~	~~1.7391~~	~~0.0186~~	~~0.16985~~	~~0.0008~~	~~0.05144~~	~~0.0007~~	~~0.5~~	~~1011~~	~~4~~	~~1023~~	~~7~~	~~1047~~	~~18~~	~~1047~~	~~18~~	~~3.4~~
Gt0319 037	52	55	1.06	0.05236	0.002	0.25793	0.0101	0.03573	0.0003	0.01116	0.0002	0.2	226	2	233	8	301	83	226	2	3.0
Gt0319 038	143	155	1.08	0.05019	0.0011	0.24805	0.0054	0.03592	0.0002	0.01107	0.0002	0.3	227	1	225	4	204	47	227	1	-0.9
Gt0319 039	273	289	1.06	0.05157	0.0008	0.25105	0.0043	0.03531	0.0002	0.01099	0.0002	0.4	224	1	227	4	266	35	224	1	1.3
Gt0319 040	56	39	0.70	0.05428	0.0019	0.28059	0.0101	0.03755	0.0005	0.01275	0.0003	0.3	238	3	251	8	383	74	238	3	5.2
Gt0319 041	92	100	1.09	0.05594	0.0011	0.26826	0.0056	0.0347	0.0002	0.01091	0.0002	0.3	220	1	241	5	450	43	220	1	8.7
Gt0319 042	77	42	0.55	0.0535	0.0017	0.2575	0.0083	0.03501	0.0003	0.01079	0.0003	0.3	222	2	233	7	350	67	222	2	4.7
Gt0319 043	108	121	1.12	0.05685	0.0013	0.2743	0.0066	0.03498	0.0003	0.01108	0.0002	0.3	222	2	246	5	486	49	222	2	9.8
Gt0319 044	188	248	1.32	0.05517	0.0012	0.24863	0.0057	0.03263	0.0002	0.01032	0.0001	0.3	207	1	225	5	419	47	207	1	8.0
Gt0319 045	67	76	1.12	0.05234	0.0024	0.24291	0.0131	0.03366	0.0004	0.01057	0.0001	0.3	213	2	221	11	300	101	213	2	3.6
Gt0319 046	230	315	1.37	0.05512	0.0011	0.25823	0.0052	0.03387	0.0002	0.01082	0.0002	0.3	215	1	233	4	417	41	215	1	7.7
Gt0319 047	129	163	1.27	0.05076	0.0016	0.24913	0.0079	0.0356	0.0003	0.01124	0.0002	0.2	226	2	226	6	230	69	226	2	0.0
Gt0319 048	55	51	0.92	0.05411	0.0033	0.26475	0.0174	0.03549	0.0004	0.01109	0.0001	0.3	225	2	238	14	376	131	225	2	5.5
Gt0319 049	105	73	0.70	0.05038	0.0012	0.25276	0.0063	0.03638	0.0002	0.01162	0.0002	0.3	230	1	229	5	213	53	230	1	-0.4
Gt0319 050	87	125	1.43	0.05655	0.0018	0.27414	0.0088	0.03533	0.0003	0.01121	0.0002	0.3	224	2	246	7	474	66	224	2	8.9
Gt0319 051	243	271	1.12	0.05041	0.0008	0.24875	0.0043	0.03579	0.0002	0.01118	0.0002	0.4	227	1	226	3	214	36	227	1	-0.4
~~Gt0319 052~~	~~302~~	~~440~~	1.46	~~0.01213~~	~~0.0009~~	~~0.05978~~	~~0.0046~~	~~0.03502~~	~~0.0002~~	~~0.01103~~	~~0.0001~~	~~0.1~~	~~222~~	~~1~~	~~59~~	4	~~-1199~~	~~53~~	~~222~~	~~1~~	~~-276.3~~
Gt0319 053	77	83	1.08	0.05724	0.0021	0.30673	0.0116	0.03885	0.0003	0.01591	0.0004	0.2	246	2	272	9	501	78	246	2	9.6
Gt0319 054	257	424	1.65	0.0508	0.0009	0.23996	0.0047	0.03426	0.0003	0.0106	0.0001	0.4	217	2	218	4	232	40	217	2	0.5
Gt0319 055	203	228	1.12	0.05244	0.0012	0.25258	0.0058	0.03492	0.0002	0.01068	0.0002	0.3	221	1	229	5	305	48	221	1	3.5
Gt0319 056	188	219	1.17	0.05084	0.001	0.25009	0.005	0.03564	0.0002	0.01112	0.0002	0.3	226	1	227	4	234	42	226	1	0.4
Gt0319 057	163	168	1.03	0.05094	0.001	0.24975	0.0051	0.03557	0.0003	0.01088	0.0001	0.4	225	2	226	4	238	42	225	2	0.4
Gt0319 058	118	91	0.78	0.05032	0.0012	0.24181	0.0058	0.03495	0.0003	0.01083	0.0002	0.3	221	2	220	5	210	51	221	2	-0.5
Gt0319 059	337	461	1.37	0.05028	0.0007	0.24739	0.0037	0.03568	0.0002	0.01109	0.0001	0.4	226	1	224	3	208	31	226	1	-0.9
Gt0319 060	71	86	1.20	0.05629	0.0015	0.27013	0.0077	0.0349	0.0003	0.01088	0.0002	0.3	221	2	243	6	464	57	221	2	9.1
Gt0320, deformed gabbro. 14°57'56.9" 90°32'49"																					
Gt0320 001	159	219	1.38	0.05193	0.0013	0.2425	0.0063	0.03389	0.0003	0.01083	0.0002	0.3	215	2	220	5	282	57	215	2	2.3
Gt0320 002	127	165	1.30	0.05008	0.002	0.22839	0.0102	0.03308	0.0003	0.01044	8E-05	0.3	210	2	209	8	198	84	210	2	-0.5
Gt0320 003	218	147	0.67	0.05047	0.0009	0.24749	0.0047	0.03559	0.0002	0.01153	0.0002	0.3	225	1	225	4	217	41	225	1	0.0
Gt0320 006	32	17	0.54	0.05578	0.0026	0.26003	0.0123	0.03382	0.0004	0.01043	0.0003	0.2	214	2	235	10	444	101	214	2	8.9
Gt0320 008	34	26	0.76	0.05062	0.003	0.23971	0.0164	0.03434	0.0006	0.01082	0.0002	0.4	218	4	218	13	224	131	218	4	0.0
Gt0320 009	113	147	1.30	0.05359	0.0013	0.25896	0.0065	0.03509	0.0003	0.01086	0.0002	0.3	222	2	234	5	354	54	222	2	5.1
Gt0320 010	176	245	1.39	0.05617	0.001	0.26754	0.0051	0.0346	0.0002	0.01085	0.0001	0.3	219	1	241	4	459	37	219	1	9.1
Gt0320 011	80	97	1.22	0.05419	0.0015	0.26309	0.0074	0.03528	0.0003	0.01077	0.0002	0.3	224	2	237	6	379	56	224	2	5.5
Gt0320 012	99	125	1.26	0.05035	0.0013	0.24619	0.0066	0.03548	0.0003	0.01126	0.0002	0.3	225	2	223	5	211	56	225	2	-0.9
Gt0320 013	84	55	0.66	0.0523	0.0015	0.25756	0.0077	0.03574	0.0003	0.011	0.0002	0.2	226	2	233	6	299	62	226	2	3.0
Gt0320 014	75	53	0.70	0.05437	0.0016	0.26781	0.008	0.03571	0.0003	0.01137	0.0002	0.3	226	2	241	6	386	61	226	2	6.2
~~Gt0320 015~~	~~114~~	~~140~~	1.23	~~0.05915~~	~~0.0012~~	~~0.26566~~	~~0.0059~~	~~0.0326~~	~~0.0002~~	~~0.01097~~	~~0.0002~~	~~0.3~~	~~207~~	~~1~~	~~239~~	~~5~~	~~573~~	~~42~~	~~207~~	~~1~~	~~13.4~~
Gt0320 016	158	215	1.36	0.05474	0.0024	0.25174	0.0119	0.03336	0.0002	0.01041	7E-05	0.2	212	1	228	10	401	91	212	1	7.0
~~Gt0320 017~~	~~85~~	~~103~~	1.21	~~0.06418~~	~~0.002~~	~~0.28442~~	~~0.0092~~	~~0.03209~~	~~0.0003~~	~~0.01138~~	~~0.0002~~	~~0.3~~	~~204~~	~~2~~	~~254~~	~~7~~	~~748~~	~~65~~	~~204~~	~~2~~	~~19.7~~

DOI: 10.1344/105.000001695

TABLE II | **Continued**

				CORRECTED RATIOS[2]									CORRECTED AGES (Ma)								
Sample number	U[1] (ppm)	Th[1] (ppm)	Th/U	$^{207}Pb/^{206}Pb$	±1σ[3]	$^{207}Pb/^{235}U$	±1σ[3]	$^{206}Pb/^{238}U$	±1σ[3]	$^{208}Pb/^{232}Th$	±1σ[3]	Rho	$^{206}Pb/^{238}U$	±1σ	$^{207}Pb/^{235}U$	±1σ	$^{207}Pb/^{206}Pb$	±1σ	Best age (Ma)	±1σ	% disc
Gt0320 018	49	24	0.49	0.05201	0.0017	0.25288	0.0086	0.03528	0.0003	0.01138	0.0003	0.2	224	2	229	7	286	70	224	2	2.2
~~Gt0320 019~~	~~74~~	~~50~~	0.67	~~0.06414~~	~~0.0019~~	~~0.27876~~	~~0.0086~~	~~0.03149~~	~~0.0003~~	~~0.01253~~	~~0.0003~~	~~0.3~~	~~200~~	~~2~~	~~250~~	~~7~~	~~746~~	~~60~~	~~200~~	~~2~~	~~20.0~~
Gt0320 020	147	101	0.69	0.05243	0.0011	0.26328	0.0055	0.03647	0.0002	0.01154	0.0002	0.3	231	1	237	4	304	42	231	1	2.5
Gt0320 021	105	115	1.10	0.05131	0.0013	0.25308	0.0068	0.03583	0.0003	0.01126	0.0002	0.3	227	2	229	6	255	55	227	2	0.9
Gt0320 022	89	33	0.38	0.05156	0.0013	0.25543	0.0066	0.03599	0.0003	0.01245	0.0003	0.3	228	2	231	5	266	53	228	2	1.3
Gt0320 023	96	62	0.65	0.05087	0.0016	0.24895	0.0087	0.03549	0.0003	0.01118	9E-05	0.3	225	2	226	7	235	67	225	2	0.4
~~Gt0320 024~~	~~65~~	~~65~~	1.00	~~0.06372~~	~~0.0028~~	~~0.283~~	~~0.014~~	~~0.03221~~	~~0.0004~~	~~0.00988~~	~~0.0001~~	~~0.3~~	~~204~~	~~2~~	~~253~~	~~11~~	~~732~~	~~91~~	~~204~~	~~2~~	~~19.4~~
Gt0320 025	74	68	0.92	0.05165	0.0024	0.26023	0.0124	0.0366	0.0004	0.01163	0.0002	0.3	232	3	235	10	270	104	232	3	1.3
Gt0320 026	101	74	0.74	0.05144	0.0011	0.2544	0.006	0.03591	0.0003	0.01167	0.0002	0.4	227	2	230	5	261	47	227	2	1.3
Gt0320 027	67	79	1.17	0.0527	0.0016	0.26	0.0083	0.03585	0.0003	0.0113	0.0002	0.3	227	2	235	7	316	65	227	2	3.4
Gt0320 028	74	70	0.95	0.05382	0.0017	0.26713	0.0085	0.03596	0.0003	0.01153	0.0002	0.2	228	2	240	7	364	69	228	2	5.0
Gt0320 029	37	31	0.84	0.05355	0.0026	0.24643	0.0133	0.03338	0.0004	0.01045	0.0001	0.3	212	2	224	11	352	107	212	2	5.4
Gt0320 030	52	48	0.91	0.05399	0.0026	0.25513	0.0135	0.03427	0.0004	0.01072	0.0001	0.3	217	2	231	11	371	106	217	2	6.1
~~Gt0320 031~~	~~141~~	~~182~~	1.30	~~0.05767~~	~~0.0016~~	~~0.25175~~	~~0.0073~~	~~0.03159~~	~~0.0002~~	~~0.01064~~	~~0.0002~~	~~0.3~~	~~200~~	~~1~~	~~228~~	~~6~~	~~517~~	~~60~~	~~200~~	~~1~~	~~12.3~~
Gt0320 032	74	86	1.16	0.0553	0.0018	0.26207	0.0087	0.03457	0.0003	0.01093	0.0002	0.3	219	2	236	7	424	70	219	2	7.2
Gt0320 033	63	55	0.86	0.05121	0.0015	0.25297	0.0078	0.03599	0.0003	0.01101	0.0002	0.2	228	2	229	6	250	68	228	2	0.4
Gt0320 034	85	40	0.47	0.05283	0.0016	0.25602	0.0079	0.03528	0.0003	0.0117	0.0002	0.3	224	2	231	6	322	67	224	2	3.0
Gt0320 035	60	57	0.95	0.05174	0.0016	0.23192	0.0072	0.03259	0.0003	0.01055	0.0002	0.3	207	2	212	6	274	68	207	2	2.4
Gt0320 036	195	175	0.90	0.05192	0.0009	0.24781	0.0047	0.03461	0.0002	0.01048	0.0002	0.4	219	1	225	4	282	40	219	1	2.7
Gt0320 037	88	60	0.68	0.05301	0.0015	0.26491	0.0079	0.03625	0.0004	0.01132	0.0002	0.4	230	2	239	6	329	62	230	2	3.8
Gt0320 038	180	299	1.66	0.05174	0.0009	0.24858	0.0047	0.03491	0.0002	0.0106	0.0002	0.3	221	1	225	4	274	41	221	1	1.8
Gt0320 039	240	260	1.09	0.05072	0.0008	0.24573	0.0042	0.03517	0.0002	0.01101	0.0002	0.3	223	1	223	3	228	36	223	1	0.0
Gt0320 040	247	303	1.23	0.052	0.0008	0.25266	0.0043	0.03528	0.0002	0.01106	0.0001	0.3	224	1	229	3	285	36	224	1	2.2
Gt0320 041	185	120	0.65	0.05303	0.001	0.26095	0.0052	0.03571	0.0002	0.01141	0.0002	0.3	226	1	235	4	330	43	226	1	3.8
Gt0320 042	104	140	1.34	0.05217	0.0015	0.25558	0.0075	0.03561	0.0003	0.01131	0.0002	0.3	226	2	231	6	293	63	226	2	2.2
Gt0320 043	203	176	0.87	0.0521	0.0008	0.25456	0.0044	0.03549	0.0002	0.01096	0.0002	0.4	225	1	230	4	290	36	225	1	2.2
Gt0320 044	66	66	1.00	0.05325	0.0016	0.25415	0.0079	0.03475	0.0003	0.01079	0.0002	0.2	220	2	230	6	339	67	220	2	4.3
Gt0321, Agua Caliente River felsic orthogneiss. 14°56'07.8" 90°30'10.9"																					
Gt0321 006	431	218	0.51	0.05126	0.0017	0.24029	0.0088	0.03395	0.0004	0.01079	0.0003	0.4	215	3	219	7	253	72	215	3	1.8
Gt0321 007	179	95	0.53	0.05188	0.0032	0.20801	0.0136	0.02908	0.0004	0.00914	0.0001	0.3	185	3	192	11	280	127	185	3	3.6
~~Gt0321 008~~	~~188~~	~~160~~	0.85	~~0.06164~~	~~0.0036~~	~~0.21883~~	~~0.0133~~	~~0.02578~~	~~0.0005~~	~~0.00981~~	~~0.0003~~	~~0.3~~	~~164~~	~~3~~	~~201~~	~~11~~	~~662~~	~~115~~	~~164~~	~~3~~	~~18.4~~
Gt0321 009	74	46	0.62	0.05423	0.004	0.24508	0.0196	0.03277	0.0006	0.01024	0.0002	0.2	208	3	223	16	381	153	208	3	6.7
Gt0321 010	937	726	0.78	0.05064	0.0013	0.23386	0.0064	0.03344	0.0004	0.00932	0.0002	0.4	212	2	213	5	224	53	212	2	0.5
~~Gt0321 012~~	~~179~~	~~162~~	0.90	~~0.05747~~	~~0.0034~~	~~0.27443~~	~~0.0175~~	~~0.03463~~	~~0.0004~~	~~0.01075~~	~~0.0001~~	~~0.2~~	~~219~~	~~2~~	~~246~~	~~14~~	~~510~~	~~119~~	~~219~~	~~2~~	~~11.0~~
Gt0321 013	193	155	0.81	0.05688	0.0022	0.27085	0.0106	0.03462	0.0004	0.01024	0.0003	0.3	219	2	243	9	487	77	219	2	9.9
~~Gt0321 014~~	~~261~~	~~191~~	0.73	~~0.05866~~	~~0.0025~~	~~0.29499~~	~~0.0141~~	~~0.03647~~	~~0.0003~~	~~0.01129~~	~~9E-05~~	~~0.3~~	~~231~~	~~2~~	~~262~~	~~11~~	~~554~~	~~87~~	~~231~~	~~2~~	~~11.8~~
~~Gt0321 015~~	~~116~~	~~86~~	0.75	~~0.06322~~	~~0.0037~~	~~0.32086~~	~~0.0189~~	~~0.03664~~	~~0.0004~~	~~0.01119~~	~~0.0003~~	~~0.2~~	~~232~~	~~2~~	~~283~~	~~15~~	~~716~~	~~114~~	~~232~~	~~2~~	~~18.0~~
Gt0321 016	170	176	1.04	0.05536	0.0032	0.28553	0.0166	0.03745	0.0004	0.01045	0.0003	0.2	237	3	255	13	427	118	237	3	7.1
~~Gt0321 018~~	~~177~~	~~52~~	0.29	~~0.06761~~	~~0.0051~~	~~0.317~~	~~0.025~~	~~0.034~~	~~0.0004~~	~~0.01036~~	~~0.0003~~	~~0.3~~	~~216~~	~~2~~	~~280~~	~~19~~	~~857~~	~~144~~	~~216~~	~~2~~	~~22.9~~
Gt0321 019	162	128	0.79	0.05307	0.0022	0.26791	0.0119	0.03634	0.0005	0.01046	0.0003	0.3	230	3	241	9	332	88	230	3	4.6
Gt0321 020	263	185	0.70	0.0561	0.0031	0.30224	0.0178	0.03908	0.0003	0.01216	0.0001	0.2	247	2	268	14	456	113	247	2	7.8
Gt0321 021	635	574	0.90	0.05042	0.0014	0.23915	0.0071	0.03437	0.0003	0.00984	0.0002	0.3	218	2	218	6	214	60	218	2	0.0
Gt0321 022	747	666	0.89	0.05077	0.001	0.23847	0.0053	0.03399	0.0003	0.01053	0.0002	0.4	215	2	217	4	230	43	215	2	0.9
~~Gt0321 024~~	~~217~~	~~177~~	0.82	~~0.05957~~	~~0.0017~~	~~0.2938~~	~~0.0087~~	~~0.03582~~	~~0.0003~~	~~0.01142~~	~~0.0003~~	~~0.3~~	~~227~~	~~2~~	~~262~~	~~7~~	~~588~~	~~56~~	~~227~~	~~2~~	~~13.4~~
~~Gt0321 025~~	~~217~~	~~195~~	0.90	~~0.05706~~	~~0.0019~~	~~0.29318~~	~~0.0104~~	~~0.03711~~	~~0.0004~~	~~0.01073~~	~~0.0003~~	~~0.3~~	~~235~~	~~2~~	~~261~~	~~8~~	~~494~~	~~69~~	~~235~~	~~2~~	~~10.0~~
~~Gt0321 026~~	~~143~~	~~92~~	0.64	~~0.05845~~	~~0.0027~~	~~0.27575~~	~~0.013~~	~~0.03424~~	~~0.0004~~	~~0.01105~~	~~0.0003~~	~~0.2~~	~~217~~	~~2~~	~~247~~	~~10~~	~~547~~	~~93~~	~~217~~	~~2~~	~~12.1~~
Gt0321 027	121	91	0.76	0.05678	0.0023	0.30485	0.0129	0.03885	0.0004	0.01191	0.0003	0.3	246	3	270	10	483	83	246	3	8.9
~~Gt0321 028~~	~~213~~	~~163~~	0.76	~~0.06631~~	~~0.0057~~	~~0.33287~~	~~0.0306~~	~~0.03641~~	~~0.0005~~	~~0.01112~~	~~0.0001~~	~~0.2~~	~~231~~	~~3~~	~~292~~	~~23~~	~~816~~	~~167~~	~~231~~	~~3~~	~~20.9~~
Gt0321 030	167	66	0.39	0.04961	0.0053	0.22667	0.0254	0.03314	0.0005	0.01047	0.0007	0.2	210	3	207	21	177	215	210	3	-1.4
~~Gt0321 031~~	~~86~~	~~48~~	0.56	~~0.0671~~	~~0.0042~~	~~0.32966~~	~~0.021~~	~~0.03567~~	~~0.0005~~	~~0.01069~~	~~0.0004~~	~~0.2~~	~~226~~	~~3~~	~~289~~	~~16~~	~~841~~	~~124~~	~~226~~	~~3~~	~~21.8~~
~~Gt0321 032~~	~~147~~	~~100~~	0.68	~~0.05806~~	~~0.003~~	~~0.28733~~	~~0.0155~~	~~0.03586~~	~~0.0007~~	~~0.01169~~	~~0.0003~~	~~0.3~~	~~227~~	~~4~~	~~256~~	~~12~~	~~532~~	~~107~~	~~227~~	~~4~~	~~11.3~~
Gt0321 033	1942	147	0.08	0.07937	0.0013	1.96167	0.0343	0.17926	0.0012	0.05365	0.0004	0.4	1063	7	1102	12	1181	30	~~1181~~	~~30~~	10.0
Gt0321 034	464	297	0.64	0.06082	0.0013	0.48084	0.0114	0.05725	0.0005	0.01158	0.0005	0.4	359	3	399	8	633	45	~~359~~	~~3~~	10.0
~~Gt0321 036~~	~~379~~	~~151~~	0.40	~~0.07518~~	~~0.0014~~	~~1.6405~~	~~0.0329~~	~~0.1583~~	~~0.001~~	~~0.03983~~	~~0.0009~~	~~0.3~~	~~947~~	~~6~~	~~986~~	~~13~~	~~1073~~	~~36~~	~~1073~~	~~36~~	~~11.7~~
Gt0321 037	1453	291	0.20	0.07227	0.0012	1.5936	0.0283	0.15958	0.0012	0.05373	0.0011	0.4	954	7	968	11	994	31	~~954~~	~~7~~	1.4
~~Gt0321 038~~	~~201~~	~~197~~	0.98	~~0.06541~~	~~0.0018~~	~~0.31677~~	~~0.0094~~	~~0.0353~~	~~0.0004~~	~~0.01139~~	~~0.0003~~	~~0.3~~	~~224~~	~~2~~	~~279~~	~~7~~	~~788~~	~~55~~	~~224~~	~~2~~	~~19.7~~
~~Gt0321 039~~	~~186~~	~~218~~	1.17	~~0.08744~~	~~0.0061~~	~~0.40081~~	~~0.0324~~	~~0.03324~~	~~0.0007~~	~~0.00985~~	~~0.0002~~	~~0.4~~	~~211~~	~~4~~	~~342~~	~~23~~	~~1370~~	~~130~~	~~211~~	~~4~~	~~38.3~~
~~Gt0321 040~~	~~213~~	~~11~~	0.05	~~0.06939~~	~~0.0033~~	~~0.15727~~	~~0.0077~~	~~0.01641~~	~~0.0002~~	~~0.03163~~	~~0.0013~~	~~0.2~~	~~104.9~~	~~1~~	~~148~~	~~7~~	~~910~~	~~94~~	~~105~~	~~1~~	~~29.1~~
~~Gt0321 042~~	~~191~~	~~170~~	0.89	~~0.05955~~	~~0.0024~~	~~0.29392~~	~~0.0122~~	~~0.03582~~	~~0.0004~~	~~0.0114~~	~~0.0003~~	~~0.3~~	~~227~~	~~2~~	~~262~~	~~10~~	~~587~~	~~82~~	~~227~~	~~2~~	~~13.4~~
~~Gt0321 043~~	~~114~~	~~100~~	0.88	~~0.05677~~	~~0.0025~~	~~0.27619~~	~~0.0125~~	~~0.03523~~	~~0.0004~~	~~0.01114~~	~~0.0003~~	~~0.2~~	~~223~~	~~2~~	~~248~~	~~10~~	~~483~~	~~93~~	~~223~~	~~2~~	~~10.1~~
Gt0321 044	581	619	1.07	0.05299	0.0019	0.24317	0.0089	0.03328	0.0003	0.00966	0.0002	0.3	211	2	221	7	328	75	211	2	4.5
Gt0321 045	1163	959	0.82	0.04827	0.0012	0.22207	0.0058	0.03327	0.0003	0.0099	0.0003	0.4	211	2	204	5	113	53	211	2	-3.4
~~Gt0321 046~~	~~493~~	~~506~~	1.03	~~0.06325~~	~~0.0036~~	~~0.29986~~	~~0.0186~~	~~0.03438~~	~~0.0003~~	~~0.01055~~	~~0.0001~~	~~0.2~~	~~218~~	~~2~~	~~266~~	~~14~~	~~717~~	~~116~~	~~218~~	~~2~~	~~18.0~~
~~Gt0321 048~~	~~159~~	~~142~~	0.89	~~0.05622~~	~~0.0024~~	~~0.2632~~	~~0.0115~~	~~0.03386~~	~~0.0004~~	~~0.01024~~	~~0.0003~~	~~0.3~~	~~215~~	~~3~~	~~237~~	~~9~~	~~461~~	~~89~~	~~215~~	~~3~~	~~9.3~~

TABLE II | **Continued**

				CORRECTED RATIOS[2]									CORRECTED AGES (Ma)								
Sample number	U[1] (ppm)	Th[1] (ppm)	Th/U	$^{207}Pb/^{206}Pb$	$\pm1\sigma^3$	$^{207}Pb/^{235}U$	$\pm1\sigma^3$	$^{206}Pb/^{238}U$	$\pm1\sigma^3$	$^{208}Pb/^{232}Th$	$\pm1\sigma^3$	Rho	$^{206}Pb/^{238}U$	$\pm1\sigma$	$^{207}Pb/^{235}U$	$\pm1\sigma$	$^{207}Pb/^{206}Pb$	$\pm1\sigma$	Best age (Ma)	$\pm1\sigma$	% disc
Gt0321 049	206	202	0.98	0.05473	0.0022	0.28063	0.0118	0.03714	0.0004	0.01061	0.0003	0.2	235	2	251	9	401	87	235	2	6.4
~~Gt0321 050~~	~~185~~	~~116~~	0.63	~~0.06559~~	~~0.0046~~	~~0.32865~~	~~0.0233~~	~~0.03666~~	~~0.0004~~	~~0.01289~~	~~0.0009~~	~~0.2~~	~~232~~	~~3~~	~~289~~	~~18~~	~~793~~	~~142~~	~~232~~	~~3~~	~~19.7~~
Gt0321 051	268	217	0.81	0.0552	0.0032	0.26841	0.0175	0.03527	0.0005	0.011	0.0001	0.3	223	3	241	14	420	124	223	3	7.5
Gt0321 052	450	364	0.81	0.04911	0.0011	0.2339	0.0057	0.03455	0.0003	0.01084	0.0003	0.4	219	2	213	5	153	51	219	2	-2.8
~~Gt0321 054~~	~~294~~	~~209~~	0.71	~~0.12527~~	~~0.0058~~	~~0.4311~~	~~0.0206~~	~~0.02427~~	~~0.0003~~	~~0.01601~~	~~0.0009~~	~~0.3~~	~~155~~	~~2~~	~~364~~	~~15~~	~~2033~~	~~77~~	~~2033~~	~~77~~	~~57.4~~
Gt0321 055	533	459	0.86	0.05149	0.0014	0.25623	0.0072	0.03599	0.0003	0.01169	0.0003	0.3	228	2	232	6	263	59	228	2	1.7
Gt0321 056	761	739	0.97	0.05314	0.0012	0.25035	0.0061	0.03414	0.0003	0.01022	0.0003	0.3	216	2	227	5	335	49	216	2	4.8
Gt0321 057	488	318	0.65	0.05476	0.0015	0.26903	0.0075	0.03566	0.0003	0.01101	0.0003	0.3	226	2	242	6	402	57	226	2	6.6
Gt0321 058	709	773	1.09	0.04941	0.0013	0.24287	0.0068	0.03559	0.0003	0.01049	0.0003	0.3	225	2	221	6	167	59	225	2	-1.8
Gt0321 060	647	498	0.77	0.05343	0.0025	0.26112	0.0143	0.03544	0.0005	0.0111	0.0001	0.5	225	3	236	11	347	100	225	3	4.7
Gt0321 061	223	153	0.69	0.05441	0.0017	0.27448	0.0089	0.0366	0.0004	0.01156	0.0003	0.3	232	2	246	7	388	66	232	2	5.7
Gt0321 062	229	99	0.43	0.06956	0.0019	1.0235	0.0291	0.10704	0.0009	0.02579	0.0006	0.3	656	5	716	15	915	49	~~656~~	~~5~~	8.4
~~Gt0321 063~~	~~1319~~	~~1568~~	1.19	~~0.06004~~	~~0.0011~~	~~0.25948~~	~~0.0061~~	~~0.03141~~	~~0.0005~~	~~0.00918~~	~~0.0002~~	~~0.6~~	~~199~~	~~3~~	~~234~~	~~5~~	~~605~~	~~37~~	~~199~~	~~3~~	~~15.0~~
Gt0321 064	182	158	0.87	0.05367	0.0018	0.27447	0.0096	0.03715	0.0003	0.01174	0.0003	0.2	235	2	246	8	357	73	235	2	4.5
Gt0332, El Chol migmatite leucosome. 14°57'53.6" 90°29'12.5"																					
Gt0332 001	156	15	0.10	0.05633	0.0008	0.46378	0.0074	0.05955	0.0003	0.01948	0.0005	0.4	373	2	387	5	465	33	373	2	3.6
Gt0332 002	148	15	0.10	0.05635	0.0021	0.44983	0.0173	0.0579	0.0005	0.01801	0.0003	0.3	363	3	377	12	466	76	363	3	3.7
~~Gt0332 003~~	~~284~~	~~39~~	0.14	~~0.07629~~	~~0.0009~~	~~1.62574~~	~~0.0274~~	~~0.15456~~	~~0.0015~~	~~0.04646~~	~~0.0005~~	~~0.6~~	~~926~~	~~8~~	~~980~~	~~11~~	~~1103~~	~~23~~	~~1103~~	~~23~~	~~16.0~~
Gt0332 004	263	53	0.20	0.07297	0.0008	1.5346	0.021	0.15235	0.0012	0.04762	0.0008	0.6	914	7	944	8	1013	21	914	7	3.2
Gt0332 005	105	5	0.05	0.06633	0.0012	0.98129	0.0294	0.10606	0.0026	0.04536	0.0064	0.8	650	15	694	15	817	38	650	15	6.3
Gt0332 006	299	4	0.01	0.05772	0.0008	0.53746	0.01	0.06753	0.0009	0.02095	0.0003	0.7	421	5	437	7	519	29	421	5	3.7
Gt0332 007	100	1	0.01	0.05546	0.0015	0.26155	0.0073	0.03432	0.0002	0.01188	0.0025	0.3	218	1	236	6	431	60	218	1	7.6
Gt0332 008	350	103	0.29	0.07138	0.0007	1.367	0.0157	0.13875	0.0008	0.04191	0.0006	0.5	838	4	875	7	968	20	838	4	4.2
Gt0332 009	1100	4	0.004	0.05453	0.0006	0.40614	0.0049	0.05405	0.0003	0.04423	0.0021	0.4	339	2	346	4	393	25	339	2	2.0
~~Gt0332 010~~	~~60~~	~~20~~	0.34	~~0.07494~~	~~0.0013~~	~~1.6493~~	~~0.0298~~	~~0.15927~~	~~0.001~~	~~0.04813~~	~~0.0008~~	~~0.4~~	~~953~~	~~6~~	~~989~~	~~11~~	~~1067~~	~~32~~	~~1067~~	~~32~~	~~10.7~~
Gt0332 011	80	16	0.20	0.07027	0.002	1.27995	0.0387	0.1321	0.0009	0.04007	0.0004	0.3	800	5	837	17	936	54	800	5	4.4
Gt0332 012	414	77	0.19	0.05658	0.0007	0.42168	0.0072	0.05401	0.0006	0.01729	0.0004	0.6	339	4	357	5	475	28	339	4	5.0
Gt0332 013	133	38	0.28	0.07302	0.0008	1.5136	0.0185	0.15011	0.0008	0.04653	0.0007	0.4	902	4	936	7	1015	21	902	4	3.6
Gt0332 014	349	12	0.03	0.05626	0.0007	0.54576	0.0074	0.07036	0.0004	0.02189	0.0003	0.4	438	2	442	5	463	25	438	2	0.9
Gt0332 015	51	29	0.57	0.07281	0.0015	1.62334	0.0392	0.1617	0.0012	0.04885	0.0003	0.4	966	7	979	15	1009	39	966	7	1.3
Gt0332 016	58	12	0.20	0.07515	0.0021	1.45896	0.0413	0.1408	0.0008	0.04239	0.0003	0.2	849	5	914	17	1073	52	849	5	7.1
Gt0332 017	269	8	0.03	0.05359	0.0007	0.40993	0.0062	0.05547	0.0003	0.01736	0.0001	0.4	348	2	349	4	354	29	348	2	0.3
Gt0332 018	84	1	0.01	0.05178	0.0014	0.39775	0.0114	0.05558	0.0007	0.02382	0.0026	0.4	349	4	340	8	276	56	349	4	-2.6
~~Gt0332 019~~	~~94~~	~~1~~	0.01	~~0.06401~~	~~0.0028~~	~~0.30196~~	~~0.0137~~	~~0.03421~~	~~0.0004~~	~~0.01049~~	~~0.0014~~	~~0.3~~	~~217~~	~~2~~	~~268~~	~~11~~	~~742~~	~~92~~	~~217~~	~~2~~	~~19.0~~
Gt0332 020	329	18	0.06	0.05804	0.001	0.51963	0.0151	0.06494	0.0013	0.02013	0.0004	0.8	406	8	425	10	531	35	406	8	4.5
Gt0332 021	181	41	0.23	0.07645	0.0008	1.9312	0.0238	0.18303	0.001	0.05405	0.0008	0.5	1084	6	1092	8	1107	21	1107	21	2.1
Gt0332 022	93	1	0.01	0.05264	0.0013	0.29048	0.0084	0.04002	0.0005	0.01255	0.0003	0.5	253	3	259	7	313	57	253	3	2.3
Gt0332 023	236	18	0.07	0.06059	0.0008	0.75052	0.0112	0.08984	0.0006	0.02771	0.0002	0.4	555	3	569	6	625	26	555	3	2.5
Gt0332 024	103	1	0.01	0.05421	0.0015	0.26188	0.0077	0.03504	0.0002	0.01095	0.0004	0.2	222	1	236	6	380	60	222	1	5.9
Gt0332 025	363	32	0.09	0.058	0.0009	0.66101	0.0289	0.0802	0.0033	0.0255	0.0011	0.9	497	20	515	18	530	31	497	20	3.5
Gt0332 026	75	20	0.27	0.07045	0.001	1.4959	0.0341	0.15327	0.0028	0.04859	0.001	0.8	919	15	929	14	942	27	919	15	1.1
Gt0332 027	51	57	1.13	0.07212	0.0011	1.6353	0.0264	0.16461	0.001	0.05075	0.0007	0.4	982	5	984	10	989	29	982	5	0.2
Gt0332 028	274	89	0.32	0.07746	0.0007	2.1525	0.0228	0.20122	0.0009	0.05931	0.0008	0.4	1182	5	1166	7	1133	18	1133	18	-4.3
Gt0332 029	530	187	0.35	0.05469	0.0007	0.44225	0.0059	0.05859	0.0003	0.01763	0.0003	0.4	367	2	372	4	400	26	367	2	1.3
Gt0332 030	5	0	0.07	0.07465	0.0033	1.61938	0.0768	0.15733	0.0023	0.0474	0.0008	0.4	942	13	978	30	1059	83	1059	83	3.7
Gt0332 031	84	88	1.05	0.07159	0.0012	1.551	0.0302	0.15707	0.0015	0.04713	0.0007	0.5	940	8	951	12	974	33	940	8	1.2
~~Gt0332 032~~	~~92~~	~~75~~	0.81	~~0.07044~~	~~0.0009~~	~~1.6456~~	~~0.0239~~	~~0.16929~~	~~0.0011~~	~~0.04881~~	~~0.0007~~	~~0.4~~	~~1008~~	~~6~~	~~988~~	~~9~~	~~941~~	~~25~~	~~1008~~	~~6~~	~~-7.1~~
Gt0332 033	73	18	0.25	0.06704	0.0011	1.16447	0.022	0.12598	0.0009	0.03841	0.0003	0.4	765	5	784	10	839	32	765	5	2.4
Gt0332 034	3129	35	0.01	0.05292	0.0009	0.37554	0.0077	0.05147	0.0006	0.01613	0.001	0.7	324	3	324	6	325	35	324	3	0.0
Gt0332 035	214	79	0.37	0.06621	0.0015	0.90604	0.0296	0.09925	0.0015	0.03031	0.0004	0.7	610	9	655	16	813	45	610	9	6.9
Gt0332 036	327	145	0.44	0.07	0.001	1.18686	0.0225	0.12298	0.0009	0.03732	0.0003	0.6	748	5	795	10	928	28	748	5	5.9
Gt0332 037	13	12	0.92	0.07048	0.003	1.2357	0.0537	0.12777	0.0014	0.03853	0.0009	0.3	775	8	817	24	942	81	775	8	5.1
Gt0332 038	28	36	1.26	0.06676	0.004	1.10625	0.0737	0.12018	0.0014	0.03666	0.0004	0.4	732	8	756	36	830	117	732	8	3.2
Gt0332 039	101	15	0.14	0.07222	0.001	1.561	0.0235	0.15669	0.0009	0.04896	0.001	0.4	938	5	955	9	992	27	938	5	1.8
Gt0332 040	301	142	0.47	0.07419	0.0007	1.7429	0.0182	0.17007	0.0007	0.05168	0.0007	0.4	1012	4	1025	7	1047	18	1047	18	3.3
Gt0332 041	99	10	0.10	0.07702	0.0013	1.82071	0.0353	0.17145	0.001	0.05148	0.001	0.4	1020	6	1053	13	1122	34	1122	34	9.1
Gt0332 042	126	12	0.10	0.07199	0.0008	1.56688	0.0196	0.15786	0.0007	0.04775	0.0002	0.4	945	4	957	8	986	22	945	4	1.3
Gt0332 043	168	89	0.53	0.07603	0.0008	1.9919	0.0252	0.19007	0.0012	0.05634	0.0008	0.5	1122	6	1113	9	1096	21	1096	21	-2.4
Gt0332 044	275	80	0.29	0.0764	0.0008	1.821	0.0218	0.17278	0.0008	0.05321	0.0007	0.4	1027	4	1053	8	1106	22	1106	22	7.1
Gt0332 045	185	52	0.28	0.07685	0.0009	1.944	0.0233	0.18323	0.0009	0.05497	0.0007	0.4	1085	5	1096	8	1117	22	1117	22	2.9
Gt0332 046	54	29	0.53	0.07689	0.0012	1.8505	0.0329	0.17446	0.0017	0.05039	0.0009	0.5	1037	9	1064	12	1118	30	1118	30	7.2
Gt0332 047	533	190	0.36	0.07324	0.0007	1.7632	0.0198	0.17447	0.0012	0.05385	0.0008	0.6	1037	6	1032	7	1021	18	1021	18	-1.6
Gt0332 048	345	146	0.42	0.07387	0.0007	1.6993	0.0176	0.16665	0.0008	0.05005	0.0007	0.4	994	4	1008	7	1038	19	1038	19	4.2
~~Gt0332 049~~	~~10~~	4	0.40	~~0.0596~~	~~0.0045~~	~~0.69668~~	~~0.0563~~	~~0.08478~~	~~0.0012~~	~~0.0262~~	~~0.0004~~	~~0.3~~	~~525~~	~~7~~	~~537~~	~~34~~	~~589~~	~~166~~	~~525~~	~~7~~	~~2.2~~

TABLE II | **Continued**

				CORRECTED RATIOS[2]										CORRECTED AGES (Ma)								
Sample number	U[1] (ppm)	Th[1] (ppm)	Th/U	$^{207}Pb/^{206}Pb$	±1σ[3]	$^{207}Pb/^{235}U$	±1σ[3]	$^{206}Pb/^{238}U$	±1σ[3]	$^{208}Pb/^{232}Th$	±1σ[3]	Rho	$^{206}Pb/^{238}U$	±1σ	$^{207}Pb/^{235}U$	±1σ	$^{207}Pb/^{206}Pb$	±1σ	Best age (Ma)	±1σ	% disc
~~3t0332 050~~	~~46~~	~~32~~	0.69	~~0.13981~~	~~0.0042~~	~~1.2565~~	~~0.0392~~	~~0.06512~~	~~0.0006~~	~~0.05394~~	~~0.0048~~	~~0.3~~	~~407~~	~~3~~	~~826~~	~~18~~	~~2225~~	~~52~~	~~2225~~	~~52~~	~~81.7~~
3t0332 051	47	28	0.59	0.06315	0.0027	0.95347	0.0448	0.10951	0.0009	0.03362	0.0003	0.3	670	5	680	23	713	92	670	5	1.5
3t0332 052	60	70	1.18	0.07002	0.0012	1.3441	0.0247	0.13917	0.001	0.04448	0.0006	0.4	840	5	865	11	929	35	840	5	2.9
3t0332 053	7	7	0.98	0.07508	0.0024	1.8334	0.0627	0.17686	0.0021	0.05342	0.0011	0.4	1050	12	1057	22	1071	65	1071	65	2.0
~~3t0332 054~~	~~25~~	~~18~~	0.72	~~0.08468~~	~~0.0102~~	~~1.7152~~	~~0.2063~~	~~0.14367~~	~~0.0012~~	~~0.04416~~	~~0.0007~~	~~0.1~~	~~865~~	~~7~~	~~1014~~	~~77~~	~~1308~~	~~244~~	~~1308~~	~~244~~	~~33.9~~
3t0332 055	211	61	0.29	0.07639	0.0008	1.895	0.0214	0.17968	0.0009	0.05463	0.0008	0.5	1065	5	1079	7	1105	20	1105	20	3.6
3t0332 056	48	13	0.27	0.07443	0.0011	1.70055	0.0292	0.1657	0.0011	0.04994	0.0003	0.5	988	6	1009	11	1053	29	1053	29	6.2
3t0332 057	492	237	0.48	0.07508	0.0007	1.8209	0.0188	0.17568	0.0008	0.05174	0.0006	0.4	1043	4	1053	7	1071	19	1071	19	2.6
3t0332 058	347	134	0.39	0.07494	0.0007	1.7691	0.02	0.17103	0.001	0.05259	0.0007	0.5	1018	6	1034	7	1067	19	1067	19	4.6
3t0332 059	189	47	0.25	0.07436	0.0008	1.8223	0.0219	0.17749	0.0009	0.05417	0.0008	0.4	1053	5	1054	8	1051	22	1051	22	-0.2
3t0332 060	77	42	0.54	0.07708	0.001	1.8798	0.0265	0.17684	0.001	0.05481	0.0009	0.4	1050	5	1074	9	1123	26	1123	26	6.5
3t0332 061	578	53	0.09	0.05113	0.0024	0.26071	0.0124	0.03711	0.0005	0.02728	0.003	0.3	235	3	235	10	247	95	235	3	0.0
3t0332 062	479	42	0.09	0.05066	0.0022	0.24796	0.0114	0.03546	0.0005	0.0232	0.0028	0.3	225	3	225	9	225	91	225	3	0.0
3t0332 063	605	57	0.09	0.04994	0.0026	0.25055	0.0131	0.03651	0.0004	0.01321	0.0028	0.2	231	3	227	11	192	106	231	3	-1.8
3t0332 064	1494	110	0.07	0.05484	0.002	0.26402	0.0098	0.03496	0.0003	0.02604	0.0034	0.3	222	2	238	8	406	73	222	2	6.7
3t0332 065	1888	374	0.20	0.05049	8E-05	0.24094	0.0025	0.03461	0.0003	0.08597	0.0059	0.3	219	2	219	2	218	3	219	2	0.0
3t0332 066	87	34	0.39	0.05049	7E-05	0.24103	0.0027	0.03462	0.0004	0.04323	0.0049	0.3	219	2	219	2	218	3	219	2	0.0
3t0332 067	275	63	0.23	0.05627	0.0024	0.27975	0.0124	0.03659	0.0005	0.02926	0.0044	0.3	232	3	250	10	463	84	232	3	7.2
3t0341, orthogneiss. 15°00'22.5" 90°14'24.4"																					
3t0341 001	171	146	0.85	0.05696	0.0009	0.57685	0.0093	0.07356	0.0004	0.02256	0.0003	0.4	458	3	462	6	490	32	458	3	0.9
3t0341 002	121	90	0.75	0.05805	0.0009	0.62159	0.0106	0.07786	0.0004	0.02405	0.0003	0.3	483	3	491	7	532	35	483	3	1.6
3t0341 003	86	43	0.50	0.0726	0.0009	1.6717	0.0235	0.16698	0.0009	0.04928	0.0007	0.4	995	5	998	9	1003	26	~~995~~	~~5~~	0.3
3t0341 004	509	398	0.78	0.05594	0.0006	0.52663	0.0059	0.0684	0.0004	0.02015	0.0002	0.5	427	2	430	4	450	22	427	2	0.7
3t0341 005	825	1760	2.13	0.06273	0.0008	0.60464	0.0141	0.0698	0.0014	0.02303	0.0012	0.9	435	8	480	9	699	25	435	8	9.4
3t0341 006	608	137	0.22	0.05622	0.0006	0.56093	0.0061	0.07241	0.0003	0.0233	0.0003	0.4	451	2	452	4	461	21	451	2	0.2
3t0341 007	165	130	0.79	0.05993	0.0015	0.63942	0.0192	0.07739	0.0007	0.0239	0.0002	0.4	481	4	502	12	601	53	481	4	4.2
3t0341 008	660	606	0.92	0.05813	0.0006	0.54479	0.0075	0.06804	0.0006	0.02017	0.0004	0.6	424	3	442	5	535	23	424	3	4.1
3t0341 009	326	279	0.86	0.05944	0.0008	0.61262	0.0088	0.07485	0.0004	0.02414	0.0003	0.4	465	3	485	6	583	27	465	3	4.1
3t0341 010	170	210	1.23	0.05707	0.001	0.59089	0.0114	0.07524	0.0005	0.02335	0.0003	0.3	468	3	471	7	494	39	468	3	0.6
3t0341 011	333	224	0.67	0.05674	0.0006	0.58979	0.0073	0.07552	0.0004	0.02228	0.0003	0.5	469	3	471	5	481	24	469	3	0.4
3t0341 012	429	241	0.56	0.05584	0.0006	0.57358	0.0064	0.07459	0.0004	0.02316	0.0003	0.5	464	2	460	4	446	22	464	2	-0.9
3t0341 013	84	103	1.22	0.05721	0.0009	0.6047	0.0104	0.07679	0.0005	0.02416	0.0003	0.4	477	3	480	7	500	35	477	3	0.6
~~3t0341 014~~	~~96~~	~~91~~	0.94	~~0.07632~~	~~0.0017~~	~~0.7605~~	~~0.0175~~	~~0.07284~~	~~0.0005~~	~~0.02695~~	~~0.0004~~	~~0.3~~	~~453~~	~~3~~	~~574~~	~~10~~	~~1103~~	~~44~~	~~453~~	~~3~~	~~21.1~~
3t0341 015	514	339	0.66	0.05649	0.0006	0.56201	0.0062	0.07225	0.0004	0.02185	0.0002	0.5	450	2	453	4	472	22	450	2	0.7
3t0341 016	653	941	1.44	0.05719	0.0006	0.56314	0.0065	0.07162	0.0004	0.02191	0.0003	0.5	446	3	454	4	499	21	446	3	1.8
3t0341 017	160	209	1.31	0.05624	0.0008	0.59385	0.0092	0.07674	0.0005	0.02436	0.0003	0.4	477	3	473	6	462	31	477	3	-0.8
3t0341 018	396	740	1.87	0.05658	0.0007	0.55058	0.0071	0.07072	0.0003	0.02142	0.0002	0.4	440	2	445	5	475	26	440	2	1.1
3t0341 019	463	585	1.26	0.05709	0.0006	0.56762	0.0064	0.07227	0.0004	0.02268	0.0003	0.5	450	2	456	4	495	22	450	2	1.3
3t0341 020	1187	1065	0.90	0.0559	0.0005	0.40887	0.0079	0.05314	0.0009	0.01643	0.0002	0.9	334	6	348	6	448	20	334	6	4.0
3t0341 021	215	89	0.41	0.05773	0.0008	0.58327	0.0081	0.07341	0.0004	0.02287	0.0003	0.4	457	2	467	5	520	28	457	2	2.1
3t0341 022	780	461	0.59	0.057	0.0005	0.56357	0.0062	0.07181	0.0004	0.02246	0.0003	0.5	447	2	454	4	492	21	447	2	1.5
3t0341 023	227	163	0.72	0.05571	0.0008	0.5853	0.0087	0.07639	0.0004	0.02386	0.0003	0.4	475	2	468	6	441	31	475	2	-1.5
3t0341 024	429	137	0.32	0.09328	0.0008	3.2453	0.0315	0.25199	0.0011	0.07075	0.0008	0.5	1449	6	1468	8	1494	16	~~1494~~	~~16~~	3.0
3t0341 025	429	160	0.37	0.05931	0.001	0.74541	0.015	0.09115	0.0005	0.02819	0.0001	0.4	562	3	566	9	579	38	562	3	0.7
3t0341 026	226	267	1.18	0.05684	0.0008	0.59058	0.0089	0.07545	0.0004	0.02336	0.0003	0.4	469	2	471	6	485	31	469	2	0.4
3t0341 027	120	150	1.26	0.05832	0.0011	0.60226	0.0116	0.07504	0.0005	0.02407	0.0003	0.4	466	3	479	7	542	39	466	3	2.7
3t0341 028	388	476	1.23	0.0578	0.0006	0.57568	0.0071	0.07234	0.0004	0.02303	0.0003	0.4	450	2	462	5	522	24	450	2	2.6
3t0341 029	364	216	0.59	0.05687	0.0007	0.57738	0.0076	0.0738	0.0004	0.02344	0.0003	0.4	459	2	463	5	487	26	459	2	0.9
3t0341 030	214	94	0.44	0.05744	0.0008	0.56823	0.0088	0.07187	0.0005	0.02234	0.0003	0.4	447	3	457	6	509	30	447	3	2.2
3t0341 031	305	258	0.85	0.06192	0.0009	0.63361	0.014	0.07444	0.0013	0.02034	0.0012	0.8	463	8	498	9	671	30	463	8	7.0
3t0341 032	331	130	0.39	0.05708	0.0006	0.59749	0.0073	0.07595	0.0004	0.02361	0.0003	0.4	472	2	476	5	495	24	472	2	0.8
3t0341 033	117	90	0.77	0.058	0.0013	0.36057	0.0092	0.04619	0.0005	0.02554	0.0005	0.4	291	3	313	7	530	50	291	3	7.0
3t0341 034	144	86	0.59	0.0571	0.0007	0.57709	0.0082	0.07341	0.0004	0.02258	0.0003	0.4	457	2	463	5	495	28	457	2	1.3
3t0341 035	94	257	2.74	0.05771	0.001	0.57238	0.0104	0.07208	0.0005	0.02227	0.0003	0.4	449	3	460	7	519	37	449	3	2.4
3t0341 036	105	224	2.13	0.05773	0.0009	0.59391	0.0096	0.0747	0.0004	0.02229	0.0003	0.4	464	3	473	6	520	33	464	3	1.9
3t0341 037	379	412	1.09	0.05791	0.0006	0.58736	0.007	0.07353	0.0004	0.02252	0.0003	0.4	457	2	469	4	526	24	457	2	2.6
3t0341 038	430	619	1.44	0.06178	0.0007	0.62011	0.0081	0.07274	0.0004	0.02355	0.0003	0.4	453	2	490	5	667	25	453	2	7.6
3t0341 039	630	500	0.79	0.05766	0.0006	0.57184	0.0064	0.07198	0.0004	0.02112	0.0005	0.4	448	2	459	4	517	22	448	2	2.4
3t0341 040	320	234	0.73	0.05752	0.0012	0.60057	0.0142	0.07572	0.0004	0.0235	0.0001	0.4	471	2	478	9	512	45	471	2	1.5
3t0341 041	674	478	0.71	0.05624	0.0006	0.55142	0.0061	0.07124	0.0003	0.02154	0.0002	0.4	444	2	446	4	462	22	444	2	0.4
3t0341 042	479	176	0.37	0.05789	0.0006	0.56778	0.0069	0.07121	0.0004	0.02575	0.0004	0.4	443	2	457	4	526	24	443	2	3.1
3t0341 043	1090	607	0.56	0.05645	0.001	0.56649	0.0119	0.07278	0.0004	0.02264	0.0001	0.5	453	2	456	8	470	40	453	2	0.7
3t0341 044	472	206	0.44	0.05706	0.0006	0.56638	0.0069	0.07217	0.0004	0.02267	0.0003	0.4	449	2	456	4	494	24	449	2	1.5
~~3t0341 045~~	~~205~~	~~132~~	0.64	~~0.05683~~	~~0.0007~~	~~0.59865~~	~~0.0082~~	~~0.07648~~	~~0.0005~~	~~0.02345~~	~~0.0003~~	~~0.5~~	~~475~~	~~3~~	~~476~~	~~5~~	~~485~~	~~26~~	~~475~~	~~3~~	~~0.2~~

TABLE II | **Continued**

				CORRECTED RATIOS[2]										CORRECTED AGES (Ma)								
Sample number	U[1] (ppm)	Th[1] (ppm)	Th/U	$^{207}Pb/^{206}Pb$	±1σ[3]	$^{207}Pb/^{235}U$	±1σ[3]	$^{206}Pb/^{238}U$	±1σ[3]	$^{208}Pb/^{232}Th$	±1σ[3]	Rho	$^{206}Pb/^{238}U$	±1σ	$^{207}Pb/^{235}U$	±1σ	$^{207}Pb/^{206}Pb$	±1σ	Best age (Ma)	±1σ	% disc
Gt0341 046	620	355	0.57	0.05663	0.0006	0.57147	0.0063	0.07329	0.0004	0.02283	0.0003	0.4	456	2	459	4	477	22	456	2	0.7
Gt0341 047	223	378	1.70	0.06149	0.0008	0.58726	0.0089	0.06937	0.0005	0.02113	0.0004	0.5	432	3	469	6	656	27	432	3	7.9
Gt0341 048	550	345	0.63	0.05665	0.0006	0.57569	0.0069	0.07386	0.0003	0.02323	0.0003	0.4	459	2	462	4	478	24	459	2	0.6
Gt0341 049	222	293	1.32	0.05911	0.0009	0.58091	0.0096	0.07134	0.0005	0.02469	0.0003	0.4	444	3	465	6	571	32	444	3	4.5
Gt0341 050	195	47	0.24	0.05777	0.0009	0.56646	0.0092	0.07126	0.0004	0.02264	0.0004	0.4	444	3	456	6	521	32	444	3	2.6
Gt03113 pegmatite dike. 15°03'24" 90°23'36.8"																					
Gt03113 001	256	80	0.31	0.07737	0.0009	2.0375	0.0243	0.19089	0.0009	0.05905	0.0009	0.4	1126	5	1128	8	1131	20	1131	20	0.4
Gt03113 002	300	92	0.31	0.07233	0.001	1.59942	0.0261	0.16037	0.0008	0.04848	0.0002	0.4	959	4	970	10	995	28	959	4	1.1
Gt03113 003	1051	122	0.12	0.06444	0.0013	1.00002	0.0223	0.11255	0.0006	0.03447	0.0005	0.5	688	4	704	11	756	41	688	4	2.3
~~Gt03113 004~~	~~106~~	~~19~~	0.18	~~0.05129~~	~~0.0157~~	~~0.82331~~	~~0.2728~~	~~0.11641~~	~~0.0032~~	~~0.03663~~	~~0.0238~~	~~0.2~~	~~710~~	~~18~~	~~610~~	~~152~~	~~254~~	~~498~~	~~710~~	~~18~~	~~-16.4~~
Gt03113 005	277	102	0.37	0.07603	0.0008	1.8186	0.0202	0.17351	0.0009	0.05358	0.0008	0.5	1031	5	1052	7	1096	19	1096	19	5.9
Gt03113 006	486	79	0.16	0.07096	0.0016	1.41842	0.0354	0.14498	0.0009	0.04393	0.0004	0.3	873	5	897	15	956	45	873	5	2.7
Gt03113 007	245	86	0.35	0.07668	0.0008	1.9842	0.0214	0.18765	0.0008	0.05568	0.0008	0.4	1109	5	1110	7	1113	19	1113	19	0.4
~~Gt03113 008~~	~~856~~	~~145~~	0.17	~~0.07219~~	~~0.0007~~	~~0.96358~~	~~0.0111~~	~~0.09689~~	~~0.0006~~	~~0.05909~~	~~0.0009~~	~~0.5~~	~~596~~	~~3~~	~~685~~	~~6~~	~~991~~	~~19~~	~~596~~	~~3~~	~~13.0~~
~~Gt03113 009~~	~~126~~	~~54~~	0.43	~~0.08395~~	~~0.0009~~	~~1.8372~~	~~0.0222~~	~~0.15822~~	~~0.0008~~	~~0.04441~~	~~0.0008~~	~~0.4~~	~~947~~	~~4~~	~~1059~~	~~8~~	~~1291~~	~~20~~	~~1291~~	~~20~~	26.6
Gt03113 010	386	102	0.27	0.07497	0.0007	1.6892	0.0183	0.16336	0.0008	0.0484	0.0007	0.4	975	4	1004	7	1068	19	1068	19	8.7
~~Gt03113 011~~	~~179~~	~~35~~	0.20	~~0.07672~~	~~0.005~~	~~1.77126~~	~~0.1238~~	~~0.16746~~	~~0.0018~~	~~0.0503~~	~~0.0007~~	~~0.2~~	~~998~~	~~10~~	~~1035~~	~~45~~	~~1114~~	~~128~~	~~1114~~	~~128~~	~~10.4~~
Gt03113 012	1113	88	0.08	0.05837	0.0011	0.60878	0.0123	0.07564	0.0004	0.02343	0.0003	0.4	470	2	483	8	544	39	470	2	2.7
Gt03113 013	109	32	0.29	0.07575	0.0009	2.0461	0.0264	0.19606	0.0009	0.05932	0.0009	0.4	1154	5	1131	9	1088	23	1088	23	-2.0
~~Gt03113 014~~	~~135~~	~~48~~	0.35	~~0.08283~~	~~0.0197~~	~~2.12074~~	~~0.5456~~	~~0.1857~~	~~0.0065~~	~~0.05532~~	~~0.0042~~	~~0.3~~	~~1098~~	~~36~~	~~1156~~	~~178~~	~~1265~~	~~511~~	~~1265~~	~~511~~	~~13.2~~
Gt03113 015	247	72	0.29	0.07676	0.0009	1.97327	0.0262	0.18645	0.0009	0.056	0.0003	0.4	1102	5	1106	9	1115	22	1115	22	1.2
Gt03113 016	98	32	0.33	~~0.07216~~	~~0.0146~~	~~1.61372~~	~~0.35~~	~~0.16218~~	~~0.0033~~	~~0.04905~~	~~0.0034~~	~~0.2~~	969	18	976	136	991	436	969	18	0.7
Gt03113 017	348	62	0.18	0.07423	0.0012	1.65157	0.0301	0.16137	0.0009	0.04865	0.0004	0.4	964	5	990	12	1048	32	1048	32	8.0
Gt03113 018	383	125	0.33	0.0774	0.0007	2.0198	0.0212	0.18931	0.0009	0.05888	0.0008	0.4	1118	5	1122	7	1132	18	1132	18	1.2
Gt03113 019	117	52	0.45	0.07405	0.0016	1.76258	0.0414	0.17264	0.0009	0.05206	0.0003	0.3	1027	5	1032	15	1043	41	1043	41	1.5
Gt03113 020	115	38	0.33	0.07731	0.0009	2.018	0.0244	0.1894	0.001	0.0553	0.0008	0.4	1118	5	1122	8	1129	21	1129	21	1.0
Gt03113 021	966	149	0.15	0.05726	0.0008	0.61043	0.0101	0.07731	0.0004	0.02401	0.0002	0.4	480	2	484	6	502	31	480	2	0.8
Gt03113 022	240	71	0.30	0.07466	0.0008	1.7564	0.0193	0.17075	0.0008	0.05223	0.0007	0.4	1016	4	1030	7	1059	19	1059	19	4.1
Gt03113 023	113	28	0.25	0.07301	0.002	1.71135	0.0556	0.17	0.0018	0.05134	0.0005	0.5	1012	10	1013	21	1014	55	1014	55	0.2
Gt03113 024	509	67	0.13	0.07067	0.0017	1.34641	0.0351	0.13817	0.0008	0.04188	0.0007	0.4	834	4	866	15	948	47	834	4	3.7
Gt03113 025	368	95	0.26	0.07109	0.0011	1.53755	0.0271	0.15686	0.0008	0.04752	0.0003	0.4	939	5	946	11	960	30	939	5	0.7
Gt03113 026	558	157	0.28	0.07294	0.0008	1.56093	0.0222	0.15522	0.0009	0.04688	0.0003	0.5	930	5	955	9	1012	22	930	5	2.6
Gt03113 027	522	137	0.26	0.07276	0.0013	1.62392	0.0329	0.16187	0.0011	0.04891	0.0004	0.5	967	6	980	13	1007	34	967	6	1.3
Gt03113 028	212	49	0.23	0.07609	0.0008	1.9658	0.0219	0.18741	0.0009	0.05855	0.0008	0.4	1107	5	1104	7	1097	19	1097	19	-0.9
Gt03113 029	208	50	0.24	0.07413	0.0007	1.7159	0.0193	0.16797	0.0009	0.05563	0.0008	0.5	1001	5	1014	7	1045	19	1045	19	4.2
Gt03113 030	120	50	0.42	0.07579	0.0008	1.9	0.0234	0.18189	0.001	0.05603	0.0008	0.5	1077	5	1081	8	1090	21	1090	21	1.2
Gt0405 migmatite Rio Pasabien. 15°02'21.4" 89°41'02.4"																					
~~Gt0405 001~~	~~91~~	~~70~~	0.77	~~0.05895~~	~~0.0054~~	~~0.31666~~	~~0.0303~~	~~0.03896~~	~~0.0004~~	~~0.01206~~	~~0.0002~~	~~0.2~~	~~246~~	~~3~~	~~279~~	~~23~~	~~565~~	~~211~~	~~246~~	~~3~~	~~11.8~~
Gt0405 002	411	143	0.35	0.05009	0.001	0.28745	0.0062	0.04166	0.0003	0.01242	0.0002	0.4	263	2	257	5	199	43	263	2	-2.3
Gt0405 003	99	34	0.34	0.07037	0.001	1.4623	0.0222	0.15106	0.0009	0.04561	0.0007	0.4	907	5	915	9	939	30	~~907~~	~~5~~	0.9
Gt0405 004	150	88	0.59	0.05505	0.0011	0.53816	0.0107	0.07111	0.0004	0.02147	0.0003	0.3	443	3	437	7	414	44	443	3	-1.4
Gt0405 005	178	70	0.39	0.05912	0.0026	0.59211	0.0272	0.07263	0.0004	0.02247	0.0002	0.3	452	3	472	17	572	99	452	3	4.2
Gt0405 006	169	69	0.41	0.05746	0.001	0.59155	0.0107	0.07492	0.0005	0.024	0.0004	0.3	466	3	472	7	509	38	466	3	1.3
Gt0405 007	466	181	0.39	0.0553	0.0007	0.56879	0.0074	0.0748	0.0004	0.02359	0.0003	0.4	465	2	457	5	424	27	465	2	-1.8
Gt0405 008	132	50	0.38	0.05595	0.0011	0.5506	0.0115	0.07158	0.0004	0.02195	0.0004	0.3	446	3	445	8	450	46	446	3	-0.2
~~Gt0405 009~~	~~403~~	~~262~~	0.65	~~0.16292~~	~~0.0033~~	~~1.8602~~	~~0.0402~~	~~0.08162~~	~~0.0007~~	~~0.06371~~	~~0.0019~~	~~0.4~~	~~506~~	~~4~~	~~1067~~	~~14~~	~~2486~~	~~35~~	~~2486~~	~~35~~	~~52.6~~
~~Gt0405 010~~	~~264~~	~~137~~	0.52	~~0.06109~~	~~0.0079~~	~~0.33609~~	~~0.0454~~	~~0.0399~~	~~0.0005~~	~~0.0123~~	~~0.0003~~	~~0.3~~	~~252~~	~~3~~	~~294~~	~~34~~	~~642~~	~~257~~	~~252~~	~~3~~	~~14.3~~
Gt0405 011	195	71	0.36	0.05627	0.001	0.55607	0.01	0.07184	0.0004	0.02203	0.0003	0.3	447	3	449	7	463	35	447	3	0.4
Gt0405 012	561	200	0.36	0.05594	0.0006	0.55692	0.0062	0.07232	0.0004	0.02237	0.0003	0.5	450	2	450	4	450	20	450	2	0.0
~~Gt0405 013~~	~~5108~~	~~2791~~	0.55	~~0.07245~~	~~0.0032~~	~~0.2156~~	~~0.0104~~	~~0.02158~~	~~0.0002~~	~~0.00652~~	~~8E-05~~	~~0.5~~	~~138~~	~~1~~	~~198~~	~~9~~	~~999~~	~~81~~	~~138~~	~~1~~	~~30.3~~
Gt0405 014	595	292	0.49	0.05195	0.0007	0.2837	0.0043	0.03964	0.0002	0.01237	0.0002	0.4	251	1	254	3	283	30	251	1	1.2
Gt0405 015	2490	342	0.14	0.05852	0.0018	0.46303	0.0151	0.05739	0.0004	0.01777	0.0003	0.4	360	2	386	11	549	61	360	2	6.7
~~Gt0405 016~~	~~4015~~	~~101~~	0.03	~~0.06211~~	~~0.0009~~	~~0.37609~~	~~0.006~~	~~0.04446~~	~~0.0002~~	~~0.06733~~	~~0.0024~~	~~0.3~~	~~280~~	~~1~~	~~324~~	~~4~~	~~678~~	~~30~~	~~280~~	~~1~~	~~13.6~~
Gt0405 017	570	295	0.52	0.05145	0.0007	0.27898	0.0042	0.03939	0.0002	0.01262	0.0002	0.4	249	1	250	3	261	30	249	1	0.4
Gt0405 018	220	102	0.46	0.05642	0.0012	0.55387	0.0132	0.0712	0.0004	0.02215	0.0001	0.3	443	2	448	9	469	44	443	2	1.1
Gt0405 019	764	519	0.68	0.05312	0.0007	0.27705	0.0039	0.03792	0.0002	0.01195	0.0002	0.4	240	1	248	3	334	27	240	1	3.2
Gt0405 020	705	195	0.28	0.05233	0.0006	0.29051	0.0038	0.04029	0.0002	0.0122	0.0002	0.4	255	1	259	3	300	25	255	1	1.5
Gt0405 021	315	130	0.41	0.056	0.0007	0.54684	0.0076	0.07097	0.0004	0.02172	0.0003	0.4	442	2	443	5	452	30	442	2	0.2
Gt0405 023	154	77	0.50	0.05595	0.0009	0.56322	0.0095	0.07301	0.0004	0.02281	0.0003	0.3	454	2	454	6	450	37	454	2	0.0
Gt0405 024	1488	37	0.02	0.05153	0.0018	0.28573	0.0103	0.04021	0.0002	0.01265	0.0011	0.3	254	1	255	8	265	82	254	1	0.4
~~Gt0405 025~~	~~432~~	~~147~~	0.34	~~0.05632~~	~~0.0007~~	~~0.55761~~	~~0.0072~~	~~0.07201~~	~~0.0004~~	~~0.02242~~	~~0.0003~~	~~0.4~~	~~448~~	~~2~~	~~450~~	~~5~~	~~465~~	~~27~~	~~448~~	~~2~~	~~0.4~~

DOI: 10.1344/105.000001695

TABLE II | **Continued**

				CORRECTED RATIOS[2]									CORRECTED AGES (Ma)								
Sample number	U[1] (ppm)	Th[1] (ppm)	Th/U	$^{207}Pb/^{206}Pb$	±1σ[3]	$^{207}Pb/^{235}U$	±1σ[3]	$^{206}Pb/^{238}U$	±1σ[3]	$^{208}Pb/^{232}Th$	±1σ[3]	Rho	$^{206}Pb/^{238}U$	±1σ	$^{207}Pb/^{235}U$	±1σ	$^{207}Pb/^{206}Pb$	±1σ	Best age (Ma)	±1σ	% disc
Gt0405 026	543	50	0.09	0.05476	0.0007	0.46443	0.0065	0.06143	0.0003	0.0236	0.0004	0.4	384	2	387	5	402	30	384	2	0.8
~~Gt0405 027~~	~~4341~~	~~861~~	~~0.20~~	~~0.05924~~	~~0.0069~~	~~0.40377~~	~~0.0494~~	~~0.04943~~	~~0.0007~~	~~0.01529~~	~~0.0006~~	~~0.4~~	~~311~~	~~4~~	~~344~~	~~36~~	~~576~~	~~268~~	~~311~~	~~4~~	~~9.6~~
Gt0405 028	388	185	0.48	0.05604	0.0007	0.58126	0.0079	0.07531	0.0005	0.02363	0.0003	0.5	468	3	465	5	454	27	468	3	-0.6
Gt0405 029	1608	114	0.07	0.05291	0.0005	0.35923	0.0042	0.04921	0.0003	0.02119	0.0003	0.5	310	2	312	3	325	23	310	2	0.6
Gt0405 030	425	307	0.72	0.05068	0.0008	0.26803	0.0043	0.03844	0.0002	0.01194	0.0002	0.4	243	1	241	3	226	36	243	1	-0.8
Gt0405 031	188	100	0.53	0.06236	0.001	0.6206	0.0104	0.07239	0.0004	0.02528	0.0004	0.3	451	2	490	6	686	35	451	2	8.0
~~Gt0405 032~~	~~807~~	~~175~~	0.22	~~0.06298~~	~~0.0082~~	~~0.56481~~	~~0.0779~~	~~0.06504~~	~~0.0008~~	~~0.01997~~	~~0.0013~~	~~0.4~~	406	~~5~~	455	~~51~~	~~708~~	~~302~~	406	~~5~~	~~10.8~~
~~Gt0405 033~~	~~2971~~	~~67~~	0.02	~~0.06245~~	~~0.0051~~	~~0.33815~~	~~0.0289~~	~~0.03927~~	~~0.0003~~	~~0.01207~~	~~0.0047~~	~~0.3~~	~~248~~	~~2~~	~~296~~	~~22~~	~~690~~	~~185~~	~~248~~	~~2~~	~~16.2~~
Gt0405 034	590	414	0.70	0.05989	0.0006	0.60858	0.0068	0.07379	0.0004	0.02311	0.0003	0.4	459	2	483	4	600	22	459	2	5.0
Gt0405 035	186	142	0.77	0.05703	0.001	0.56871	0.0106	0.07249	0.0006	0.02337	0.0004	0.4	451	3	457	7	493	38	451	3	1.3
Gt0405 036	4761	79	0.02	0.05076	0.0005	0.26191	0.003	0.03742	0.0002	0.01179	0.0002	0.4	237	1	236	2	230	25	237	1	-0.4
~~Gt0405 037~~	~~3872~~	~~414~~	0.11	~~0.08749~~	~~0.0234~~	~~0.60095~~	~~0.1609~~	~~0.04982~~	~~0.0016~~	~~0.01475~~	~~0.0049~~	~~0.2~~	~~313~~	~~10~~	~~478~~	~~108~~	~~1371~~	~~597~~	~~313~~	~~10~~	~~34.5~~
Gt0405 038	7036	78	0.01	0.05097	0.0005	0.27027	0.0029	0.03846	0.0002	0.01211	0.0002	0.5	243	1	243	2	239	22	243	1	0.0
Gt0405 039	5709	113	0.02	0.05571	0.0041	0.29857	0.0225	0.03887	0.0003	0.01211	0.0028	0.2	246	2	265	18	441	170	246	2	7.2
~~Gt0405 040~~	~~3298~~	~~47~~	0.01	~~0.05967~~	~~0.0463~~	~~0.29217~~	~~0.2744~~	~~0.03551~~	~~0.0028~~	~~0.01097~~	~~0.3102~~	~~0.7~~	225	~~18~~	260	~~216~~	~~592~~	###	225	~~18~~	~~13.5~~
~~Gt0405 041~~	~~6747~~	~~112~~	0.02	~~0.06819~~	~~0.0224~~	~~0.33609~~	~~0.1225~~	~~0.03575~~	~~0.0015~~	~~0.01088~~	~~0.0642~~	~~0.5~~	226	~~9~~	294	~~93~~	~~874~~	~~695~~	226	~~9~~	~~23.1~~
Gt0405 042	4903	55	0.01	0.05251	0.0011	0.27846	0.0065	0.03846	0.0002	0.01207	0.0011	0.3	243	1	249	5	308	50	243	1	2.4
~~Gt0405 043~~	~~6407~~	~~90~~	0.01	~~0.08375~~	~~0.0255~~	~~0.41899~~	~~0.1408~~	~~0.03628~~	~~0.0014~~	~~0.0108~~	~~0.0477~~	~~0.5~~	~~230~~	~~9~~	~~355~~	~~101~~	~~1287~~	~~681~~	~~230~~	~~9~~	~~35.2~~
Gt0405 044	3838	74	0.02	0.05101	0.0005	0.25501	0.0027	0.03628	0.0002	0.01243	0.0002	0.5	230	1	231	2	241	21	230	1	0.4
Gt0405 045	3095	117	0.04	0.05716	0.0013	0.46073	0.0119	0.05846	0.0004	0.01816	0.001	0.5	366	2	385	8	498	51	366	2	4.9
Gt0405 046	1431	8	0.01	0.05068	0.0006	0.2418	0.0032	0.03466	0.0002	0.01143	0.0005	0.4	220	1	220	3	226	28	220	1	0.0
~~Gt0405 047~~	~~7850~~	~~101~~	0.01	~~0.06913~~	~~0.0144~~	~~0.35174~~	~~0.0782~~	~~0.0369~~	~~0.0009~~	~~0.01121~~	~~0.025~~	~~0.3~~	~~234~~	~~5~~	~~306~~	~~59~~	~~903~~	~~461~~	~~234~~	~~5~~	~~23.5~~
Gt0405 048	5658	105	0.02	0.05148	0.0005	0.27134	0.0037	0.03826	0.0004	0.01608	0.0006	0.8	242	2	244	3	262	21	242	2	0.8
~~Gt0405 049~~	~~2008~~	~~22~~	0.01	~~0.07552~~	~~0.0013~~	~~0.3937~~	~~0.0069~~	~~0.03809~~	~~0.0002~~	~~0.34427~~	~~0.0169~~	~~0.3~~	~~241~~	~~1~~	~~337~~	~~5~~	~~1082~~	~~34~~	~~241~~	~~1~~	~~28.5~~
Gt0405 050	2428	36	0.01	0.05111	0.0005	0.26734	0.0029	0.03797	0.0002	0.01583	0.0005	0.5	240	1	241	2	246	22	240	1	0.4
Gt0405 051	3299	53	0.02	0.05166	0.0008	0.25688	0.0044	0.03606	0.0002	0.01134	0.0009	0.4	228	1	232	4	271	36	228	1	1.7
Gt0405 052	7887	216	0.03	0.05272	0.0025	0.28703	0.0147	0.03949	0.0003	0.01238	0.0015	0.4	250	2	256	12	317	109	250	2	2.3
Gt0405 053	2522	29	0.01	0.05129	0.0005	0.26119	0.003	0.03693	0.0002	0.01162	0.0002	0.4	234	1	236	2	254	23	234	1	0.8
~~Gt0405 054~~	~~2118~~	~~64~~	0.03	~~0.06224~~	~~0.0056~~	~~0.45052~~	~~0.0422~~	~~0.0525~~	~~0.0005~~	~~0.01614~~	~~0.0023~~	~~0.2~~	~~330~~	~~3~~	~~378~~	~~30~~	~~682~~	~~198~~	~~330~~	~~3~~	~~12.7~~
~~Gt0405 055~~	~~1522~~	~~19~~	0.01	~~0.05607~~	~~0.0107~~	~~0.26928~~	~~0.0549~~	~~0.03483~~	~~0.0006~~	~~0.01084~~	~~0.038~~	~~0.3~~	~~221~~	~~4~~	~~242~~	~~44~~	~~455~~	~~399~~	~~221~~	~~4~~	~~8.7~~

[1]: U and Th concetrations are calibrated relative to the analysis of NIST 612 trace element standard glass

[2]: Isotopic ratios are corrected relative to analysis of a standard zircon for mass bias and down-hole fractionation (see text for further explanations and the used zircon standards). The Andersen (2002) common Pb correction m

[3]: Isotopic ratio errors are absolute and expressed at 1-sigma level. See text for further explanations

Apparent age errors are expressed at ± 1 sigma

Strikethrough analyses were discarded from calculations because >10% <-5% discordant. This criteria was released to >15% for the sample Gt0315 because of the difficulty to measure 207Pb in such young zircons

DOI: 10.1344/105.000001695